

Linköping studies in science and technology  
Licentiate Thesis. No. 1616

# Modeling and Estimation for Dry Clutch Control

Andreas Myklebust



**Linköping University**  
**INSTITUTE OF TECHNOLOGY**

Department of Electrical Engineering  
Linköping University, SE-581 33 Linköping, Sweden

Linköping 2013

Linköping studies in science and technology  
Licentiate Thesis. No. 1616

This is a Swedish Licentiate's Thesis.

Swedish postgraduate education leads to a Doctor's degree and/or a Licentiate's degree.

A Doctor's degree comprises 240 ECTS credits (4 years of full-time studies).

A Licentiate's degree comprises 120 ECTS credits,  
of which at least 60 ECTS credits constitute a Licentiate's thesis.

Andreas Myklebust  
`andreas.myklebust@liu.se`  
`www.vehicular.isy.liu.se`  
Division of Vehicular Systems  
Department of Electrical Engineering  
Linköping University  
SE-581 33 Linköping, Sweden

Copyright © 2013 Andreas Myklebust.  
All rights reserved.

Myklebust, Andreas  
Modeling and Estimation for Dry Clutch Control  
ISBN 978-91-7519-523-0  
ISSN 0280-7971  
LIU-TEK-LIC-2013:50

Typeset with L<sup>A</sup>T<sub>E</sub>X 2<sub>ε</sub>  
Printed by LiU-Tryck, Linköping, Sweden 2013

*“A mathematical model does not have to be exact; it just has to be close enough to provide better results than can be obtained by common sense.”*

— Herbert A. Simon



## ABSTRACT

Increasing demands on comfort, performance, and fuel efficiency in vehicles lead to more complex transmission solutions. One such solution is the Automated Manual Transmission (AMT). It works just like an ordinary manual transmission but the clutch and gear selection are computer controlled. In this way high efficiency can be accomplished with increased comfort and performance. To be able to control and fully utilize an AMT it is of great importance to have knowledge about how torque is transmitted in the clutch. The transmitted torque in a slipping dry clutch is therefore studied in experiments with a heavy duty truck (HDT). It is shown that material expansion with temperature can explain torque variations up to 700 Nm for the same clutch actuator position. A dynamic clutch temperature model that can describe the torque variations is developed. The dynamic model is validated in experiments, and shown to reduce the error in transmitted torque from 7 % to 3 % of the maximum engine torque compared to a static model.

The clutch model is extended with lock-up/break-a-part dynamics and an extra state describing wear. The former is done using a state machine and the latter using a slow random walk for a parameter corresponding to the clutch disc thickness. An observability analysis shows that the augmented model is fully or partially observable depending on the mode of operation. In particular, by measuring the actuator position the temperature states are observable, both during slipping of the clutch and when it is fully closed. An Extended Kalman Filter (EKF) was developed and evaluated on measurement data. The estimated states converged from poor initial values, enabling prediction of the translation of the torque transmissibility curve. The computational complexity of the EKF is low and it is thus suitable for real-time applications.

The clutch model is also integrated into a driveline model capable of capturing vehicle shuffle (longitudinal speed oscillations). Parameters are estimated to fit an HDT and the complete model shows good agreement with data. It is used to show that the effect of thermal expansion, even for moderate temperatures, is significant in launch control applications.

An alternative use of the driveline model is also investigated here. It is found that the amplitude discretization in production road-slope sensors can excite vehicle shuffle dynamics in the model, which is not present in the real vehicle. To overcome this problem road-slope information is analyzed and it is shown that a third-order butterworth low-pass filter can attenuate the vehicle shuffle, while the shape of the road profile is maintained.

All experiments in the thesis are performed using production HDTs only, i.e. production sensors only. Since all modeling, parameter estimation, observer design and validation are performed with production sensors it is straight forward to implement the results in a production HDT following the presented methodology.



## ACKNOWLEDGMENTS

I like to thank my beloved girlfriend Elin "White Darling" Julin for always supporting me and cheering me on in my work, you sure made it easier to reach this far. I also have to thank my supervisor Lars "Lasse" Eriksson for reaching this far. I would not even have started without your motivational skills. More thanks go to Karl Redbrandt, my contact at Scania, a busy man that still managed to give plenty of support, not only with measurements but also with ideas and thoughts. More people at Scania that I like to thank are my former contact person, Jörgen Hansson and Kristian Hellgren for valuable clutch information.

Further thanks go to my co-workers at Vehicular Systems for contributing to a pleasant working atmosphere. Special thanks to many roommates, both current, Neda Nickmehr and Jörgen Albrektsson, as well as former, Carl Svård, Peter Nyberg, and Erik Höckerdal. A special thank also goes to Kristoffer Lundahl for bringing more vehicular interest and vehicular discussions to Vehicular Systems.

A lot of friends and again, my Elin, are thanked for filling up my spare time with activities, which definitely is necessary when progress at work is slow. My family is thanked for creating an environment that nurtured a great science and engineering interest. There are many engineers in my family but, at the time of writing, no licentiates. A special note is made to my dad, Einar Myklebust, who have supported me when developing my practical vehicular skills. And I suppose also to my RX-7 "Black Darling" for constantly breaking down at a rate slightly higher than my "fixing rate". Last, and perhaps least, just to be on the safe side, thanks to anyone who feels forgotten in this acknowledgment!



---

# Contents

<b>1</b>	<b>Introduction</b>	<b>1</b>
1.1	Contributions . . . . .	3
1.2	Publications . . . . .	4
<b>2</b>	<b>Introduction to Clutch and Driveline Modeling</b>	<b>7</b>
2.1	Survey of Clutch and Driveline Models . . . . .	8
2.1.1	Clutch Models . . . . .	9
2.1.2	Driveline Models . . . . .	10
<b>3</b>	<b>Experimental Observations and Model Structure</b>	<b>13</b>
3.1	Motivating Experiment . . . . .	14
3.2	Actuator Dynamics . . . . .	14
3.3	Clutch Variables . . . . .	17
3.4	Wear . . . . .	18
3.5	Slip . . . . .	18
3.6	Rotational Speed . . . . .	19
3.7	Temperature . . . . .	20
3.7.1	Vehicle Speed Dependency . . . . .	23
3.7.2	Engine Speed Dependency . . . . .	24
3.8	Model Summary and Usage in Papers . . . . .	25
	References . . . . .	26
	<b>Publications</b>	<b>31</b>
<b>A</b>	<b>Torque Model with Fast and Slow Temperature Dynamics of a Slipping Dry Clutch</b>	<b>33</b>
1	Introduction . . . . .	36
2	Experimental Setup . . . . .	37
3	Modeling Outline . . . . .	37
4	Slip dependency . . . . .	38
5	Temperature Effects and Models . . . . .	40

5.1	Material Expansion Analysis . . . . .	41
5.2	Expansion Model . . . . .	42
5.3	Including Fast Dynamics . . . . .	44
6	Model Validation . . . . .	46
7	Conclusion . . . . .	48
	References . . . . .	50
<b>B</b>	<b>The Effect of Thermal Expansion in a Dry Clutch on Launch Control</b>	<b>51</b>
1	Introduction . . . . .	54
2	Driveline Model . . . . .	55
2.1	Internal Combustion Engine . . . . .	56
2.2	Clutch . . . . .	56
2.3	Transmission . . . . .	59
2.4	Propeller Shaft . . . . .	59
2.5	Final Drive . . . . .	59
2.6	Drive Shafts . . . . .	59
2.7	Vehicle Dynamics . . . . .	60
3	Parameter Estimation . . . . .	60
4	Model Validation . . . . .	63
5	Thermal Effect on Launching . . . . .	64
6	Conclusion . . . . .	66
	References . . . . .	67
<b>C</b>	<b>Modeling, Observability and Estimation of Thermal Effects and Aging on Transmitted Torque in a Heavy Duty Truck with a Dry Clutch</b>	<b>69</b>
1	Introduction . . . . .	72
1.1	Outline and Contributions . . . . .	72
1.2	Survey of Clutch Models . . . . .	72
2	Experimental Setup . . . . .	74
3	Clutch Model . . . . .	75
3.1	Lock-Up/Break-Apart Logic . . . . .	76
3.2	Slipping Torque Model Structure . . . . .	76
3.3	Slip dependency . . . . .	78
3.4	Temperature Effects and Models . . . . .	78
3.5	Clutch Model Validation . . . . .	85
4	Observer . . . . .	87
4.1	Observability . . . . .	88
4.2	Observer Selection and Precautions . . . . .	89
4.3	Selection of EKF Covariance Matrices . . . . .	90
4.4	Observer Evaluation . . . . .	90
5	Conclusion . . . . .	93
	References . . . . .	94

**D Road Slope Analysis and Filtering for Driveline Shuffle Simulation** **97**

1 Introduction . . . . . 100

2 Powertrain model . . . . . 100

    2.1 Internal Combustion Engine . . . . . 101

    2.2 Clutch . . . . . 101

    2.3 Transmission . . . . . 103

    2.4 Propeller Shaft . . . . . 104

    2.5 Final Drive . . . . . 104

    2.6 Drive Shafts . . . . . 104

    2.7 Vehicle Dynamics . . . . . 104

    2.8 State-Space Model . . . . . 107

    2.9 Linearization . . . . . 107

    2.10 Model Validation . . . . . 108

3 Slope Signal Effect on Simulation . . . . . 110

4 Road Frequency . . . . . 112

5 Filter Design . . . . . 114

6 Results . . . . . 116

7 Conclusions . . . . . 116

References . . . . . 118



# Chapter 1

---

## Introduction

In order to propel a vehicle the engine must be connected to the wheels somehow and different driveline solutions are available to create this connection. In a common rear-wheel-drive setup, see Figure 1.1, the tractive wheels (two or more) are connected to a drive shaft each. These drive shafts are, through a final drive (a differential), driven by a propeller shaft that is connected to the transmission. The transmission consists of two parts, the actual transmission part where torque and speed is changed by a gear ratio and a connection between the Internal Combustion Engine (ICE) and transmission that is capable of decoupling the speeds between the engine and transmission. Historically comfort was best accomplished with a classical Automatic Transmission (AT) and high efficiency with a Manual Transmission (MT).

An AT actuates different gear ratios through clutches and brakes that locks different parts of planetary gear sets. The coupling between engine and transmission is handled by a torque converter. These two technologies put together enable seamless gear shifts that can be controlled through simple hydraulics, the AT was put in production as early as 1939, (Nunney, 1998). The drawbacks are lower efficiency, mainly due to pumping of oil in the torque converter, and the increased complexity and cost, compared to an MT.

The MT is coupled to the engine via a clutch that is operated by the driver via the clutch pedal. A simple explanation of the clutch is that it consists of two rotating plates that can be pressed together. When pressed together friction will arise and transmit a torque between the plates, which acts to reduce the speed difference. See Chapter 2 for a more detailed explanation. Gear selection is realized using two shafts, both with a set of cog wheels, that mesh together. One pair of cog wheels, corresponding to a certain gear, can be engaged by a mechanical linkage connected to the gear lever. This type of transmission has a high efficiency and simple construction but requires the clutch to be disengaged during shifting (torque interrupt) and manual input from the driver. For more



Figure 1.1: A rear-wheel-drive driveline from a Scania HDT. The engine, transmission, propeller shaft, differential (final drive) and drive shafts can be seen.

details on possible transmission constructions see Newton et al. (1996) or Nunney (1998).

Increasing demands on comfort, performance, and fuel efficiency in vehicles lead to more complex transmission solutions. The Automated Manual Transmission (AMT) is one way to combine the best from two worlds. It has the same components and basic operation as an MT but the gear selection and clutch operation have been made automatic. This has become possible thanks to technological advances within actuators and computer controllers. The AMT has the benefits of the MT but without the need of driver attention. However it still has the drawback of torque interrupt during gear changes. Another option, capable of removing the torque interrupt, is the Dual Clutch Transmission (DCT). The DCT further improves comfort and performance with the drawbacks of increased complexity and cost. An important part in both an AMT and a DCT is clutch control, which has a profound effect on vehicle performance. A poorly controlled clutch can make starts, stops and gearshifts slow, rough on the hardware or uncomfortable. An example can be seen in Figure 1.2. In this case driveline oscillations, which cause discomfort, are induced by too rapid disengagement/engagement of the clutch. The driveline oscillations can be seen in both the speed graphs and in the acceleration graphs. This type of oscillations can be clearly felt by the driver and passengers.

To be able to control the clutch in a fast and comfortable manner, without causing excessive wear it is of importance to know the torque transmitted in the clutch with high precision. Moreover the clutch torque is of great interest if the clutch is to be integrated in a powertrain control scheme that is of, as common, torque based structure, (Eriksson and Nielsen, 2014). Models have come to play an important role in estimation and control of the transmitted torque, since torque sensors are expensive. Therefore modeling and observation of the clutch torque is in focus here. Since the purpose of the observer is improved clutch control, the model and observer are required to be light-weight enough to run in real-time. Previous experimental investigations of the clutch characteristics,

(Velardocchia et al., 1999; Moon et al., 2004; Vasca et al., 2011) and (Deur et al., 2012), have been carried out in test rigs equipped with various sensors. Here the experimental platform is limited to production vehicles without additional sensors. On one hand this choice imposes certain difficulties in setting up useful experiments. On the other hand the resulting model and observer can be directly applied to the intended vehicle, in or after production.

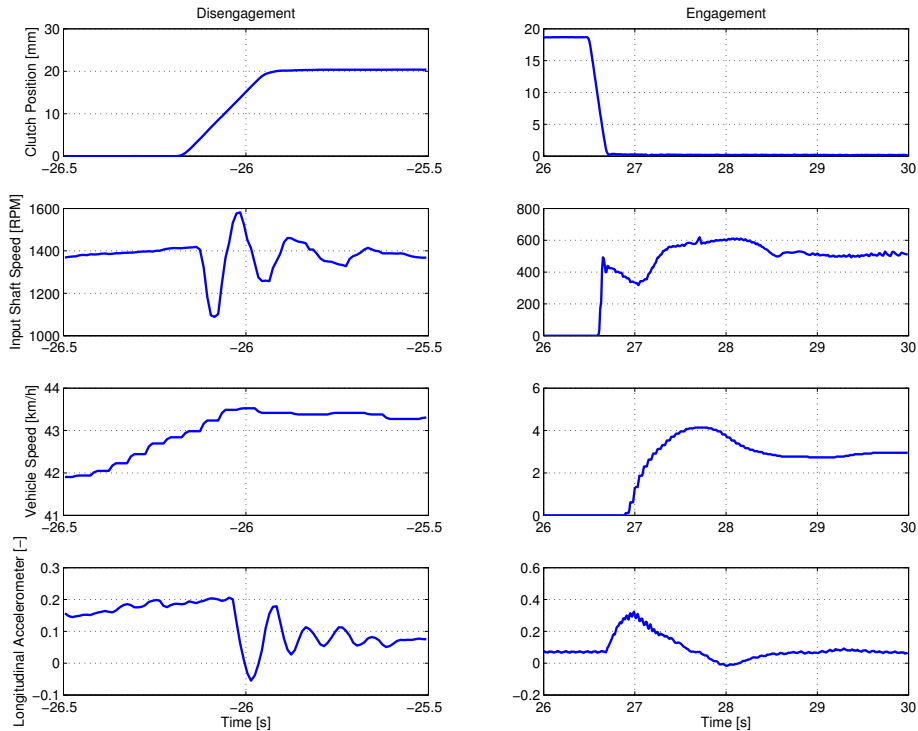


Figure 1.2: The left graphs show measurements of driveline oscillations due to (too) rapid disengagement of the clutch; a scenario possible during gear shifting. The right graphs shows the same measurements but in the case of rapid engagement from standstill, which could be the case if the driver wants a quick launch. In both cases the oscillations could clearly be felt by the driver and passenger.

## 1.1 CONTRIBUTIONS

A set of experiments for determining significant effects in the clutch and their characteristics is proposed. Since the experimental platforms used here are production vehicles the methodology proposed can easily be applied to new

platforms without the use of additional test equipment. Moreover the clutch is put in its true thermal environment, between a transmission and a warm combustion engine, which affects the temperature dynamics. Further contributions are found in the attached papers A-D. Their main contributions are summarized below.

## PAPER A

The main contribution of Paper A is a novel clutch model that includes the temperature dynamics and thermal effects on the transmitted torque during slipping. The model is developed using a method that utilizes production sensors only. The resulting model is simple enough to run in real time.

## PAPER B

Paper B integrates the clutch model of Paper A into the complete driveline model of Paper D and models clutch lock-up/break-a-part with a simple approach. The complete model is validated against data of HDT launches. The main contribution is the demonstration of the importance of considering the thermal dynamics during vehicle launch.

## PAPER C

Paper C extends the clutch model of Paper A with a wear parameter corresponding to thinning of the clutch disc. The main contributions are an observability analysis and observer design for the augmented model. The observability of the augmented model is found to be dependent on the mode of the system. An Extended Kalman Filter (EKF) that can observe the temperatures and the wear parameter is designed and tested on data from production vehicles.

## PAPER D

A driveline model is presented in Paper D and shown to be appropriate for vehicle longitudinal shuffle simulation. The main contribution is an investigation, using the model, of how and why a discretized slope signal needs to be filtered.

## 1.2 PUBLICATIONS

The following papers are included in the thesis.

### CONFERENCE PAPERS

- Andreas Myklebust and Lars Eriksson. Torque model with fast and slow temperature dynamics of a slipping dry clutch. Published in *2012 IEEE Vehicle Power and Propulsion Conference*. Seoul, South Korea, 2012. **(Paper A)**

- Andreas Myklebust and Lars Eriksson. The effect of thermal expansion in a dry clutch on launch control. Accepted for publication in *7th IFAC Symposium on Advances in Automotive Control*. Tokyo, Japan, 2013. **(Paper B)**
- Andreas Myklebust and Lars Eriksson. Road slope analysis and filtering for driveline shuffle simulation. Published in *2012 IFAC Workshop on Engine and Powertrain Control, Simulation and Modeling*. Rueil-Malmaison, France, 2012. **(Paper D)**

## SUBMITTED

- Andreas Myklebust and Lars Eriksson. Modeling, observability and estimation of thermal effects and aging on transmitted torque in a heavy duty truck with a dry clutch. Submitted to *IEEE/ASME Transactions on Mechatronics*. **(Paper C)**



# Introduction to Clutch and Driveline Modeling

A schematic of the dry clutch and actuator studied in this thesis is found in Figure 2.1. It has an electro-hydraulic actuator and the clutch construction is typical for a dry clutch. Double clutches have slightly altered constructions but the main principle is the same.

The electric motor rotates a worm gear that pushes into the hydraulic fluid, in an MT the clutch pedal would do this. When the opening to the reservoir is passed the hydraulic fluid pushes on a piston that through a lever pulls the throw-out bearing away from the clutch, the depicted clutch is hence called a pull-type clutch.

The throw-out bearing pulls on the fingers of the diaphragm (also called belleville, washer, slotted disc) spring. This spring is radially pivoted and angularly fixed to the clutch cover that is bolted to the flywheel. The bolting of the clutch cover pre-loads the diaphragm spring so that it exerts a force on the pressure (push) plate and thus clamps the clutch disc between the pressure plate and the flywheel. The pressure plate is also angularly fixed to the clutch cover and thereby flywheel. When the throw-out bearing is pulling the fingers of the diaphragm spring load is taken off the pressure plate. As the pressure plate exerts less clamp load, the cushion (flat) spring inside the clutch disc expands leading to a new equilibrium position for all of the clutch linkage. The connection between positions, spring characteristics and bearing force can be seen in Figure 2.2. Through this arrangement a certain actuator positions will correspond to a certain clamp loads, which facilitates control, especially in the manual case.

The clutch disc is angularly fixed to the transmission input shaft and can therefore rotate with a different speed than the engine and flywheel. When the clamp load becomes greater than zero a friction force will arise if there is a speed difference. This force will result in a torque around the crank and input shafts working to reduce the speed difference. With a larger normal force a larger

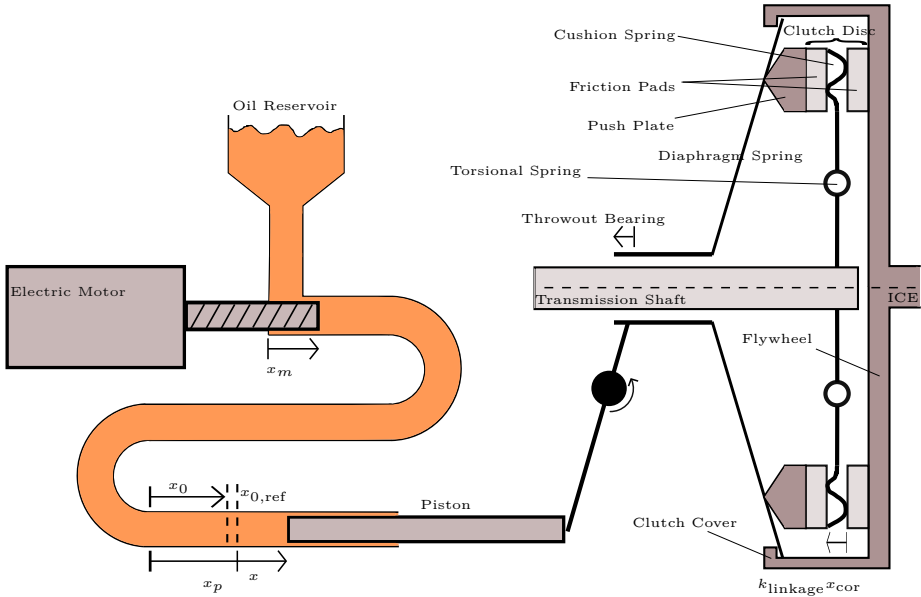


Figure 2.1: A schematic over the actuator and the dry single-plate pull-type clutch studied here.  $k_{\text{linkage}}$  is the combined ratio of all levers between the piston and the push plate. Sometimes the measurement  $x$  is used instead of  $x_p$  as a wear compensated piston position that is in the same range as  $x_m$ .

torque will be transmitted and if the speed difference gets reduced to zero the clutch will lock up, i.e. static friction will take place. When locked up the clutch acts as a solid unit and transmit the engine torque as long as it does not exceed the stiction torque. The engine torque is oscillative and in order to damp these oscillations there are torsional springs inside the clutch disc. For more detailed descriptions of how a clutch works see Mashadi and Crolla (2012); Newton et al. (1996); Dolcini et al. (2010) or Vasca et al. (2011).

## 2.1 SURVEY OF CLUTCH AND DRIVELINE MODELS

When modeling for control purposes not every detail has to be captured. It is sufficient if significant dynamics are captured and preferable if the model complexity can be kept low, (Ljung, 1999). In the case of the clutch the transmitted torque is an important quantity to model. However the importance of clutch torque control becomes clearer if it is put into the wider context of driveline control. For advanced driveline control a driveline model is useful, either for simulation during development or for model based control. The model should capture the dynamics in the driveline, such as shunt and shuffle, that affects the driver (and passenger) comfort.

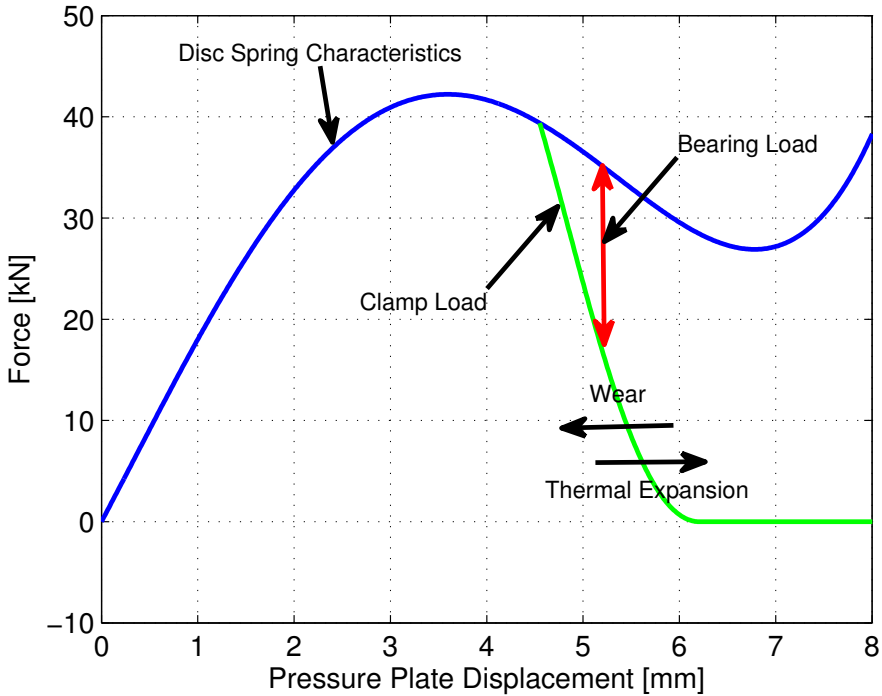


Figure 2.2: Illustration of how the two spring forces in the clutch and the throw-out bearing force interact. The clutch disc spring characteristics are the spring torque at the pivot point divided by the length of the lever between the pivot and the pressure plate. The throw-out bearing force is multiplied with the length of the lever between the bearing and the pivot and then divided with the length of the lever between the pivot and the pressure plate.

### 2.1.1 CLUTCH MODELS

In the literature a wide range of models have been proposed. The most simple models have a clutch torque that is assumed to be a controllable input, see for example Dolcini et al. (2008) or Garofalo et al. (2002). These models rely on the assumption that there is perfect knowledge of how the clutch behaves. More advanced models include submodels for slipping and sticking torques. For example a LuGre model is used in Dolcini et al. (2005) and a Karnopp model in Bataus et al. (2011). The former is a one-state model that captures stick-slip behavior, varying break-away force, Stribeck effect, and viscous friction. The latter includes a dead-zone around zero speed to ease the simulation of stick-slip behavior. The clutch torque during slipping is commonly modeled using a

function with the following structure,

$$M_{\text{trans},k} = \text{sgn}(\Delta\omega) n \mu R_e F_N \quad (2.1)$$

where  $\Delta\omega$  is the clutch slip (speed),  $n$  the number of friction surfaces,  $\mu$  the friction coefficient,  $R_e$  the effective radius and  $F_N$  the clamping (normal) force. In these models  $F_N$  is often either given as input or a static nonlinear function of clutch position,  $x$ , i.e.  $F_N = F_N(x)$ , see for example Vasca et al. (2011) or Glielmo and Vasca (2000). In particular Dolcini et al. (2010) mentions that a third-order polynomial is suitable to describe the connection between throwout-bearing position and clutch transmitted torque, mainly governed by the cushion spring characteristics. In Deur et al. (2012)  $\mu$  is fitted to the following regression curve:

$$\begin{aligned} \mu = & a_0 + a_1 (e^{-a_2\Delta\omega} - 1) T_b + (a_3 - a_4 \ln(\Delta\omega)) T_b^2 \\ & + (a_5 - a_6\Delta\omega) F_N + a_7 T_b F_N \end{aligned} \quad (2.2)$$

where  $T_b$  is the temperature of the clutch body and assumed to be an input signal.  $a_0 - a_7$  are curve parameters.  $F_N$  is mapped against actuator position and  $T_b$  in Deur et al. (2012). More advanced FEM models of the clutch are also found in the literature. To name some Nam et al. (2000) investigates the stresses in the diaphragm spring, Sfarni et al. (2008) has studied how the clutch disc characteristics change with wear and Cappetti et al. (2012b) examines the temperature effect on the cushion spring. Especially temperature distributions are popular to investigate using FEM. Both in clutch parts, Abdullah and Schlattmann (2012a) examines temperature distributions in clutch discs with different grooves and Lee et al. (2007) investigates the temperature distribution in the pressure plate, and in the clutch as a whole, (Abdullah and Schlattmann, 2012b) and (Sun et al., 2013). These FEM models point out interesting effects but are of little use here as the computational complexity is too high.

In Velardocchia et al. (2000) and Wikdahl and Ågren (1999) simpler temperature models are established. However these two models do not include the effect of the temperature on  $M_{\text{trans},k}$ . The models in Velardocchia et al. (2000) and Wikdahl and Ågren (1999) could be combined with the model presented in Deur et al. (2012), where the clutch temperature is an input, in order to give the clutch torque. Although that approach requires a map of the normal force as function of actuator position and temperature, whereas the approach in Paper A, (Myklebust and Eriksson, 2012b), is completely model based. Furthermore the clamping load and temperatures, which is not available in production vehicles, need to be measured during the parameter estimation procedure. In Paper A, (Myklebust and Eriksson, 2012b), only sensors available in production vehicles are used.

### 2.1.2 DRIVELINE MODELS

When modeling for control purposes it is common in the literature to include one or more flexibilities. In Pettersson (1997) active shuffle damping and clutch-less

gear-shift control is studied. There the model includes flexibilities in the clutch, propeller shaft and drive shafts. The clutch torsion springs are modeled both in a linear and a piece-wise linear fashion. Also Fredriksson and Egardt (2003) looks at clutch-less gear-shift control, but this time in a transmission without synchronizers. There only the drive shaft flexibility is modeled. Garofalo et al. (2002) and Dolcini et al. (2008) study optimal control of clutch engagement. For that the former models two flexibilities in the driveline, one before the transmission and one after. Whereas the latter models only the flexibility after the gearbox. A clutch-by-wire system is built in Moon et al. (2004), there a non-linear clutch and drive-shaft flexibilities are used. Clutch judder is examined in Crowther et al. (2004) using a driveline model with two flexibilities. A paper about AMT modeling in general, (Lucente et al., 2007), states that three flexibilities are useful, one in the engine, one before the transmission and one after.



---

## Experimental Observations and Model Structure

As seen in Chapter 2 there are different ways to model the clutch. In order to chose a suitable model structure an experimental platform and data is required. Here Scania Heavy Duty Trucks (HDTs) with standard production sensors are used. A variety of trucks have been used but the two most used are Ara and Ernfrid. Both are equipped with a 14-speed AMT and a 16.4 liter V8 capable of producing 3500 Nm. Ara weighs 105 tonnes and Ernfrid 21 tonnes. The clutch was described in Chapter 2. A list of the measurement signals used is found in Table 3.1 and their respective location in the driveline can be seen in Figure 3.1. Hence no exact torque measurement, is available. In order to get a measurement of the clutch torque the reported engine torque is used with added compensation for inertia effects of the engine and flywheel.

The main benefit of this setup, with only production sensors, is that the resulting model and observer is directly applicable on a production truck. Furthermore the procedure for experiments, model building, model validation, and

Table 3.1: A list over the different measurements used in the HDTs

Notation	Explanation
$\omega_e$	Engine speed
$\omega_t$	Transmission input-shaft speed
$\omega_p$	Transmission output-shaft speed
$\omega_w$	Tractive-wheel speed
$v$	Vehicle speed, actually speed of the free rolling (front) wheels
$T_{\text{coolant}}$	Engine coolant temperature
$T_{\text{amb}}$	Ambient temperature
$x_m$	Clutch actuator motor position
$x_p$	Clutch actuator piston position
$M_e$	Engine torque, reported from ECU

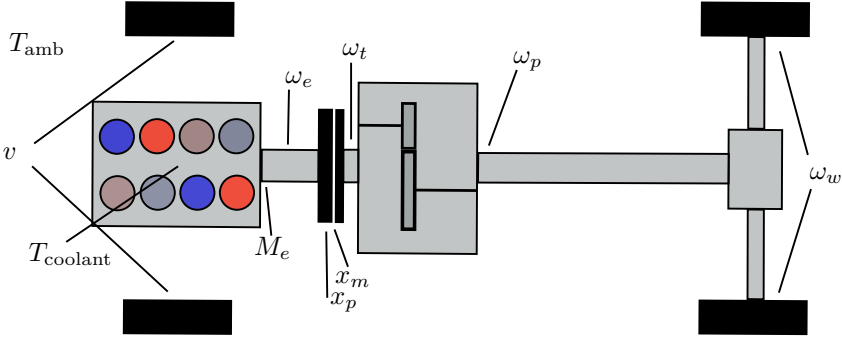


Figure 3.1: Sketch of a typical HDT driveline and where the sensors are placed. See Table 3.1 for an explanation of the notation.

observer evaluation can easily be performed on other vehicles equipped with a dry clutch. On the other hand, the drawback, compared to a test stand, e.g. Velardocchia et al. (1999); Moon et al. (2004) or Deur et al. (2012), is fewer and less precise sensors. All the cited test stands consist of a stand-alone dry clutch that is cooled towards the stagnated room-temperature air. In a truck there might be an airflow, the clutch is installed below the truck floor, bolted to the transmission, and especially the flywheel is bolted to a 1 tonne,  $\sim 90$  °C warm engine. Naturally all this leads to different temperature dynamics.

### 3.1 MOTIVATING EXPERIMENT

As a first investigation of the clutch characteristics the actuator position has been ramped back and forth several times while the clutch torque has been measured. Every second ramp pair the actuator has moved a shorter path. This is performed in order to study possible hysteresis effects. The results from such an experiment is presented in Figure 3.2. There the ramps are seen to follow a curve that can be fitted to a third order polynomial, (Dolcini et al., 2010; Myklebust and Eriksson, 2012b). However the polynomial is different for each ramp, there is clearly some dynamics present.

### 3.2 ACTUATOR DYNAMICS

The clutch actuator has a built in position controller, the benefit of this setup is that effects causing hysteresis in the actuator force, e.g. friction or the diaphragm spring, will not effect the actuator output/clutch torque relation, (Deur et al., 2012). Furthermore a position measurement of the piston effectively makes the piston position the output of the actuator. Since the actuator output is known the clutch torque can be modeled without knowing the actuator dynamics.

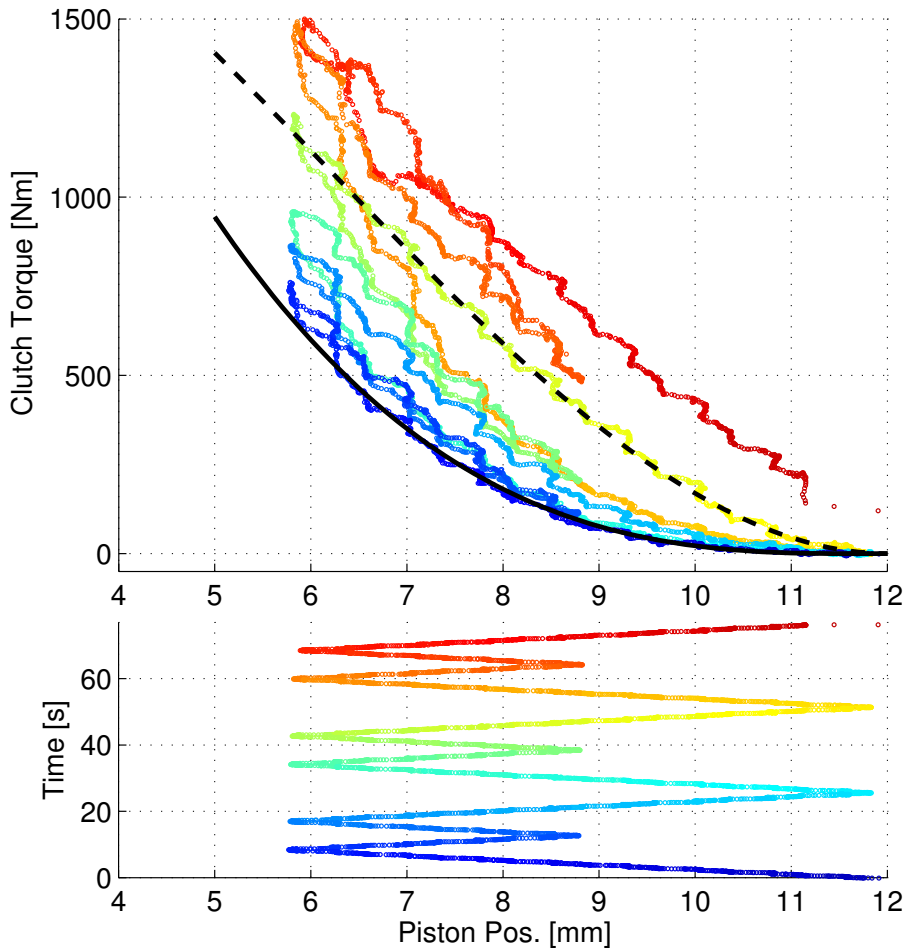


Figure 3.2: The clutch position,  $x$ , has been ramped back and forth while the clutch torque has been measured, top plot. The transmitted torque clearly depends on something more than the clutch position, in particular there is a drift with time. The time scale can be viewed by following the position into the lower plot. The time scale is also color coded, blue=0 s and red=75 s. The torque difference between the first and last ramp is up to 900 Nm. The two black lines are two possible parameterizations of a third order polynomial.

However for control applications the limitations of the actuator need to be considered. Conveniently the motor in the actuator is both accurate and fast, see Figure 3.3. The motor position can therefore be modeled as the requested position rate limited to 82 mm/s.

Some dynamics exists in the hydraulics of the actuator but the piston still

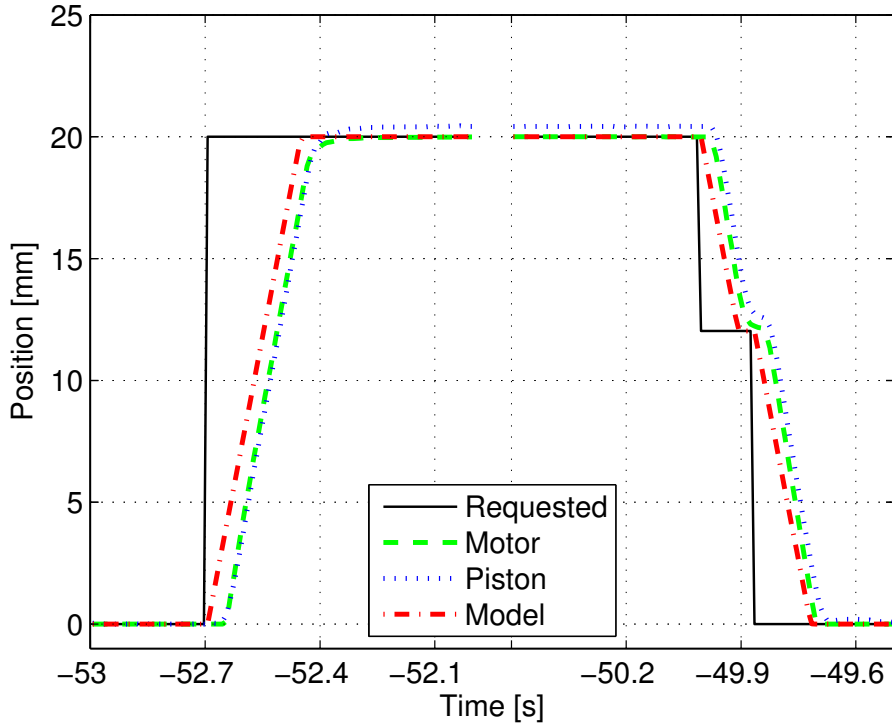


Figure 3.3: A step change in actuator (motor) position has been demanded. The corresponding response in both motor and piston position can be seen. The actuator is fast and can be modeled as a rate limiter of 82 mm/s.

moves at approximately the same rate as the motor, so control of the piston position have similar performance. During intense use of the clutch the hydraulic oil can be heated and thereby expand. This will cause a change in the relation between the motor and piston position. However since the piston position is measured and controlled this is of small concern. It should be noted that the clutch is located inside the bell housing (the housing surrounding the clutch) whereas the actuator is outside the bell housing. Therefore the temperature dynamics of the actuator has little to do with the temperature dynamics of the clutch discussed in Section 3.7.

### 3.3 CLUTCH VARIABLES

Several factors could be the reason for the dynamics seen in Figure 3.2. First lets recall (2.1) from the previous chapter.

$$M_{\text{trans},k} = \text{sgn}(\Delta\omega) n \mu R_e F_N \quad (2.1)$$

Looking at (2.1) one factor that directly affects the clutch torque is the clamp load. The clamp load is dependent on the actuator position but also on other factors, mainly the cushion spring characteristics. These characteristics are reported to have a decreasing slope with temperature in Cappetti et al. (2012a). However in Cappetti et al. (2012b) thermal expansion in the axial direction of the spring is shown to be a more significant effect. Sfarni et al. (2008) reports about steeper cushion spring characteristics with wear. From a graph in Hong et al. (2012) the normal force can be seen to be speed dependent. In Dolcini et al. (2010) that speed dependency is said to be due to centrifugal forces acting on the diaphragm spring. The works Mashadi and Crolla (2012); Moon et al. (2004) and Szimandl and Németh (2012) report of hysteresis in the diaphragm spring, that could lead to hysteresis in the normal force. A decrease in diaphragm spring force with temperature is reported in Sun et al. (2013). The decrease is especially pronounced for temperatures above 200 °C. In Mattiazzo et al. (2002) a temperature and wear dependency of the normal force/bearing position characteristics is shown. The wear is reported to affect the characteristics both through thinning of the disc, as in Figure 2.2, and through fatigue of the diaphragm spring. In Mattiazzo et al. (2002) the normal force decreases with temperature. In Deur et al. (2012); Cappetti et al. (2012b) and Hoic et al. (2013) the change in normal force/bearing position characteristics is explained by thermal expansion of clutch parts and the normal force is increasing with temperature. Although with an exception for low forces in Hoic et al. (2013). There the normal force is decreasing with temperature due to the expansion of a return spring, which is not present in the more common setup studied here.

However the normal force is not the only component of (2.1) that varies. It is generally recognized that  $\mu$  can depend on temperature, slip speed, and wear while  $R_e$  can depend on temperature and wear as well, (Velardocchia et al., 1999; Sun et al., 2013). Sun et al. (2013) has data showing an increase of  $\mu$  with temperature until 200 °C, after that  $\mu$  decreases. In Vasca et al. (2011) a slip speed dependency of  $\mu R_e$  is shown, this was especially pronounced for slip speeds below  $\sim 100$  RPM.  $R_e$  has been assumed constant in Deur et al. (2012) and there  $\mu$  decreases with temperature and increases with slip for a low to medium normal force but for a high normal force no clear trend is seen. The result is explained using (2.2).

It can be difficult to separate which parameter in (2.1) that is the reason for a change in  $M_{\text{trans},k}$ . Therefore the clutch torque is often studied as a lumped model. In Velardocchia et al. (1999)  $M_{\text{trans},k}$  is seen to decrease with temperature and  $\Delta\omega$ . However there are large variations with wear. In Ercole et al. (2000)  $M_{\text{trans},k}$  initially decreases with temperature for low temperatures and then

increases for medium and high temperatures. Similarly there are variations with wear and in addition temperature-torque hysteresis are reported.

A summary of the effects and dependencies above is to express (2.1) as,

$$M_{\text{trans},k} = \text{sgn}(\Delta\omega) n \mu(\Delta\omega, T, t) R_e(T, t) F_N(x, T, \omega_e, t) \quad (3.1)$$

where  $T$  is the temperature(s) and  $t$  represents wear (with time). Since production trucks are used as experimental platforms, the number of sensors is limited. This reduces the possibilities to separate the effects in (3.1). Therefore a lumped model has been studied here.

$$M_{\text{trans},k} = M_{\text{trans},k}(\Delta\omega, \omega_e, T, t, x) \quad (3.2)$$

However the more general model (3.1) gives some insight that can be used for setting up experiments and selecting the internal structure of the model (3.2). In order to investigate how the different dependencies of (3.2) affect the torque a number of experiments have been performed. The experiments have been designed to isolate different effects from each other and to step through the dependencies of (3.2).

### 3.4 WEAR

Investigations of wear requires a lot of time consuming measurements. Luckily wear is usually a slow process that is not noticeable in single experiments. Therefore wear is omitted from the model structure,

$$M_{\text{trans},k} = M_{\text{trans},k}(\Delta\omega, \omega_e, T, x) \quad (3.3)$$

However in a production application wear have to be dealt with through e.g. adaption. The only wear effect that has been observed throughout this thesis is thinning of the clutch disc. A method for adapting the disc thickness is proposed in Paper C, (Myklebust and Eriksson, 2013b).

### 3.5 SLIP

In order to investigate the slip speed,  $\Delta\omega$ , dependency experiments have been carried out as follows. A truck has been driven to an uphill and has been kept stationary by slipping the clutch at a constant position. This way the vehicle will accelerate forwards if more torque is transmitted and backwards if less torque is transmitted. Furthermore it is easy to, at least initially, keep the input shaft speed stationary this way, and by doing so the engine speed can be used to control the slip speed. The change in slip speed will of course have a corresponding change in dissipated power and hence the temperature rate. In order to isolate the slip dependency from temperature dynamics a fast change in slip speed is desirable. Therefore slip-speed steps are made and an abrupt

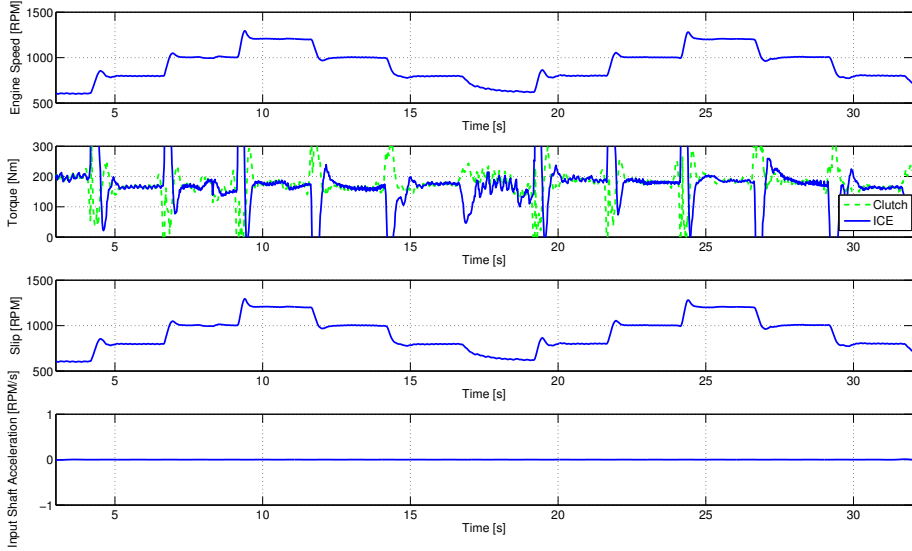


Figure 3.4: Slip steps are made through engine-speed control when the truck is held stationary in a slight uphill using a constant clutch position. No reaction is seen in neither clutch torque or input shaft acceleration.

change in torque/input shaft acceleration should be seen if there is a slip-speed dependency, see Figure 3.4. Note that the engine torque has a transient during the edges of a step, due to the acceleration of the engine. A smaller transient is present in the clutch torque signal due to imperfections in the compensation for the acceleration. No significant change is seen in the input shaft acceleration and no correlation between steady-state clutch torque and slip speed is seen neither, Figure 3.5. Based on this experiment (3.3) can be reduced to,

$$M_{\text{trans},k} = M_{\text{trans},k}(\omega_e, T, x) \quad (3.4)$$

This is somewhat in contrast to the data in Velardocchia et al. (1999) where a slip dependency is shown. The slip has only been investigated at relatively large speeds and does therefore not contrast the data in Vasca et al. (2011) where the slip dependency only is present below 100 RPM.

### 3.6 ROTATIONAL SPEED

Centrifugal effects in the diaphragm spring can be studied with the same experiment as in Section 3.5 since the engine speed (and thereby diaphragm spring speed) is varied whereas the other parameters of (3.4) are kept constant. Hence no effects are seen in the torque in Figure 3.4 no speed dependency is

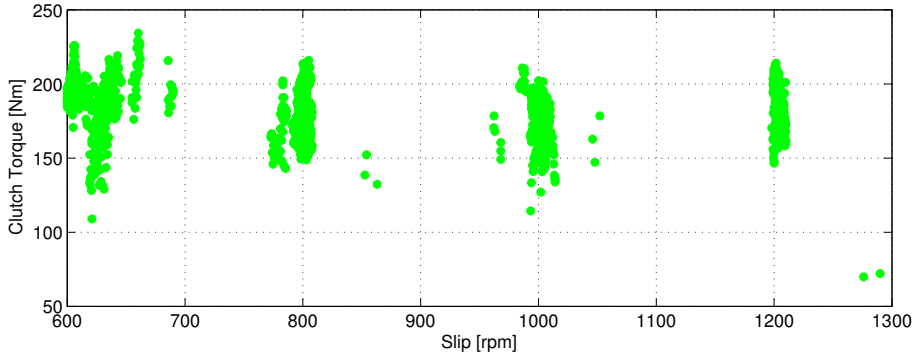


Figure 3.5: The data points from Figure 3.4 when the engine speed is constant. No correlation is seen between clutch torque and slip speed.

present either. The model can be further simplified into:

$$M_{\text{trans},k} = M_{\text{trans},k}(T, x) \quad (3.5)$$

There is a risk that an effect of  $\omega_e$  is present but canceled by an effect of  $\Delta\omega$ . In order to fully investigate this the experiment of Section 3.5 would need to be repeated with different input-shaft speeds, which would give a different combination of slip speed and engine speed. This kind of experiments have however not been performed due to practical difficulties with controlling the input-shaft speed to a constant non-zero value.

### 3.7 TEMPERATURE

A variation of the experiment of Section 3.5 can be used to isolate the thermal effect. The truck is placed in an uphill and the clutch is controlled to a point where it can keep the truck stationary. Movement of the truck is not desirable as it can make the clutch lock up (and the slip to vary). The power dissipated will heat the clutch and if that affects the transmitted torque the truck will start to move unless the clutch position is controlled to keep a constant torque. Therefore the clutch torque is put under feedback and the clutch position is measured. In Figure 3.6 it is seen to increase as more energy is dissipated into the clutch. There are clearly some temperature dynamics present.

When performing experiments for identifying the thermal dynamics the cool down process is also of interest. However a position that transmits a slipping torque can not be measured if the clutch is to cool off. One possibility then is to investigate how the contact point (kiss point), where pressure plate and clutch disc first meet, changes with cooling. This feels intuitive as the kiss point is an important parameter in clutch control. However, due to inexactness in the torque measurement and the cushion characteristics of the clutch transmissibility curve

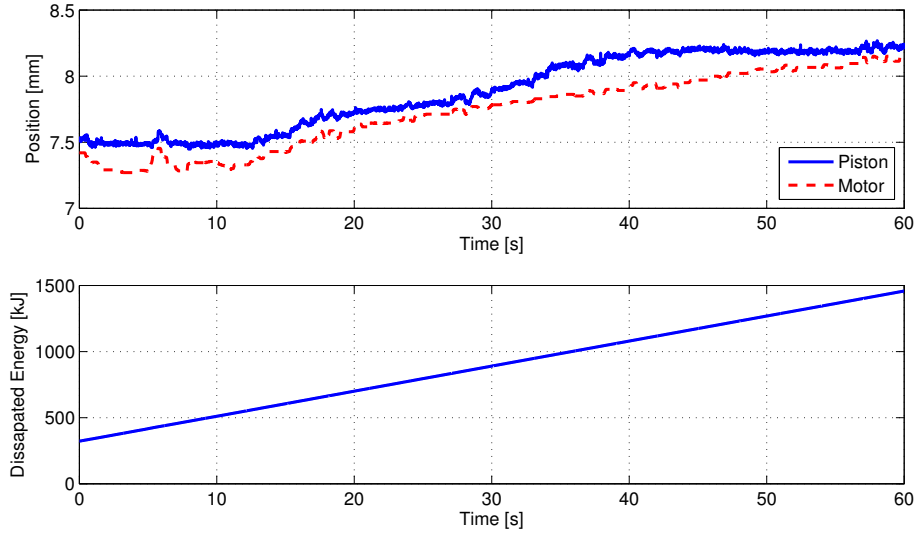


Figure 3.6: Slip and torque through the clutch has been held constant. To keep them constant the clutch position has to be varied. The motor position and piston position vary differently. The position increases with dissipated energy.

around zero torque, the exact position of the kiss point is hard to detect. One way to ease detection is to engage the clutch when neutral gear is engaged. This way the input shaft speed will respond to the transmitted torque quickly. This type of experiments have shown the kiss point to jump around, see Figure 3.7. This is thought to be because the clutch disc can slide axially along the transmission input shaft and stop in an arbitrary position in the gap between pressure plate and flywheel. The friction along the shaft can provide a sufficient clamp load to transfer enough torque to spin the input shaft when in neutral gear, but not enough to transmit any significant torque for the truck dynamics. Therefore the exact value of the kiss point is not of great concern, the point where clutch torque gets significant is of greater concern.

An alternative measure is the position where the clutch is fully closed, here called the zero position. This point is easy to determine, when the actuator motor is fully backed out (motor position zero, hence the name zero position) the clutch will, due to the diaphragm spring, be fully closed. If the clutch is closed when neutral gear is engaged no significant energy is dissipated into the clutch. The zero position does therefore give a more stable measurement, see Figure 3.7. The zero position increases when heat is dissipated into the clutch and it decreases exponentially when no heat is dissipated. A hypothesis is that thermal expansion of the clutch is the reason for the change in zero position. Therefore a rough estimate has been made of the thermal expansion.

The clutch mass is estimated as the flywheel and pressure plate,  $m_c =$

$m_{fw} + m_{pp} = 47 + 34 = 81$  kg. They are made out of cast iron and according to Nording and Österman (1999) the expansion coefficient is  $e_{ci} = 11 \cdot 10^{-6}$  1/K and the specific heat capacity  $c_p = 500$  J/(kg K). If 4 MJ of energy is dissipated into the clutch through slipping, as in Figure 3.7, the clutch will heat up with approximately 98 K and expand by 0.11 %. The clutch is about 100 mm deep, which means it will expand by 0.11 mm. At the actuator this is seen as 0.96 mm (ratio of 8.8 measured in drawings). When comparing this number with the change in the zero position seen in Figure 3.7, the numbers are in the same order of magnitude. During the warm up the zero position increases with  $\sim 1.2$  mm and during cool down it decreases  $\sim 0.8$  mm asymptotically. This gives further support for the hypothesis that this effect is due to the thermal expansion of the clutch.

In order to observe the zero position not only when the clutch is cooling but also when the clutch is heated the following procedure has been used. The clutch has been slipped for a short time while the truck has been in gear and kept stationary by the parking brake. After the slipping phase the clutch has been closed in neutral gear so that the zero position can be measured. The slipping phase and measurement phase is alternated like this for an extended period of time. The result of such an experiment can be seen in Figure 3.8. A simple temperature model can be fitted to this data, see Paper A, (Myklebust and Eriksson, 2012b), or Paper C, (Myklebust and Eriksson, 2013b), for details.

However if the dynamics seen in Figure 3.8 is compared to those seen in Figure 3.6 two things can be noticed. First the change in position is much greater in Figure 3.6. Second the time constant in Figure 3.6 is much smaller. This smaller time constant could correspond to a smaller thermal mass, e.g. the clutch disc. The thermal behavior of the cushion spring inside the clutch disc is investigated in Cappetti et al. (2012b) and could explain the faster dynamics seen here. A second expansion term with faster dynamics is useful in order to explain the clutch thermal dynamics, again see Paper A, (Myklebust and Eriksson, 2012b), or Paper C, (Myklebust and Eriksson, 2013b), for details.

The temperature dynamics can consist of several temperature but in common

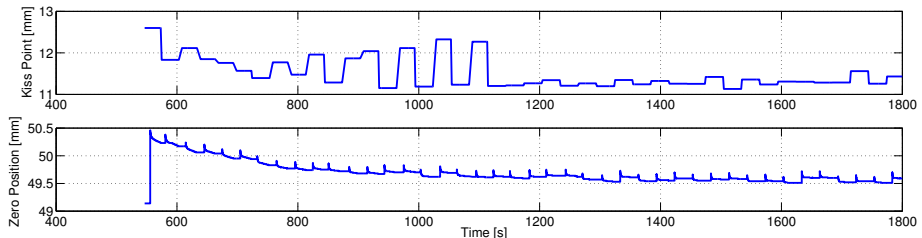


Figure 3.7: About 4 MJ of energy has been dissipated in the clutch. Afterwards the truck has been standing still with neutral gear engaged while the kiss point and zero position has been monitored.

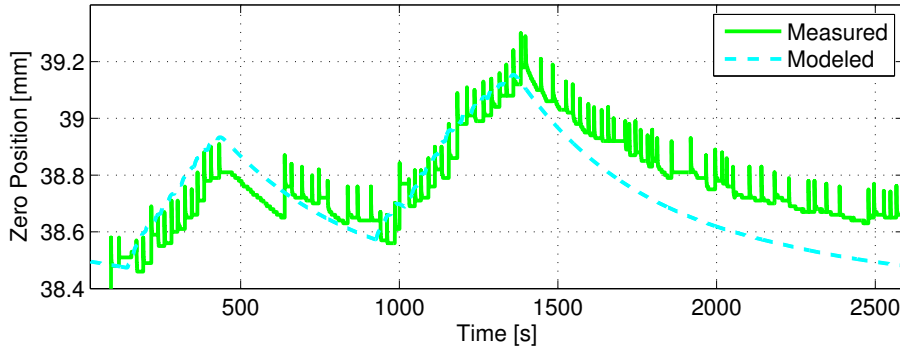


Figure 3.8: The clutch has been heated through slipping and then left to cool down. The zero position has been recorded as a measure of the expansion. A simple temperature model can explain the behavior.

for all temperatures will be that energy is gained through the power dissipated in the clutch,

$$P = M_{\text{trans},k} \Delta\omega \quad (3.6)$$

and energy is dissipated to the ambient air and the ICE, but not so much the transmission, (Wikdahl and Ågren, 1999). Since the truck is moving and the clutch is spinning there will be forced convection. Therefore also the vehicle and clutch speed are possible variables.

$$\dot{T} = f(T, P, T_{\text{ICE}}, T_{\text{amb}}, \omega_e, v) \quad (3.7)$$

where  $T$  is a temperature vector,  $T_{\text{ICE}}$  is the coolant temperature of the ICE,  $T_{\text{amb}}$  is the ambient temperature and the engine speed is used as clutch speed.

### 3.7.1 VEHICLE SPEED DEPENDENCY

The speed of the truck directly affects the speed by which air is flowing past the bell housing. This forced convection will naturally increase the cooling of the clutch. In most experiments performed here the truck has been held stationary in order to keep the clutch from locking up. Although this should be of smaller concern when using the observer of Paper C, (Myklebust and Eriksson, 2013b), since the bell housing temperature only affects the clutch torque indirectly through the ambient conditions of the flywheel and pressure plate. Equation (3.7) can be reduced to,

$$\dot{T} = f(T, P, T_{\text{ICE}}, T_{\text{amb}}, \omega_e) \quad (3.8)$$

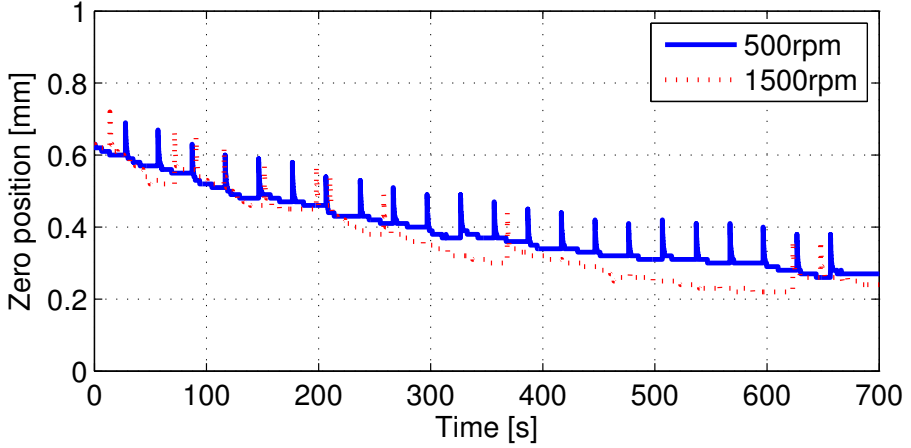


Figure 3.9: Zero position measurements when the clutch is cooling. In one case the engine speed has been 500 RPM and the coolant temperature has been 77 °C. In the other case the engine speed has been 1500 RPM and the coolant temperature has been 82 °C. The two trajectories are similar. The zero position has been adjusted with an offset to compensate for different wear levels in the two experiments.

### 3.7.2 ENGINE SPEED DEPENDENCY

If the clutch is spinning at a higher speed there should be more forced convection and the clutch body should cool faster towards clutch housing temperatures. Therefore experiments have been carried out where the zero position has been measured during cooling of the clutch with two different engine speeds, and hence two different clutch body speeds. Looking at the data in Figure 3.9 there is no significant difference in the curve shapes indicating that the clutch speed has no significant effect on the clutch temperature. Therefore (3.7) can be further reduced to,

$$\dot{T} = f(T, P, T_{ICE}, T_{amb}) \quad (3.9)$$

Using the observer from Paper C, (Myklebust and Eriksson, 2013b), it can be verified that both measurements start at the same temperature level. For the 500 RPM case and the 1500 RPM case the clutch body temperature is 109 °C and 107 °C, respectively and the clutch housing temperature is 83 °C and 85 °C, respectively. The engine coolant temperature was measured to 77 °C and 82 °C respectively.

### 3.8 MODEL SUMMARY AND USAGE IN PAPERS

In this and the previous chapter a literature survey of dry-clutch models and experiments is summarized into the model structure (3.2). Thereafter a set of experiments are designed to investigate which variables in (3.2) that are significant. In all experiments the platform has been a production truck driven on roads. Therefore this set of experiments can easily be adapted to new platforms. After performing the experiments the model structure is:

$$\begin{aligned}\dot{T} &= f(T, P, T_{\text{ICE}}, T_{\text{amb}}) \\ M_{\text{trans},k} &= M_{\text{trans},k}(T, x)\end{aligned}\tag{3.10}$$

This model structure is developed and parameterized in Paper A, (Myklebust and Eriksson, 2012b). The model that results from Paper A, (Myklebust and Eriksson, 2012b), is the foundation for Paper B, (Myklebust and Eriksson, 2013a), and Paper C, (Myklebust and Eriksson, 2013b). In Paper B, (Myklebust and Eriksson, 2013a), simulations of the clutch model and the driveline model from Paper D, (Myklebust and Eriksson, 2012a), are used to demonstrate the importance of considering the thermal dynamics in clutch control applications. One way to do that is to build an observer using the model. This is done in Paper C, (Myklebust and Eriksson, 2013b), where a clutch torque and temperature observer is designed.

## REFERENCES

- Oday I. Abdullah and Josef Schlattmann. Finite element analysis for grooved dry friction clutch. *Advances in Mechanical Engineering and its Applications*, 2(1):2167–6380, 2012a.
- O.I. Abdullah and J. Schlattmann. Finite element analysis of temperature field in automotive dry friction clutch. *Tribology in Industry*, 34(4):206–216, 2012b.
- Marius Bataus, Andrei Maciac, Mircea Oprean, and Nicolae Vasiliu. Automotive clutch models for real time simulation. *Proceedings of the Romanian Academy, Series A*, 12(2):109–116, 2011.
- Nicola Cappetti, Mario Pisaturo, and Adolfo Senatore. Modelling the cushion spring characteristic to enhance the automated dry-clutch performance: The temperature effect. *Proc IMechE, Part D: Journal of Automobile Engineering*, 226(11):1472–1482, 2012a.
- Nicola Cappetti, Mario Pisaturo, and Adolfo Senatore. Cushion spring sensitivity to the temperature rise in automotive dry clutch and effects on the frictional torque characteristic. *Mechanical Testing and Diagnosis*, 3(2):28–38, 2012b.
- A Crowther, N Zhang, D K Liu, and J K Jeyakumaran. Analysis and simulation of clutch engagement judder and stick-slip in automotive powertrain systems. *Proc IMechE, Part D: Journal of Automobile Engineering*, 218(12):1427–1446, December 2004.
- Josko Deur, Vladmir Ivanovic, Zvonko Herold, and Milan Kostelac. Dry clutch control based on electromechanical actuator position feedback loop. *International Journal of Vehicle Design*, 60(3-4):305–326, 2012.
- Pietro Dolcini, Carlos Canudas de Wit, and Hubert Béchart. Improved optimal control of dry clutch engagement. *Proceedings of the 16th IFAC World Congress*, 16(1), 2005.
- Pietro Dolcini, Carlos Canudas de Wit, and Hubert Béchart. Lurch avoidance strategy and its implementation in AMT vehicles. *Mechatronics*, 18(1):289–300, May 2008.
- Pietro J. Dolcini, Carlos Canudas de Wit, and Hubert Béchart. *Dry Clutch Control for Automotive Applications*. Advances in Industrial Control. Springer-Verlag London, 2010.
- G. Ercole, G. Mattiazzo, S. Mauro, M. Velardocchia, F. Amisano, and G. Serra. Experimental methodologies to determine diaphragm spring clutch characteristics. In *SAE Technical Paper: 2000-01-1151*, March 2000.

- Lars Eriksson and Lars Nielsen. *Modeling and Control of Engines and Drivelines*. John Wiley & Sons, 2014.
- Jonas Fredriksson and Bo Egardt. Active engine control for gear shifting in automated manual transmissions. *International Journal of Vehicle Design*, 32(3-4):216–230, 2003.
- Franco Garofalo, Luigi Glielmo, Luigi Iannelli, and Francesco Vasca. Optimal tracking for automotive dry clutch engagement. In *2002 IFAC, 15th Triennial World Congress*, 2002.
- Luigi Glielmo and Francesco Vasca. Optimal control of dry clutch engagement. In *SAE Technical Paper: 2000-01-0837*, March 2000.
- Matija Hoic, Zvonko Herold, Nenad Kranjcevic, Josko Deur, and Vladimir Ivanovic. Experimental characterization and modeling of dry dual clutch thermal expansion effects. In *SAE Technical Paper: 2013-01-0818*, April 2013.
- Sungwha Hong, Sunghyun Ahn, Beakyou Kim, Heera Lee, and Hyunsoo Kim. Shift control of a 2-speed dual clutch transmission for electric vehicle. In *2012 IEEE Vehicle Power and Propulsion Conference*, October 2012.
- Choon Yeol Lee, Ilsup Chung, and Young Suck Chai. Finite element analysis of an automobile clutch system. *Key Engineering Materials*, 353-358(1):2707–2711, September 2007.
- Lennart Ljung. *System Identification Theory for the user*. Prentice Hall Information and System Sciences Series. Prentice-Hall, Inc, 2nd edition, 1999.
- Gianluca Lucente, Marcello Montanari, and Carlo Rossi. Modelling of an automated manual transmission system. *Mechatronics*, 17(1):73–91, November 2007.
- Behrooz Mashadi and David Crolla. *Vehicle Powertrain Systems*. John Wiley & Sons Ltd, first edition, 2012.
- G. Mattiazzo, S. Mauro, M. Velardocchia, F. Amisano, G. Serra, and G. Ercole. Measurement of torque transmissibility in diaphragm spring clutch. In *SAE Technical Paper: 2002-01-0934*, March 2002.
- S.E. Moon, M.S. Kim, H. Yeo, H.S Kim, and S.H Hwang. Design and implementation of clutch-by-wire system for automated manual transmissions. *International Journal Vehicle Design*, 36(1):83–100, 2004.
- Andreas Myklebust and Lars Eriksson. Road slope analysis and filtering for driveline shuffle simulation. In *2012 IFAC Workshop on Engine and Powertrain Control, Simulation and Modeling*, October 2012a.

Andreas Myklebust and Lars Eriksson. Torque model with fast and slow temperature dynamics of a slipping dry clutch. In *2012 IEEE Vehicle Power and Propulsion Conference*, October 2012b.

Andreas Myklebust and Lars Eriksson. The effect of thermal expansion in a dry clutch on launch control. In *7th IFAC Symposium on Advances in Automotive Control*, September 2013a.

Andreas Myklebust and Lars Eriksson. Modeling, observability and estimation of thermal effects and aging on transmitted torque in a heavy duty truck with a dry clutch. *Submitted to IEEE/ASME Transactions on Mechatronics*, (?): ?–?, 2013b.

Wook-Hee Nam, Choon-Yeol Lee, Young S. Chai, and Jae-Do Kwon. Finite element analysis and optimal design of automobile clutch diaphragm spring. In *Seoul 2000 FISITA World Automotive Congress*, June 2000.

K Newton, W Steeds, and T K Garrett. *The Motor Vehicle*. Butterworth-Heinemann, 1996.

Carl Nording and Jonny Österman. *Physics Handbook*. Studentlitteratur, 1999.

M J Nunney. *Automotive Technology*. Butterworth-Heinemann, third edition, 1998.

Magnus Pettersson. *Driveline Modeling and Control*. PhD thesis, Linköpings Universitet, May 1997.

Samir Sfarni, Emmanuel Bellenger, Jérôme Fortin, and Matthieu Malley. Numerical modeling of automotive riveted clutch disc for contact pressure verification. In *49th Scandinavian Conference on Simulation and Modeling*, October 2008.

Shaohua Sun, Yulong Lei, Yao Fu, Cheng Yang, and ShunBo Li. Analysis of thermal load for dry clutch under the frequent launching condition. In *SAE Technical Paper: 2013-01-0814*, April 2013.

Barna Szimandl and Huba Németh. Dynamic hybrid model of an electro-pneumatic clutch system. *Mechatronics*, 23(1):21–36, 2012.

Francesco Vasca, Luigi Iannelli, Adolfo Senatore, and Gabriella Reale. Torque transmissibility assessment for automotive dry-clutch engagement. *IEEE/ASME transactions on Mechatronics*, 16(3):564–573, June 2011.

M. Velardocchia, G. Ercole, G. Mattiazzo, S. Mauro, and F. Amisano. Diaphragm spring clutch dynamic characteristic test bench. In *SAE Technical Paper: 1999-01-0737*, March 1999.

M. Velardocchia, F. Amisano, and R. Flora. A linear thermal model for an automotive clutch. In *SAE Technical Paper: 2000-01-0834*, March 2000.

Anna Wikdahl and Åsa Ågren. Temperature distribution in a clutch. Master's thesis, Linköping University, 1999.



# Publications



Torque Model with Fast and Slow Temperature  
Dynamics of a Slipping Dry Clutch\*

A

---

\*Published in *The 8th IEEE Vehicle Power and Propulsion Conference*.



---

# Torque Model with Fast and Slow Temperature Dynamics of a Slipping Dry Clutch

Andreas Myklebust and Lars Eriksson

*Vehicular Systems, Department of Electrical Engineering,  
Linköping University, SE-581 83 Linköping, Sweden*

## ABSTRACT

---

The transmitted torque in a slipping dry clutch is studied in experiments with a heavy duty truck. It is shown that the torque characteristic has little or no dependence on slip speed, but that there are two dynamic effects that make the torque vary up to 900 Nm for the same clutch actuator position. Material expansion with temperature can explain both phenomena and a dynamic clutch temperature model with two different time constants is developed. The dynamic model is validated in experiments, with an error of only 3 % of the maximum engine torque, and is shown to improve the behavior significantly compared to a static model.

---

## 1 INTRODUCTION

Increasing demands on comfort, performance, and fuel efficiency in vehicles lead to more complex transmission solutions. Historically high efficiency was best met with a classical Manual Transmission and comfort with a classical Automatic Transmission. The Automated Manual Transmission (AMT) is one way to combine the best from two worlds. An important part in an AMT is clutch control that has a profound effect on vehicle performance. Therefore it is of importance to know the torque transmitted in the clutch with high precision. Models have come to play an important role in estimation and control of the transmitted torque, since torque sensors are expensive.

A sketch of a dry single-plate clutch is found in Fig. 1, while in-depth explanations are found in for example Mashadi and Crolla (2012) and Vasca et al. (2011). In clutch-modeling literature a wide range of models are proposed. The most simple models have a clutch torque that is assumed to be a controllable input, see for example Dolcini et al. (2008); Garofalo et al. (2002). These models rely on the assumption that there is perfect knowledge of how the clutch behaves. More advanced models include submodels for slipping and sticking torques. For example a LuGre model is used in Dolcini et al. (2005) and a Karnopp model in Bataus et al. (2011). The former is a one-state model that captures stick-slip behavior, varying break-away force, Stribeck effect, and viscous friction. The latter simply applies a dead-zone around zero speed to ease the simulation of stick-slip behavior.

Models for the clutch torque during slipping commonly use a function with the following structure,

$$M_c = \text{sgn}(\Delta\omega) \mu R_e F_N \quad (1)$$

where  $\Delta\omega$  is the clutch slip (speed),  $\mu$  the friction coefficient,  $R_e$  the effective radius and  $F_N$  the clamping (normal) force. In these models  $F_N$  is often either given as input or a static nonlinear function of clutch position,  $x$ , i.e.  $F_N = F_N(x)$ , see for example Vasca et al. (2011); Glielmo and Vasca (2000). In particular Dolcini et al. (2010) mentions that a third-order polynomial is suitable to describe the connection between throwout-bearing position and clutch transmitted torque, mainly governed by the flat (cushion) spring characteristics. Furthermore a slight speed dependency of the normal force is hinted in Dolcini et al. (2010), centrifugal forces acting on the springs in the clutch. Mashadi and Crolla (2012) reports of hysteresis in the diaphragm spring, that could lead to hysteresis in the normal force. In Mattiazzo et al. (2002) a temperature and wear dependency of the normal force/bearing position characteristics is shown.

Concerning the other model components it is generally recognized that  $\mu$  can depend on temperature, slip speed, and wear and that  $R_e$  can depend on temperature and wear as well, see Velardocchia et al. (1999). In Vasca et al. (2011) a slip speed dependency of  $\mu R_e$  is shown, this was especially pronounced for slip speeds below  $\sim 100$  RPM.

It can be difficult to separate which parameter in (1) that is the reason for a change in  $M_c$ . Therefore the clutch torque is often studied as a lumped model. In Velardocchia et al. (1999)  $M_c$  is seen to decrease with temperature and  $\Delta\omega$ . However there are large variations with wear. In Ercole et al. (2000)  $M_c$  initially decreases with temperature for low temperatures and then increases for medium and high temperatures. Similarly there are variations with wear and in addition temperature-torque hysteresis are reported. In Velardocchia et al. (2000) and Wikdahl and Ågren (1999) temperature models are established, but no work seems to include the temperature effect on  $M_c$ . In view of this the main contribution in this paper is the analysis and model of a clutch that includes temperature dynamics and the corresponding effects on the transmitted torque.

The clutch model presented here is built solely from the observation made on the data presented in this paper. No slip dependency is seen and the torque is increasing with temperature. A limitation of the problem statement is that the clutch is only studied when it is slipping.

## 2 EXPERIMENTAL SETUP

The AMT clutch in a Heavy Duty Truck (HDT) is studied. The clutch, that is in focus here, is a dry single-plate pull-type normally closed clutch. A schematic is seen in Fig. 1. The clutch is actuated by an electric motor that through a worm gear moves a hydraulic master cylinder that in turn moves a slave piston and via a lever pulls the throwout bearing. Both motor position,  $x_m$ , and slave position,  $x$ , are measured.

The truck used here is only equipped with production sensors, engine speed, idle shaft speed and slave position. Hence no exact torque measurement, is available. In order to get a measurement of the clutch torque the reported engine torque has been compensated for inertia effects of the engine and flywheel. The limited amount of sensors add to the difficulty in making a clutch model and validating it.

## 3 MODELING OUTLINE

As mentioned in Section 1,  $M_c$  depends on several factors such as, actuator position, temperatures, rotational speeds and wear. In Fig. 2 it is seen how the transmitted torque varies with up to 900 Nm for a given position. Furthermore components are non-linear e.g. spring characteristics, hysteresis, etc. However during experiments no clear hysteresis have been detected and therefore not modeled. Due to the difficulties involved in measuring wear, especially when access to test equipment is limited and non-exclusive, wear has been assumed slow enough to not have a significant effect in the experiments. The only exception is the parameter  $x_{0,\text{ref}}$  of Section 5, which is directly affected by the thickness of the friction pads.  $x_{0,\text{ref}}$  had to be parameterized to each measurement session

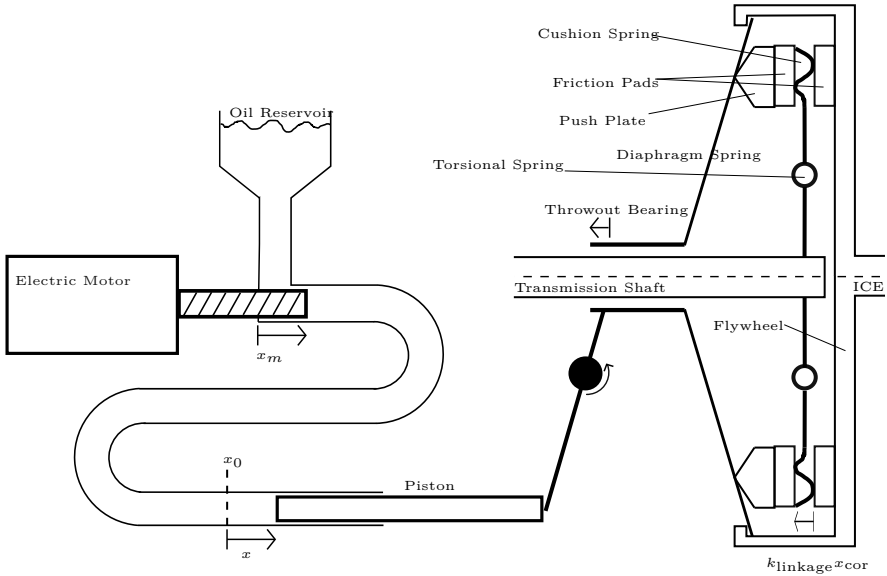


Figure 1: A schematic over the actuator and the dry single-plate pull-type clutch studied here.  $k_{\text{linkage}}$  is the combined ratio of all levers between the piston and the push plate.

(months apart). In an on-line application of the model, such as an observer or controller, more parameters would probably need to be adapted continuously.

In the collected measurement  $\Delta\omega > 0$  has always hold, hence the  $\text{sgn}$ -function from (1) has not been considered. And since the clutch is only considered during slipping no advanced friction model, e.g. LuGre, is needed as they tend to be focused around lock up. All these simplifications leave the model structure at

$$M_c = \mu(\Delta\omega, T) R_e(T) F_N(x, T, \Delta\omega) \quad (2)$$

In Section 5 the temperature effect will be explained by a changing  $F_N$ , at least for medium temperatures of the clutch. Nevertheless with the available sensors there is no way to truly separate the effects between the parameters. Therefore the model structure will be,

$$M_c = M_c(x, T, \Delta\omega) \quad (3)$$

In the next section the slip dependency will be investigated and in the subsequent section the position and temperature dependency will be handled.

## 4 SLIP DEPENDENCY

Slip speed,  $\Delta\omega$ , dependency is recognized in the literature, (Vasca et al., 2011), (Velardocchia et al., 1999). Therefore experiments have been carried out to

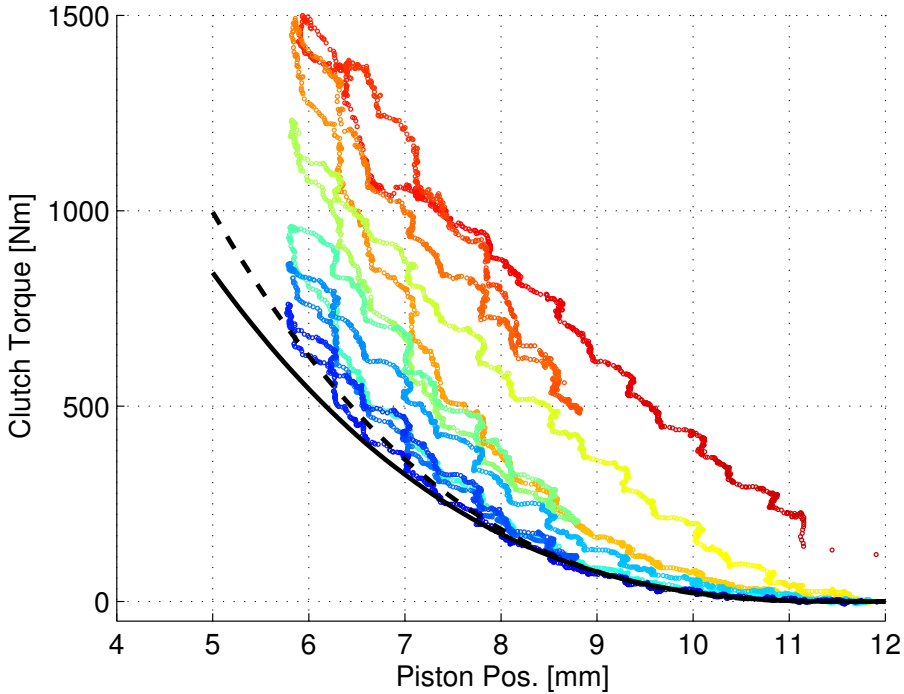


Figure 2: The clutch position has been ramped back and forth while the clutch torque has been measured. The transmitted torque clearly depends on something more than the clutch position, in particular there is a drift with time (the color changes with time, blue=0 s and red=75 s). The torque difference between the first and last ramp is up to 900 Nm. The black lines are two parameterizations of (5).

investigate this. Remember that since this work is limited to when the clutch is slipping, slip speeds have been relatively large. There has been no investigation of what happens when the clutch approaches lock up.

The experiments have been carried out as follows. The truck has been driven to an uphill and has been kept stationary by slipping the clutch at a constant position. This way the vehicle will accelerate forwards if more torque is transmitted and backwards if less torque is transmitted. Furthermore it is easy to initially keep the input shaft speed stationary this way, and by doing so the engine speed can be used to control the slip speed. Slip-speed steps are made and an abrupt change in torque/input shaft acceleration should be seen if there is a slip-speed dependency, Fig. 3. Note that the engine torque will see a transient during the flank of a step due to the acceleration of the engine. A smaller transient is present in the clutch torque signal due to imperfections in the compensation for the acceleration. No significant change is seen in the input

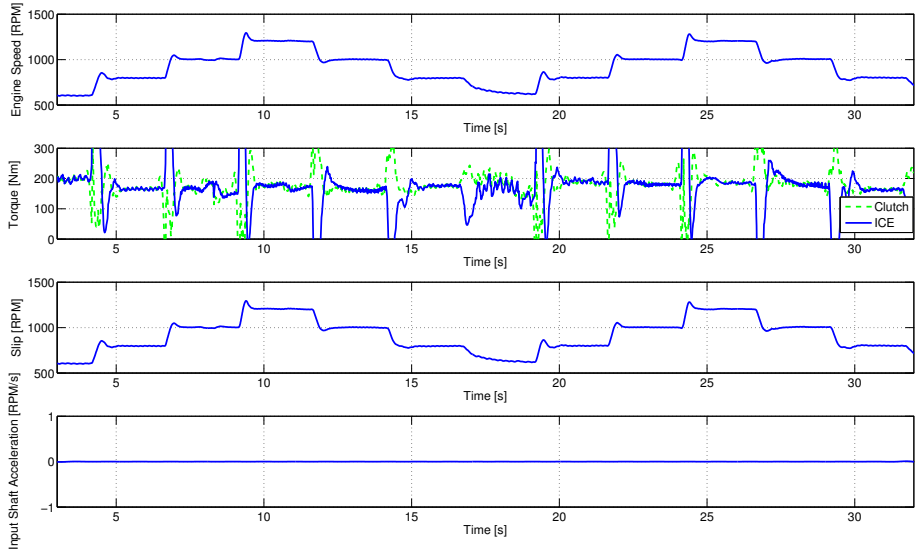


Figure 3: Slip steps are made through engine-speed control when the truck is held stationary in a slight uphill using a constant clutch position. No reaction is seen in neither clutch torque or input shaft acceleration.

shaft acceleration and no correlation between steady-state clutch torque and slip speed is seen neither, Fig 4. Therefore it is assumed that there is no slip dependency at the slip speeds of interest in this paper. Equation (3) can be reduced to

$$M_c = M_c(x, T) \quad (4)$$

This is somewhat in contrast to the data in Velardocchia et al. (1999) where a slip dependency is shown. The slip has only been investigated at relatively large speeds and does therefore not contrast the data in Vasca et al. (2011).

## 5 TEMPERATURE EFFECTS AND MODELS

The shape of the torque transmissibility curve is mainly due to the cushion spring characteristics. Dolcini et al. (2010) mentions that this curve can be described by a third order polynomial,

$$M_{\text{ref}}(x_{\text{ref}}) = \begin{cases} a(x_{\text{ref}} - x_{\text{ref,ISP}})^3 + \\ + b(x_{\text{ref}} - x_{\text{ref,ISP}})^2 & \text{if } x_{\text{ref}} < x_{\text{ref,ISP}} \\ 0 & \text{if } x_{\text{ref}} \geq x_{\text{ref,ISP}} \end{cases} \quad (5)$$

where  $x_{\text{ISP}}$  (Incipient Sliding Point) is the kiss point, where the push plate and clutch disc first meet and torque can start to transfer. There is no first or

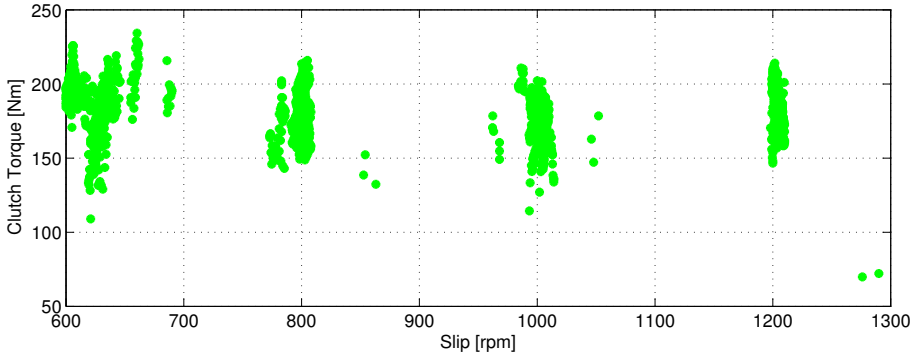


Figure 4: The data points from Fig. 3 when the engine speed is constant. No correlation is seen between clutch torque and slip speed.

zeroth order term in the equation since it is desired to have zero torque and derivative at  $x_{\text{ref,ISP}}$ . The exact value of  $x_{\text{ISP}}$  can be difficult to find since the transmissibility curve is very flat around  $x_{\text{ISP}}$ . However it is only important to find a  $x_{\text{ISP}}$  that gives a good curve fit, as errors will be small near  $x_{\text{ISP}}$ . A suggestion in Mattiazzo et al. (2002) is to define  $x_{\text{ISP}}$  as the point that transmits a certain small torque. That method should give sufficient estimates of  $x_{\text{ISP}}$  for the application described here.

Experimental data confirms (5) to be a good approximation for a given temperature,  $T_{\text{ref}}$ , see Fig. 2. However during slipping of the clutch, heat is dissipated from the friction surface into the cast iron parts of the clutch that naturally will expand. When the actuator motor is fully retracted (position=0) the expansion can be measured through the position sensor on the slave. This slave position is called the zero position,  $x_0$ , see Fig. 1.

A set of experiments has been performed to investigate the dynamics of the clutch expansion. In order to be able to measure the zero position during heating, the clutch has been alternating between closed and slipping with short time intervals. After some time of heating the clutch has been held closed for a prolonged time while the zero position has been constantly monitored as the clutch cools down. The measurement results are found in Figure 5. The zero position increases in a repeatable way with dissipated energy in the clutch and decays in an exponential manner with time. This supports the hypothesis that temperature is causing the change in zero position.

## 5.1 MATERIAL EXPANSION ANALYSIS

In order to see that the change in zero position is due to material expansion, the temperature increase is calculated in two ways. During the first heating period of Fig. 5, 1.5 MJ of energy is dissipated. The pressure plate and flywheel have a combined mass of 81 kg and are made of cast iron that has a specific

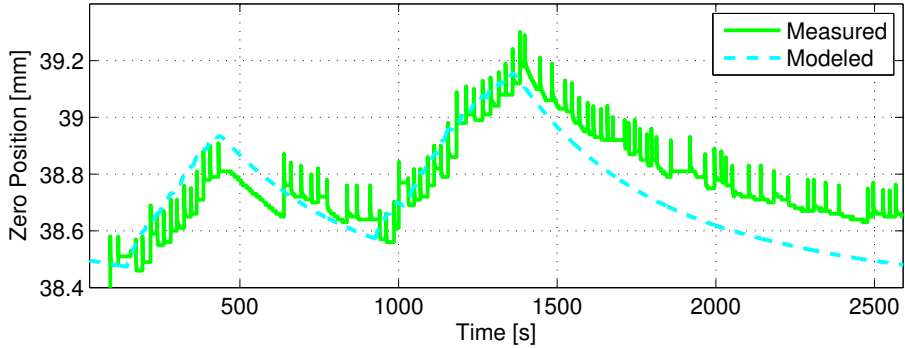


Figure 5: The clutch has been heated through slipping and then left to cool down. The zero position has been recorded as a measure of the expansion. The temperature model (6)-(9) shows good agreement with the measurement. Parameters have been fitted to a separate set of data.

heat of  $0.5 \text{ kJ}/(\text{kg K})$ , (Nording and Österman, 1999). If cooling of the clutch is neglected a slightly high estimation of the temperature increase is obtained.

$$\frac{1.5 \cdot 10^6}{500 \cdot 81} = 37 \text{ K}$$

The measured expansion of the clutch during the same period is  $0.3 \text{ mm}$  at the piston. With a linkage ratio of  $8.8$ , a  $100 \text{ mm}$  thick clutch and an expansion coefficient for cast iron of  $11 \cdot 10^{-6} \text{ K}^{-1}$ , (Nording and Österman, 1999), this corresponds to a temperature increase of,

$$\frac{0.3}{8.8 \cdot 100 \cdot 11 \cdot 10^{-6}} = 30 \text{ K}$$

The two temperature estimates are practically the same. Therefore the measured expansion can be said to depend on temperature.

## 5.2 EXPANSION MODEL

In order to model the expansion a temperature model is required. In Velardocchia et al. (2000) a linear model with one thermal mass in the pressure plate and one in the flywheel is proposed. All parts of the clutch are cooled towards the air in the clutch housing. Here the model is extended to capture the changes in the housing temperature,  $T_h$ . In contrast to Velardocchia et al. (2000) the clutch studied here is mounted in a vehicle, therefore the clutch is, in addition, thermally connected to both the ICE and transmission. However only a few percent of the dissipated power,  $P$ , goes into the transmission, Wikdahl and Ågren (1999). Therefore the heat flow to the transmission has been neglected. Moreover it has been found that the thermal masses of the flywheel and pressure

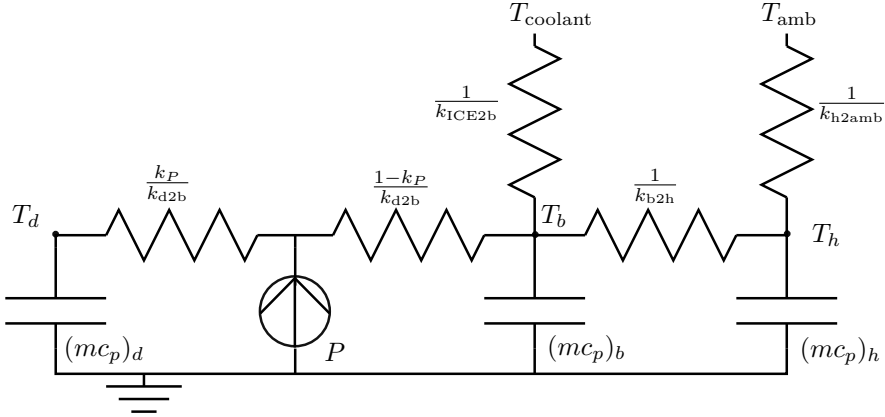


Figure 6: An electrical analogy of the temperature model (12)-(14). If  $(mc_p)_d = 0$  the model can also be described by (6)-(7).

plate can be taken as one mass,  $(mc_p)_b$ , for the clutch body, without loosing accuracy with respect to the expansion. For an electrical analogy of the model see Fig. 6. The corresponding equations are:

$$(mc_p)_b \dot{T}_b = k_{ICE2b}(T_{coolant} - T_b) + k_{b2h}(T_h - T_b) + P \quad (6)$$

$$(mc_p)_h \dot{T}_h = k_{b2h}(T_b - T_h) + k_{h2amb}(T_{amb} - T_h) \quad (7)$$

where,

$$P = M_c \Delta\omega \quad (8)$$

In order to connect the temperature model with the change in zero position, the levers and the expansion of the clutch body as function of temperature are assumed linear.

$$x_0 = k_{exp,1}(T_b - T_{ref}) + x_{0,ref} \quad (9)$$

The eight parameters in the equations have been fitted against measured data and the validation results, on a different set of data, can be seen in Fig. 5. Using these results the piston position can be corrected for the expansion effect to correspond to the actual compression of the flat spring, see Fig. 1.

$$\Delta x_0 = x_0 - x_{0,ref} \quad (10)$$

$$x_{cor} = x - \Delta x_0 \quad (11)$$

Nevertheless the expansion model does not explain the torque drift, see Fig. 7. The time scale in Fig. 2 is significantly smaller than that of Fig. 5. The torque drift is also much larger than what is explained by the expansion. This has led to the hypothesis that the clutch disc is also expanding with heat. In particular the clutch disc has a much smaller (thermal) mass, which could correspond to the faster time constant phenomenon seen in the data.

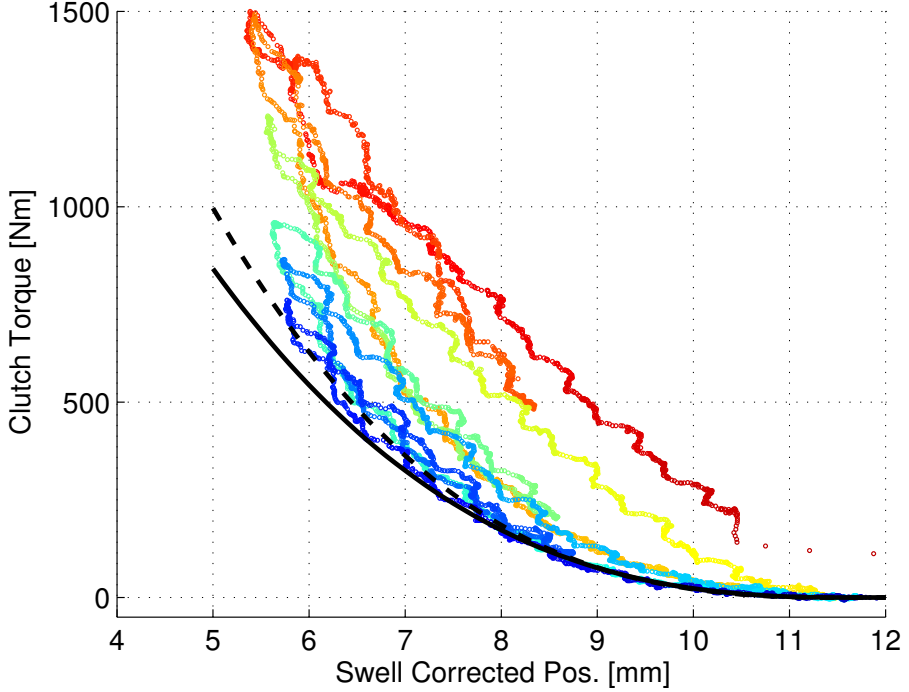


Figure 7: The data from Figure 2 has been corrected for swelling of the clutch body using (11). The correction is not sufficient to explain the torque drift.

### 5.3 INCLUDING FAST DYNAMICS

The clutch disc temperature,  $T_d$ , has been modeled in a similar fashion, see Fig. 6 for an electrical analogy and below for equations.

$$(mc_p)_b \dot{T}_b = k_{ICE2b}(T_{coolant} - T_b) + k_{b2h}(T_h - T_b) + k_{d2b}(T_d - T_b) + k_P P \quad (12)$$

$$(mc_p)_h \dot{T}_h = k_{b2h}(T_b - T_h) + k_{h2amb}(T_{amb} - T_h) \quad (13)$$

$$(mc_p)_d \dot{T}_d = k_{d2b}(T_b - T_d) + (1 - k_P)P \quad (14)$$

A new situation with this extended model is that the dissipated energy has to be split between the clutch disc and the body. In the model it is split by the parameter  $k_P$ , which is 1 if all energy goes to the body and 0 if all goes to the disc. However the model is not sensitive to  $k_P$  due to two facts. Firstly the vast difference in time constants, a factor of  $\sim 50$ , between the disc and the body decouples (12) from (14), i.e.  $k_{d2b}(T_d - T_b) + k_P P \approx (1 - k_P)P + k_P P = P$ , leaving the dynamics of  $T_b$  almost unchanged. Secondly the parameters are fitted to data, i.e. if  $k_P$  is 0 instead of 0.5 the value of  $(mc_p)_d$  and  $k_{d2b}$  will

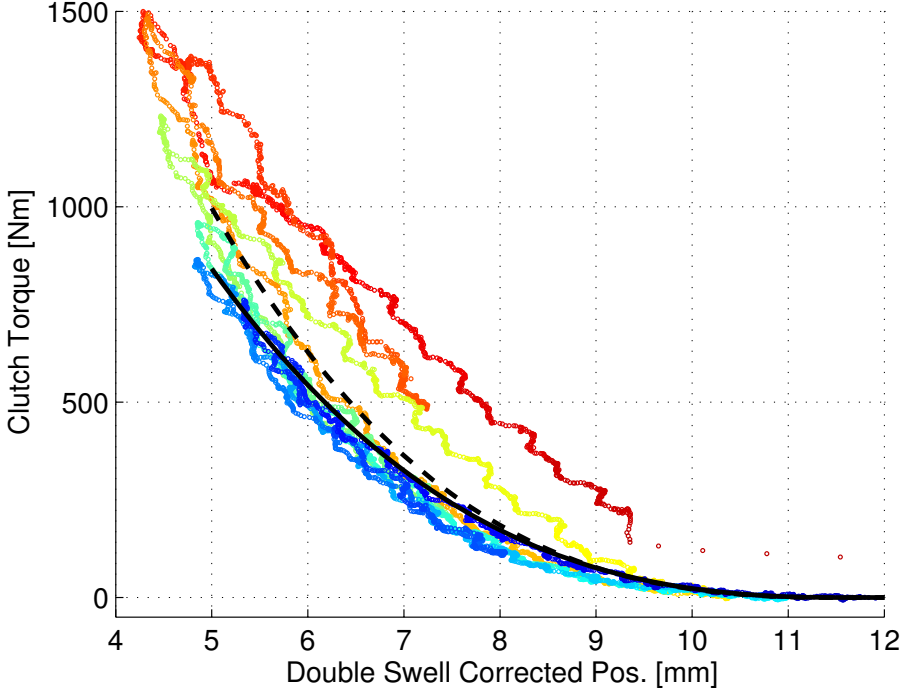


Figure 8: The data from Figure 2 has been corrected for swelling of the clutch body using (11) and (15). The correction explains the torque drift until the temperatures get too high (somewhere when state  $T_d$  becomes greater than 200 °C).

double, leaving the dynamics of  $T_d$  almost unchanged. In the data the expansion has been seen to lag the dissipated power. The lag is maximized by  $k_P = 0$  this is thus the choice of  $k_P$ .

The expansion of the clutch disc is modeled by extending (9) with an extra term

$$\begin{aligned}
 \Delta x_0 &= k_{\text{exp}} (T_b - T_{\text{ref}}) + k_{\text{exp},2} (T_d - T_{\text{ref}}) = \\
 &= k_{\text{exp}} (T_b - T_{\text{ref}}) + k_{\text{exp},2} ((T_d - T_b) + (T_b - T_{\text{ref}})) = \\
 &= \underbrace{(k_{\text{exp}} + k_{\text{exp},2})}_{k_{\text{exp},1}} (T_b - T_{\text{ref}}) + k_{\text{exp},2} (T_d - T_b) \quad (15)
 \end{aligned}$$

where the second term was practically zero during the zero-position measurements due to the fast dynamics of  $T_d$ . Therefore the new parameters can be estimated separately from the old parameters. After estimation of the new parameters the position can be corrected with (12)-(15) and Fig. 8 is obtained.

The model works well until the temperatures become too high (state  $T_d$

reaches more than 200 °C). It has been found empirically that saturating the term  $(T_d - T_b)$  at 110 °C improves the model at higher temperatures. One should note that values of the temperature states have not been validated against any measurement but they have reasonable magnitudes.

The transmitted torque can now be calculated as,

$$M_c = M_{\text{ref}}(x_{\text{cor}}) \quad (16)$$

Note that  $x_{\text{cor}}$  increases with temperature which in turn makes  $M_c$  increase with temperature. This is in contrast with the data in Velardocchia et al. (1999) where the torque is decreasing with temperature. Although in the experiments performed here the clutch mostly has a medium to high temperature and could comply with the data in Ercole et al. (2000).

In summary, the model is a three state model with one static non-linearity. All calculations are simple and therefore the model is suitable for running in real time, for example in a clutch-control application.

## 6 MODEL VALIDATION

The model has been validated on several data sets separate from those used for parameter identification. One of these validations is shown in Fig. 9. The model can be said to agree well with data. If the dissipated power is calculated from the measured torque the model agrees very well, but it still simulates a slightly low clutch torque. If instead the dissipated power is calculated from the simulated torque the torque error makes the simulated power dissipation too low and therefore the temperature states get lower. In turn this will lead to even lower simulated torque in the next torque pulse. This is the explanation for the decay in the simulated torque. In spite of this it still models the torque better than the more common static model. On one hand, calculating the power from the measured torque gives a better estimate of the current transmissibility curve, which could be used for feed forward in control applications. On the other hand the measured torque is not always available, e.g. some special driving scenarios, when evaluating new controllers through simulation, or in the prediction made by a model-based controller.

At the end of the torque pulses, the modeled torque drops faster than the measured torque, when the clutch is fully opened in 0.3 s. This is however believed to be due to delays in the computation of the engine torque, sensors and other data processing. Therefore the residuals have been filtered using a moving median of five samples (10 Hz). The result is presented in Fig. 10. The residuals are less than 200 Nm and most of the time less than 100 Nm. Considering that 100 Nm is less than 3% of maximum engine torque, the model works well. In fact the engine estimated torque can have errors of similar magnitude.

A validation of a launch is shown in Fig. 11. The static and dynamic models are compared to measurement data. The dynamic model has a small error that is always less than 104 Nm, and has better performance than the static model.

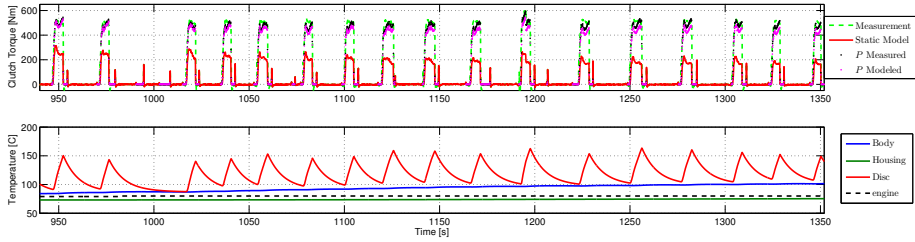


Figure 9: The dynamic torque model shows good agreement with measurements in a validation data set. There is a slight decay in torque when  $P$  is modeled instead of measured. However both implementations are significant improvements compared the static model,  $M_c = M_{\text{ref}}(x)$ . The open-loop simulation started at 0 seconds. In the lower plot  $P$  is measured.

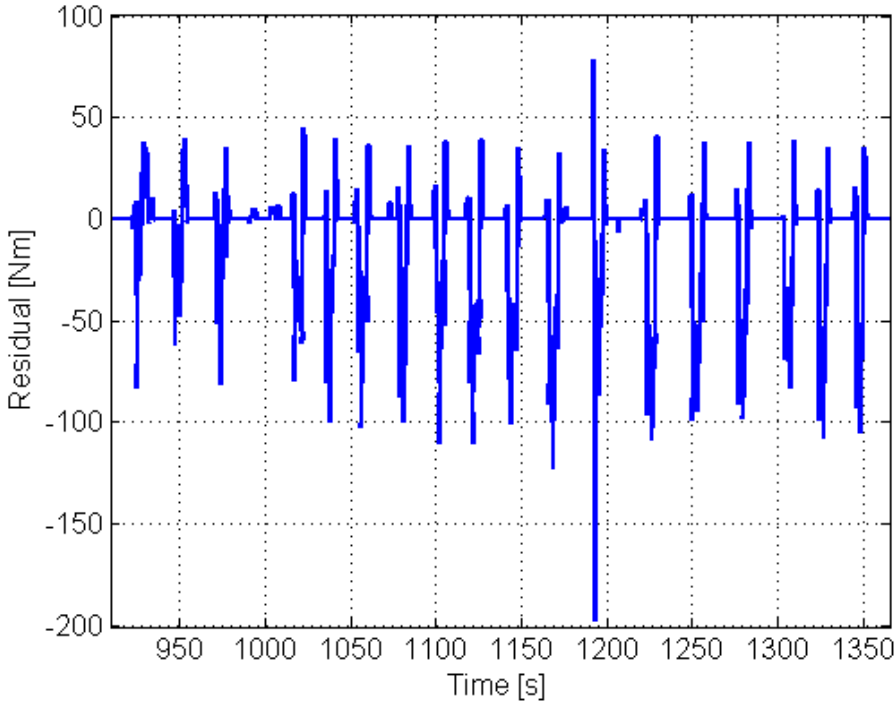


Figure 10: The residuals between the model and data presented in Figure 9. The residuals are less than 200 Nm and most of the time less than 100 Nm. Or in other words, most of the time less than 3% of maximum ICE torque.

In other data sets it has been seen that somewhere when  $T_d$  is greater than 200 °C the model deteriorates. This however is of small concern since these

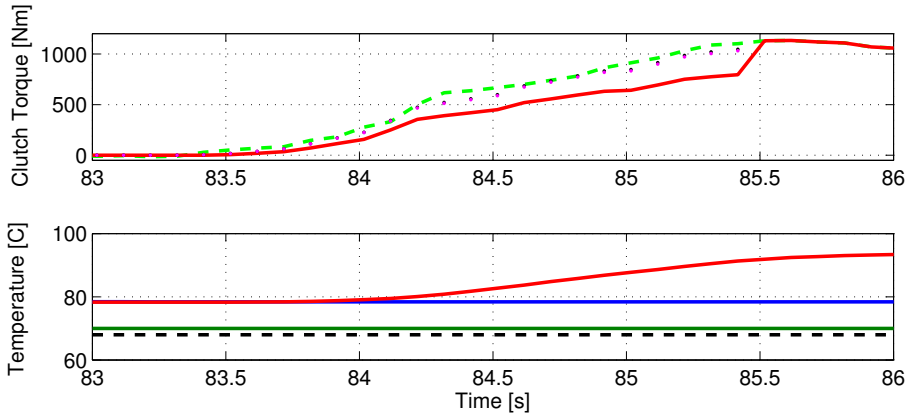


Figure 11: The dynamic torque model shows good agreement with measurement data of a start. The open-loop simulation started at 0 seconds. Line colors and styles are the same as in Fig. 9. The clutch is locked up when there are no black or magenta dots. In the lower plot  $P$  is measured.

temperatures are only reached during extreme driving. The accuracy of the model has also been seen to be less good when the truck is cold.

The clutch temperatures could not be quantitatively validated as no temperature measurements were available. Therefore only a qualitative validation is performed, showing that the magnitudes of the temperature states are reasonable for an HDT clutch, see Fig. 9 and 11.

## 7 CONCLUSION

The transmitted torque in an heavy-duty truck dry clutch at slipping conditions has been studied. Experiments showed no direct slip-speed dependency at the levels of slip investigated here, instead dynamic effects were clearly visible. In particular the measurements showed that the transmitted torque can vary with up to 900 Nm for a given position. To capture the dynamic behavior, a model with three temperature states was built. The model was developed and validated on a production HDT, where no temperature measurements were available. Therefore only a qualitative validation of the temperatures was performed, showing that they had reasonable magnitudes.

The temperature dynamics have two vastly different time constants, a factor of  $\sim 50$  apart, and the slow part could be physically explained to affect the transmitted torque through expansion of clutch parts. Due to the vast difference in the two time constants the model shows little sensitivity to how the dissipated heat enters the model.

In validations, on driving sequences with intense use of the clutch, the

open-loop simulation error was kept under 200 Nm and most of the time under 100 Nm, which is less than 3% of maximum engine torque and comparable to the accuracy of the engine torque estimate. The dynamic model was shown to give a significant improvement compared to a static model.

Finally, the model is simple and suitable for running in real time applications, such as a clutch controller or a torque observer.

## ACKNOWLEDGMENT

Vinnova industrial excellence center LINK-SIC and Scania CV have supported this work. Special thanks to Karl Redbrandt at Scania for conducting the experiments.

## REFERENCES

- Marius Bataus, Andrei Maciac, Mircea Oprean, and Nicolae Vasiliu. Automotive clutch models for real time simulation. *Proceedings of the Romanian Academy, Series A*, 12(2):109–116, 2011.
- Pietro Dolcini, Carlos Canudas de Wit, and Hubert Béchart. Improved optimal control of dry clutch engagement. *Proceedings of the 16th IFAC World Congress*, 16(1), 2005.
- Pietro Dolcini, Carlos Canudas de Wit, and Hubert Béchart. Lurch avoidance strategy and its implementation in AMT vehicles. *Mechatronics*, 18(1):289–300, May 2008.
- Pietro J. Dolcini, Carlos Canudas de Wit, and Hubert Béchart. *Dry Clutch Control for Automotive Applications*. Advances in Industrial Control. Springer-Verlag London, 2010.
- G. Ercole, G. Mattiazzo, S. Mauro, M. Velardocchia, F. Amisano, and G. Serra. Experimental methodologies to determine diaphragm spring clutch characteristics. In *SAE Technical Paper: 2000-01-1151*, March 2000.
- Franco Garofalo, Luigi Glielmo, Luigi Iannelli, and Francesco Vasca. Optimal tracking for automotive dry clutch engagement. In *2002 IFAC, 15th Triennial World Congress*, 2002.
- Luigi Glielmo and Francesco Vasca. Optimal control of dry clutch engagement. In *SAE Technical Paper: 2000-01-0837*, March 2000.
- Behrooz Mashadi and David Crolla. *Vehicle Powertrain Systems*. John Wiley & Sons Ltd, first edition, 2012.
- G. Mattiazzo, S. Mauro, M. Velardocchia, F. Amisano, G. Serra, and G. Ercole. Measurement of torque transmissibility in diaphragm spring clutch. In *SAE Technical Paper: 2002-01-0934*, March 2002.
- Carl Nording and Jonny Österman. *Physics Handbook*. Studentlitteratur, 1999.
- Francesco Vasca, Luigi Iannelli, Adolfo Senatore, and Gabriella Reale. Torque transmissibility assessment for automotive dry-clutch engagement. *IEEE/ASME transactions on Mechatronics*, 16(3):564–573, June 2011.
- M. Velardocchia, G. Ercole, G. Mattiazzo, S. Mauro, and F. Amisano. Diaphragm spring clutch dynamic characteristic test bench. In *SAE Technical Paper: 1999-01-0737*, March 1999.
- M. Velardocchia, F. Amisano, and R. Flora. A linear thermal model for an automotive clutch. In *SAE Technical Paper: 2000-01-0834*, March 2000.
- Anna Wikdahl and Åsa Ågren. Temperature distribution in a clutch. Master’s thesis, Linköping University, 1999.

The Effect of Thermal Expansion in a Dry Clutch  
on Launch Control\*

**B**

---

\*Accepted for publication in *7th IFAC Symposium on Advances in Automotive Control*.



---

# The Effect of Thermal Expansion in a Dry Clutch on Launch Control

Andreas Myklebust and Lars Eriksson

*Vehicular Systems, Department of Electrical Engineering,  
Linköping University, SE-581 83 Linköping, Sweden*

## ABSTRACT

---

A dry clutch model with thermal dynamics is added to a driveline model of a heavy-duty truck equipped with an automated manual transmission. The model captures driveline oscillations and can be used to simulate how different clutch-control strategies affect vehicle performance, drivability and comfort. Parameters are estimated to fit a heavy-duty truck and the complete model is validated with respect to shuffle, speed trajectory, clutch torque and clutch lock-up/break-apart behavior. The model shows good agreement with data. Furthermore the model is used to study the effect of thermal expansion in the clutch on launch control. It is shown that the effect of thermal expansion, even for moderate temperatures, is significant in launch control applications.

---

## 1 INTRODUCTION

Increasing demands on comfort, performance, and fuel efficiency in vehicles lead to more complex transmission solutions. Historically high efficiency was best met with a classical Manual Transmission and comfort with a classical Automatic Transmission. The Automated Manual Transmission (AMT) is one way to combine the best from two worlds. An important part in an AMT is clutch control that has a profound effect on vehicle performance. Therefore it is of importance to know the torque transmitted in the clutch with high precision. Models have come to play an important role in estimation and control of the transmitted torque, since torque sensors are expensive.

A sketch of a dry single-plate clutch is found in Fig. 1, while in-depth explanations are found in for example Mashadi and Crolla (2012) and Vasca et al. (2011). In clutch-modeling literature a wide range of models are proposed. The most simple models have a clutch torque that is assumed to be a controllable input, see for example Dolcini et al. (2008); Garofalo et al. (2002). These models rely on the assumption that there is perfect knowledge of how the clutch behaves. More advanced models include submodels for slipping and sticking torques. For example a LuGre model is used in Dolcini et al. (2005) and a Karnopp model in Bataus et al. (2011). The former is a one-state model that captures stick-slip behavior, varying break-away force, Stribeck effect, and viscous friction. The latter simply applies a dead-zone around zero speed to ease the simulation of stick-slip behavior.

Models for the transmittable clutch torque during slipping commonly use a function with the following structure,

$$M_{\text{trans},k} = \text{sgn}(\Delta\omega) \mu R_e F_N \quad (1)$$

where  $\Delta\omega$  is the clutch slip (speed),  $\mu$  the friction coefficient,  $R_e$  the effective radius and  $F_N$  the clamping (normal) force. In these models  $F_N$  is often either given as input or a static nonlinear function of clutch position,  $x$ , i.e.  $F_N = F_N(x)$ , see for example Vasca et al. (2011); Glielmo and Vasca (2000). Furthermore a graph with speed dependency of the normal force is shown in Hong et al. (2012). In Dolcini et al. (2010) that speed dependency is said to be due to centrifugal forces acting on the springs in the clutch. Mashadi and Crolla (2012); Moon et al. (2004) reports of hysteresis in the diaphragm spring, that could lead to hysteresis in the normal force. In Mattiazzo et al. (2002) a temperature and wear dependency of the normal force/bearing position characteristics is shown.

Concerning the other model components it is generally recognized that  $\mu$  can depend on temperature, slip speed, and wear and that  $R_e$  can depend on temperature and wear as well, see Velardocchia et al. (1999). In Vasca et al. (2011) a slip speed dependency of  $\mu R_e$  is shown, this was especially pronounced for slip speeds below  $\sim 100$  RPM.

It can be difficult to separate which parameter in (1) that is the reason for a change in  $M_{\text{trans},k}$ . Therefore the clutch torque is often studied as a

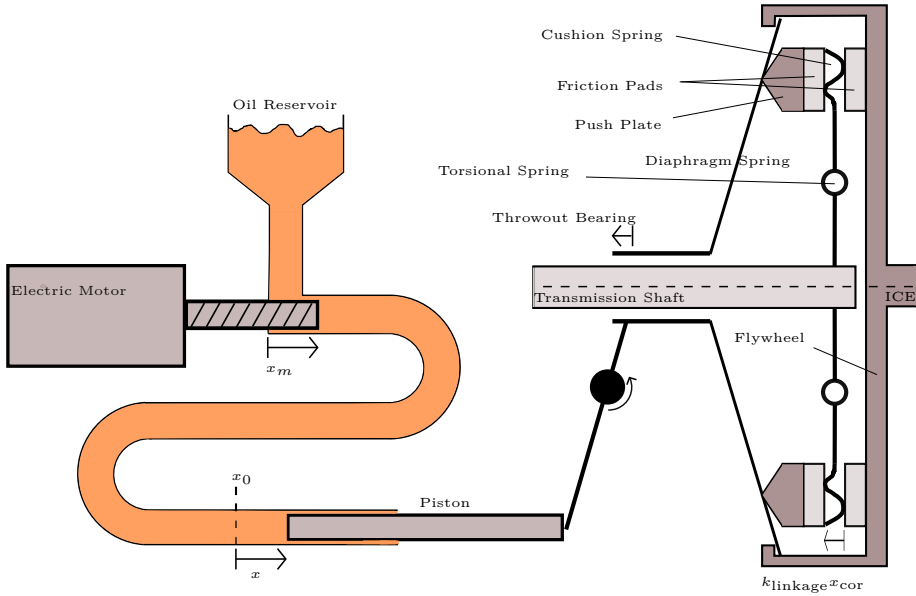


Figure 1: A sketch over the actuator and dry single-plate pull-type clutch installed in the experiment vehicle.

lumped model. In Velardocchia et al. (1999)  $M_{trans,k}$  is seen to decrease with temperature and  $\Delta\omega$ . However there are large variations with wear. In Ercole et al. (2000)  $M_{trans,k}$  initially decreases with temperature for low temperatures and then increases for medium and high temperatures. Similarly there are variations with wear and in addition temperature-torque hysteresis are reported. In Velardocchia et al. (2000), Wikdahl and Ågren (1999) and Myklebust and Eriksson (2012b) temperature models are established, but only Myklebust and Eriksson (2012b) includes the effect of the temperature on  $M_{trans}$ .

When modeling the rest of the driveline for (clutch) control purposes it is common to include one or more flexibilities, (Pettersson, 1997; Garofalo et al., 2002; Fredriksson and Egardt, 2003; Moon et al., 2004; Crowther et al., 2004; Lucente et al., 2007; Dolcini et al., 2008)

Here yet another driveline model with focus on the clutch and the control of it is presented and validated. The contribution lies in that here the thermal dynamics of the clutch are included in the model. Particularly the significance to launch performance of including the thermal part is shown.

## 2 DRIVELINE MODEL

In order to evaluate the quality of a certain launch control, a longitudinal model of the heavy-duty truck in question is required. The model has to capture

important dynamics in the driveline and how they make the truck shuffle. One such model is found in Myklebust and Eriksson (2012a). It is used here with one modification, the clutch model is replaced with the more advanced model from Myklebust and Eriksson (2012b).

An overview of the model is seen in Figure 2. There the different parts of the model, Internal Combustion Engine (ICE), clutch, gearbox, propeller shaft, final drive, drive shafts and vehicle dynamics, can be seen as well as where the flexibilities are located. Next, a quick review of the model equations are given.

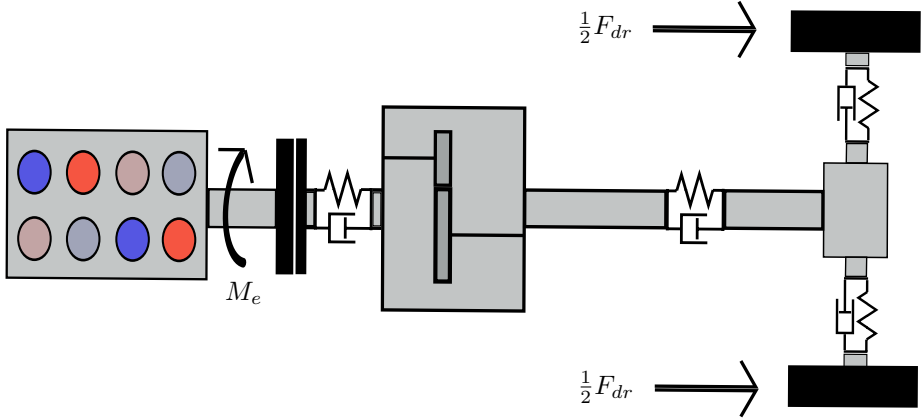


Figure 2: Sketch of the driveline model. Modeled parts and locations of flexibilities are visible.

If not otherwise stated the nomenclature follows this system:  $\theta$ =angle,  $\omega = \dot{\theta}$ ,  $v$ =velocity,  $r$ =radius,  $T$ =temperature,  $M$ =torque,  $F$ =force,  $P$ =power,  $c$ =damping or vehicle dynamics coefficient,  $k$ =spring coefficient,  $b$ =viscous friction coefficient,  $J$ =inertia,  $i$ =gear ratio, and  $x$ =clutch piston position. These quantities are often equipped with subscripts,  $e$ =engine,  $fw$ =flywheel,  $c$ =clutch transmission side,  $t$ =transmission,  $p$ =propeller shaft,  $f$ =final drive,  $d$ =drive shaft,  $w$ =wheel,  $i$ =gear number, and  $amb$ =ambient.

## 2.1 INTERNAL COMBUSTION ENGINE

The ICE produces the engine torque,  $M_e$ , that is given as model input. Note that this is the net (brake) torque of the ICE, e.g.  $M_e = 0$  with open clutch will keep the engine speed constant.

## 2.2 CLUTCH

The explanation of the clutch model is split into three parts, the friction and temperature dynamics, the mode changes between locked and slipping, and the torsional springs. An overview of the studied clutch is seen in Fig. 1.

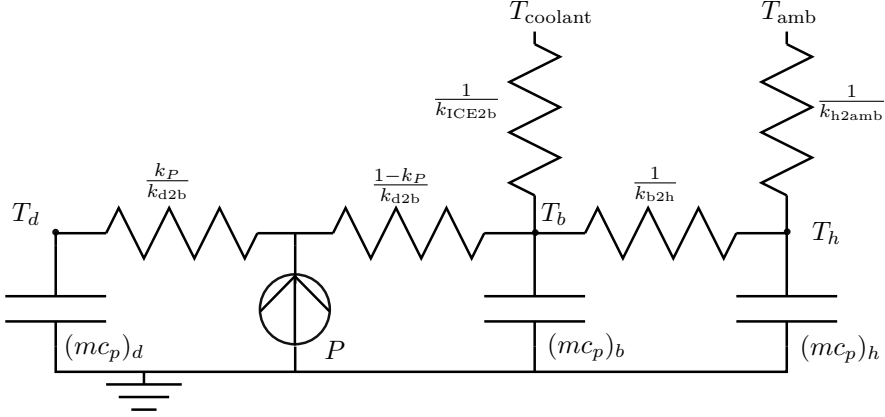


Figure 3: An electrical analogy of the temperature model (3)-(5).

### CLUTCH FRICTION

The natural output from the actuator is the clamping force,  $F_N$ . However  $F_N$  is not measurable, therefore it is directly recalculated into a transmittable torque,  $M_{\text{trans}} = k\mu F_N$ , that is used as actuator output. The shape of the torque transmissibility curve is described by a third order polynomial, (Dolcini et al., 2010; Myklebust and Eriksson, 2012b)

$$M_{\text{ref}}(x_{\text{ref}}) = \begin{cases} a(x_{\text{ref}} - x_{\text{ref,ISP}})^3 + \\ + b(x_{\text{ref}} - x_{\text{ref,ISP}})^2, & \text{if } x_{\text{ref}} < x_{\text{ref,ISP}} \\ 0, & \text{if } x_{\text{ref}} \geq x_{\text{ref,ISP}} \end{cases} \quad (2)$$

where  $x_{\text{ISP}}$  (Incipient Sliding Point) is the kiss point. The exact value of  $x_{\text{ISP}}$  can be difficult to find since the transmissibility curve is very flat around  $x_{\text{ISP}}$ . However it is only important to find a  $x_{\text{ISP}}$  that gives a good curve fit, for a certain temperature,  $T_{\text{ref}}$ , as errors will be small near  $x_{\text{ISP}}$ .

The clutch disc temperature,  $T_d$ , clutch body (flywheel and pressure plate) temperature,  $T_b$ , and the clutch housing temperature,  $T_h$ , have been modeled in order to explain the torque drift, see Fig. 5, due to temperature. An electrical analogy of the model is found in Fig. 3 and below are the equations.

$$(mc_p)_b \dot{T}_b = k_{\text{ICE2b}}(T_{\text{coolant}} - T_b) + k_{\text{b2h}}(T_h - T_b) + k_{\text{d2b}}(T_d - T_b) + k_P P \quad (3)$$

$$(mc_p)_h \dot{T}_h = k_{\text{b2h}}(T_b - T_h) + k_{\text{h2amb}}(T_{\text{amb}} - T_h) \quad (4)$$

$$(mc_p)_d \dot{T}_d = k_{\text{d2b}}(T_b - T_d) + (1 - k_P)P \quad (5)$$

where,

$$P = M_{\text{trans},k} \Delta\omega = M_{\text{trans},k} (\omega_e - \omega_c) \quad (6)$$

The temperature model is connected to the transmitted torque through a change of the position  $x_{\text{cor}}$ , see Fig. 1, corresponding to the expansion of parts in the clutch. The expansion of the clutch body and disc as a function of temperatures is assumed linear.

$$\Delta x_0 = (k_{\text{exp},1} + k_{\text{exp},2})(T_b - T_{\text{ref}}) + k_{\text{exp},2}(T_d - T_b) \quad (7)$$

$$x_{\text{cor}} = x - \Delta x_0 \quad (8)$$

The transmitted torque can now be calculated as,

$$M_{\text{trans},k} = M_{\text{ref}}(x_{\text{cor}}) \quad (9)$$

Note that  $x_{\text{cor}}$  increases with temperature which in turn makes  $M_{\text{trans},k}$  increase with temperature. The  $k$  in the subscript stands for kinetic because the friction is modeled as coulomb friction with stick-slip behavior. Define  $k_\mu$  as the ratio of the static friction coefficient over the kinetic. Then the maximum transmittable torque when sticking is:

$$M_{\text{trans},s} = k_\mu M_{\text{trans},k} \quad (10)$$

#### LOCK-UP/BREAK-APART LOGIC

The clutch model has two modes, locked and slipping mode. While in locked mode, the clutch behaves as one rigid body, whereas during slipping the clutch consists of two bodies where each one has an angular velocity and position. The equations are:

Conditions for switching from slipping to locked mode:

$$\dot{\theta}_e = \dot{\theta}_c \quad (11)$$

$$M_{\text{trans}} \leq M_{\text{trans},s} \quad (12)$$

Conditions for switching from locked to slipping mode:

$$M_{\text{trans}} \geq M_{\text{trans},s} \quad (13)$$

Equations specific for the clutch in locked mode:

$$M_e - M_c = (J_e + J_{\text{fw}} + J_c) \ddot{\theta}_e \quad (14)$$

$$\dot{\theta}_c = \dot{\theta}_e \quad (15)$$

$$M_{\text{trans}} = \frac{M_e J_c + M_c (J_e + J_{\text{fw}})}{J_e + J_{\text{fw}} + J_c} \quad (16)$$

Equations specific to the clutch in slipping mode:

$$M_{\text{trans}} = \text{sgn}(\dot{\theta}_e - \dot{\theta}_c) M_{\text{trans},k} \quad (17)$$

$$M_e - M_{\text{trans}} = (J_e + J_{\text{fw}}) \ddot{\theta}_e \quad (18)$$

$$M_{\text{trans}} - M_c = J_c \ddot{\theta}_c \quad (19)$$

## TORSIONAL PART

The main flexibility of the clutch is in the torsion springs in the clutch disc. They are located on the vehicle side of the friction surfaces and can be modeled as a separate part.

The clutch torsional part is modeled as a torsional spring and damper.

$$M_c = c_c(\dot{\theta}_c - \dot{\theta}_t) + k_c(\theta_c - \theta_t) \quad (20)$$

## 2.3 TRANSMISSION

The transmission consists of some inertia, viscous friction and a gear ratio. Note that no synchronizers are modeled and the model can not engage neutral gear. Therefore gear shifting will be instantaneous. This is an acceptable approximation when the clutch is disengaged, since the transmission input side has low inertia compared to the rest of the vehicle.

With the states  $\dot{\theta}_p$ ,  $\theta_p$ , and  $\theta_t$  the equations become:

$$M_t = M_c i_{t,i} \quad (21)$$

$$(J_{t,i} + J_p) \ddot{\theta}_p = M_t - b_t \dot{\theta}_p - M_p \quad (22)$$

$$\dot{\theta}_t = \dot{\theta}_p i_{t,i} \quad (23)$$

## 2.4 PROPELLER SHAFT

The flexible propeller shaft is modeled in the same way as the clutch flexibility, (20). The propeller-shaft equation is:

$$M_p = c_p(\dot{\theta}_p - \dot{\theta}_f) + k_p(\theta_p - \theta_f) \quad (24)$$

## 2.5 FINAL DRIVE

The final drive with differential is assumed to act symmetrically on the drive shafts. Therefore it can be modeled as the transmission but with fixed gear ratio,  $i_f$ , and inertia,  $J_f$ . With the states  $\dot{\theta}_d$ ,  $\theta_d$  the equations become:

$$(J_p i_f^2 + J_f + J_d) \ddot{\theta}_d = M_p i_f - b_f \dot{\theta}_d - M_d \quad (25)$$

$$\dot{\theta}_f = \dot{\theta}_d i_f \quad (26)$$

## 2.6 DRIVE SHAFTS

The driveline's main flexibility is in the drive shafts, which can, with a symmetrical differential, be modeled as the clutch flexibility, (20). The drive shaft equation is:

$$M_d = c_d(\dot{\theta}_f - \dot{\theta}_w) + k_d(\theta_f - \theta_w) \quad (27)$$

## 2.7 VEHICLE DYNAMICS

The wheels and non-driveline parts that affect the longitudinal dynamics are modeled in this section. Tire dynamics are neglected and rolling condition is assumed. The wheels simply consists of a radius,  $r_w$ , an inertia,  $J_w$  and a rolling resistance force,  $F_r$ .  $F_r$  is multiplied with a smoothing function in order to improve performance of the simulation, (Myklebust and Eriksson, 2012a).

Model inputs that directly affect the vehicle dynamics are braking force and road-slope angle,  $\alpha$  (in radians). The road-slope angle is used to calculate the gradient force that is added with the braking force, rolling resistance and aerodynamic drag.

With the states  $v$  ( $\dot{v} = a$ ) and  $\theta_w$  the equations become:

$$F_a = \frac{1}{2}\rho_a c_w A_f v^2, \quad F_g = mg \sin(\alpha) \quad (28)$$

$$F_r = f(v)(c_{r1} + c_{r2}|v|)mg, \quad \dot{\theta}_w = v/r_w \quad (29)$$

$$\begin{aligned} \frac{M_d}{r_w} - \text{sgn}(v)(F_r + F_a + F_b) - F_g &= \\ &= \frac{M_d}{r_w} - F_{dr} = \left( m + \frac{J_w + J_d}{r_w^2} \right) a \end{aligned} \quad (30)$$

Let torsions replace the states corresponding to angles, then the state vector is reduce to:  $\omega_e, \omega_c, \theta_c - \theta_t, \omega_p, \theta_p - \theta_f, \omega_d, \theta_d - \theta_w, \omega_w, T_b, T_h$ , and  $T_d$ . When the clutch is locked one state disappears,  $\omega_e = \omega_c$

## 3 PARAMETER ESTIMATION

The driveline model and the clutch model have both been validated separately in their respective paper. However they have not been validated when put together and the lock-up/break-a-part detection has not been validated before. In order to do that a number of launches have been recorded. However these experiments have been carried out in a different truck than those used in the previous papers. Therefore the parameters have to be estimated. The driveline parameters have been estimated using a launch where the clutch has been closed rapidly (clutch is slipping less than 0.1 s). This gives negligible clutch dynamics and large shuffle oscillations, which is appropriate when estimating the flexibilities and damping coefficients. The result can be seen in Fig. 4. Since it is difficult to do open-loop simulation of a system under feedback, the model also utilizes feedback. In the experiments the combustion engine is under speed control, therefore also the modeled engine is put under speed control. A PI-controller with feedforward of the measured engine torque is used. However since the engine model is simply an inertia, the PI-controller performs better than the real controller. Therefore the measured engine speed has been used as reference, in order to capture the

imperfections in the speed control and the inherent shuffle. The other driveline speeds follow the measurements well. The model is leading somewhat in the start due to sensor dynamics. There is some difference in the engine reported torque and the modeled engine torque, although it is hard to draw any conclusions from this, since the torque signal is inexact during transients. The parameterization seems good.

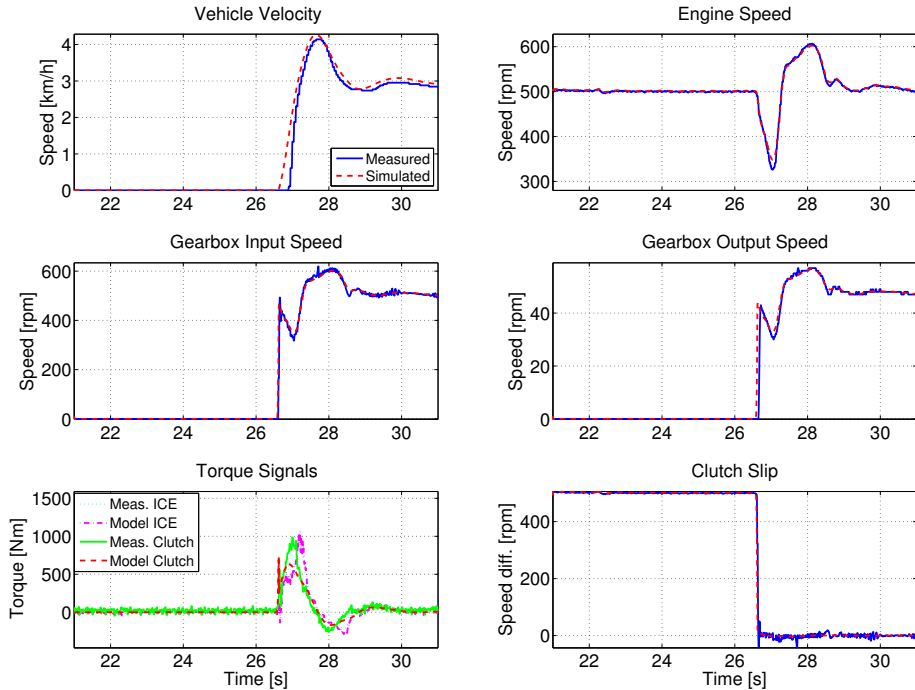


Figure 4: A quick launch (clutch locks-up in less than 0.1 s) with large oscillations was used to parameterize the driveline model. Both the real and modeled engines were under speed control. The measured output-shaft speed is lagging the model due to sensor dynamics.

Next the clutch model needs to be parameterized. The experiment conducted to do this has consisted of ramping the clutch position back and forth while the truck has been kept stationary using the parking brake. The resulting data can be seen in Fig. 5. The torque drift due to temperature can clearly be seen. By applying (3)-(8) to the data, using the same parameters as in Myklebust and Eriksson (2012b), Fig. 6 is attained. There the ramps have converged to one curve and consequently these parameters work here too. The 3rd degree polynomial, (2), has been fitted to this curve using the least square method.

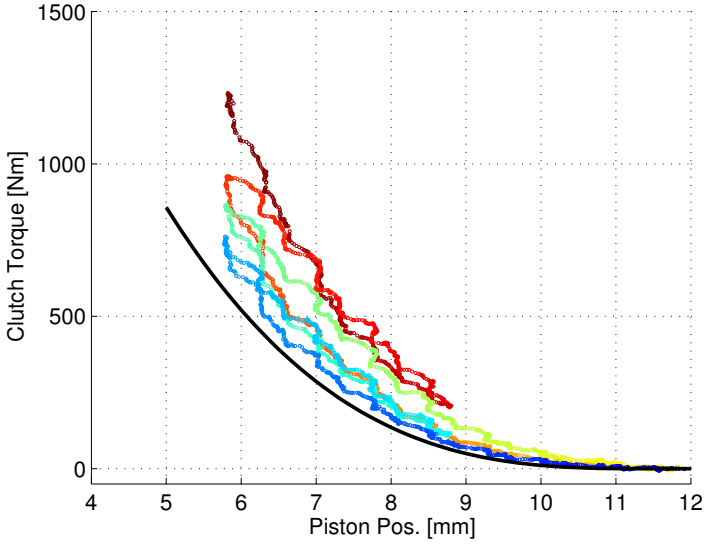


Figure 5: The data used for parameterizing the clutch model. The torque drift with temperature can be clearly seen. The color indicates time (blue=0 s, red=45 s).

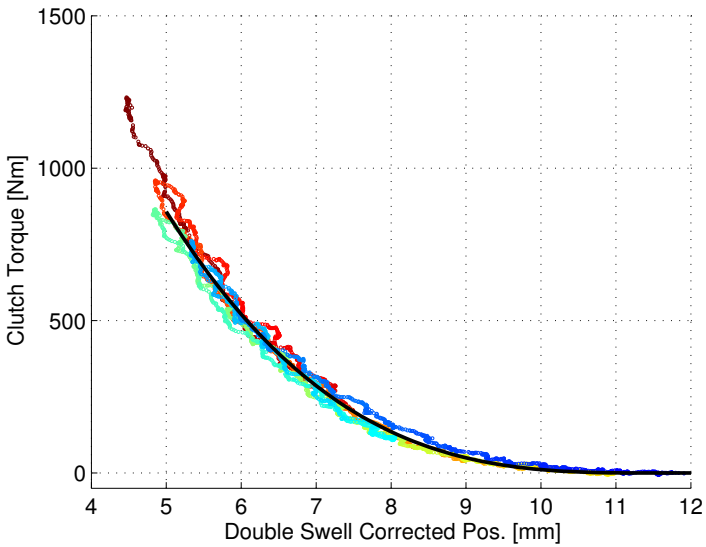


Figure 6: Same as Fig. 5 but the position has been corrected for the thermal expansion using (8). All lines converge. The black line is the least square fit of the 3rd degree polynomial, (2).

## 4 MODEL VALIDATION

A number of launches have been performed in different gears in order to validate the complete model. Here two launches are shown, one in third gear, Fig. 7, and one in sixth gear, Fig. 8. In third gear there is some drift in vehicle speed with the consequence that the clutch locks up earlier in the model compared to the measurement. During the slipping phase the clutch torque has been modeled correctly, however after lock up the torque decreases due to the engine speed controller. When the engine speed reaches a set value the controller is switched off and torque is used as model input, since then the measurement is no longer under feedback. When the controller is switched off the drift naturally returns. Nevertheless the oscillations in the driveline are captured with respect to amplitude and frequency, although the attenuation in the model is a bit too high. In sixth gear the driveline speeds and clutch torque matches the measurement very well. As a result it is easy to see that the lock-up/break-apart logic makes mode switches at the correct time points. This is a further addition to the base-line model in Myklebust and Eriksson (2012a). However when the clutch torque goes from positive to negative and vice versa there is some oscillations seen in the measurement due to backlash. These oscillations are naturally not captured in the model since the backlash is not modeled.

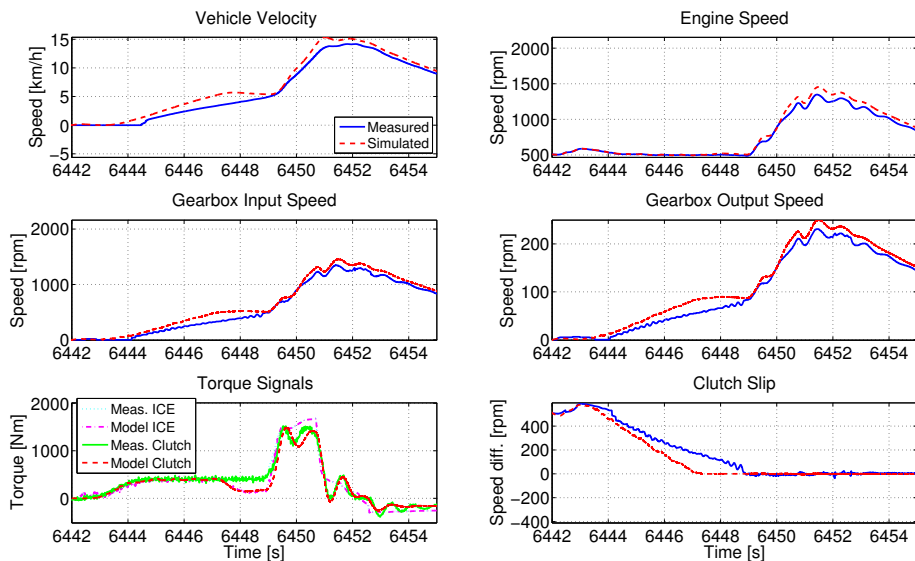


Figure 7: Validation of the complete model in 3rd gear. Vehicle oscillations are captured and the clutch torque is correct (while slipping). The engine is under speed control when the speed is close to 500 RPM and using torque as input otherwise.

In conclusion both validations look fine and the model is suitable for investigating different clutch control strategies during launch and their effect on vehicle shuffle and performance.

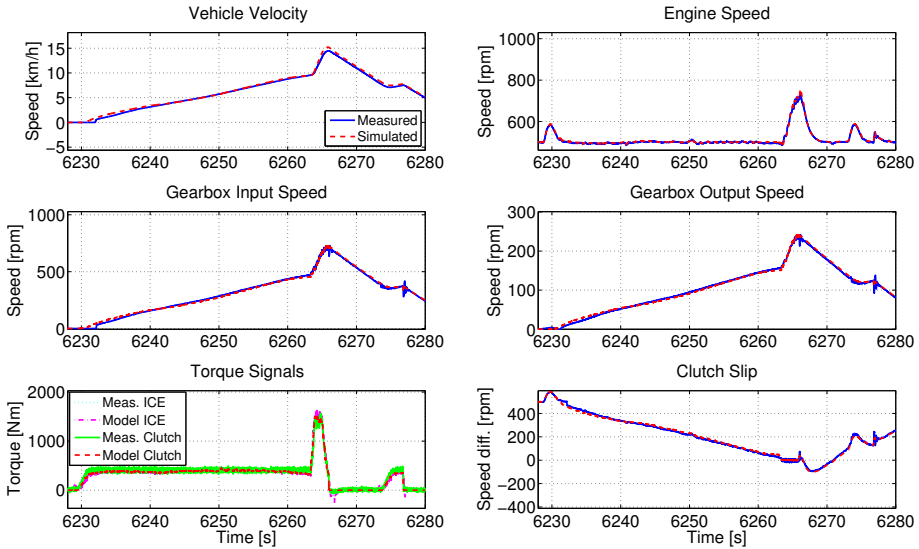


Figure 8: Validation of the complete model in 6th gear. Vehicle motion and the clutch torque are modeled with high accuracy. The lock-up/break-apart logic can be seen to work as intended at 6263/6266 s. When the torque transferred in the clutch changes between positive and negative some oscillations are seen in the measurement due to unmodeled backlash. The engine is under speed control.

## 5 THERMAL EFFECT ON LAUNCHING

This section highlights possible problems that can arise in clutch control during launch when not considering the thermal effects. Here two controllers taking requested torque as input are studied. This is a natural choice of input since it is common to use torque based driveline control, (Heintz et al., 2001). When so the driver intention over time can be interpreted as a reference torque trajectory. The first controller is the simplest possible, an open-loop controller consisting of an inversion of (2), the torque transmissibility curve at 60 °C. The second controller uses the first controller as a feedforward part but in addition it has a PI-controller in order to utilize the engine torque for feedback. For both controllers the clutch is fully open when the torque request is zero and fully closed when there is no slip in the clutch. The clutch actuator is fast and exact

and therefore it is modeled with a rate limiter of 82 mm/s on  $x$ . The ICE directly gives the requested torque and has in addition a PI idle-speed controller in order to not stall the engine if the requested torque is too low. The simulations will be evaluated mainly from a comfort perspective and a measurement relating to comfort is jerk (time derivative of the vehicle acceleration). According to Zeng et al. (2013) the maximum jerk and minimum (negative) jerk are important comfort measures.

A requested torque trajectory has been chosen as follows; starts out at zero torque until 1.5 s where it is ramped up to 3 % of maximum torque at 2.5 s. It is

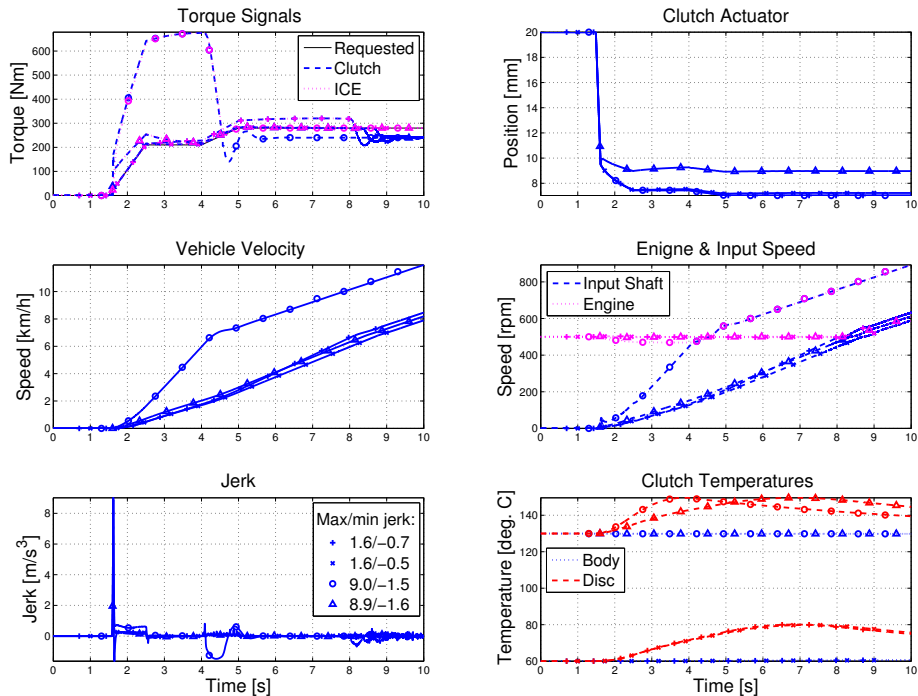


Figure 9: A simulated launch in fourth gear for four different cases, cold clutch with open loop control marked with plus signs, cold clutch with closed loop control marked with crosses, warm clutch with open loop control marked with circles and warm clutch with closed loop control marked with triangles. Cold clutch means  $[T_b, T_h, T_d] = [60, 50, 60]^{\circ}\text{C}$  and warm means  $[T_b, T_h, T_d] = [130, 120, 130]^{\circ}\text{C}$ . The cold closed loop case follows the reference torque closely whereas the cold open loop case has a slight drift due to heating of the clutch. The warm open loop case has a completely different speed trajectory that should correspond to a different accelerator input and, as in both warm cases, jerk levels are about five times higher.

kept there until 4 s when it is ramped further up to 4 % at 5 s and kept there for the rest of the simulation. This trajectory is used as input to the simulation model together with no braking, no slope, fourth gear and 500 RPM as idle speed. Simulations are run for both controllers in cold,  $[T_b, T_h, T_d] = [60, 50, 60]^\circ\text{C}$ , and warm,  $[T_b, T_h, T_d] = [120, 110, 120]^\circ\text{C}$ , conditions, four cases in total. The results are seen in Fig. 9. The maximum jerk levels can be seen to rise more than a factor of five when the clutch is warm. This is due to that the clutch controller overshoots the kiss point at 1.5 s. The feedback controller also get a large negative jerk when it tries to compensate for the excessive torque due to incorrect kiss point. In the open loop case no such compensation is present and naturally the truck receives a completely different speed trajectory although the driver input is the same. Furthermore the jerk is larger when the clutch locks-up in this case. The open-loop controller for the cold case has a drift in torque due to heating of the clutch. Only the closed-loop controller for the cold case manages to follow the desired trajectory.

Even though the example in Fig. 9 utilizes simple clutch-control algorithms it highlights a problem that will be present in any controller that does not compensate for the thermal dynamics. In order to give a quick response to driver request the clutch needs to quickly move to the kiss point. If the kiss point is overshoot large discomfort can arise, as seen in Fig. 9. An additional problem is that the large change in the torque transmissibility curve can put the controller in a situation it has not been tuned for, as demonstrated by the negative peak in the jerk for the closed loop controller in the warm case. Moreover it should be mentioned that the temperatures used in this example are normal, temperatures can even go above  $200^\circ\text{C}$ .

A remedy for this problem is to estimate the temperature and compensate the clutch piston position for the expansion using the model in Myklebust and Eriksson (2012b).

## 6 CONCLUSION

A driveline model for vehicle shuffle and a clutch model including thermal effects have been merged together in order to simulate how different clutch-control strategies affect vehicle shuffle and performance. Parameters have been estimated to fit a heavy-duty truck and the complete model has been successfully validated, including the lock-up/break-apart logic. The complete driveline model has been used to show the profound effect of thermal phenomenon in the clutch on launch control, even for moderate temperatures. The launch control example showcases the importance of incorporating a thermal model of the clutch in launch control applications.

## REFERENCES

- M. Bataus, A. Maciac, M. Oprean, and N. Vasiliu. Automotive clutch models for real time simulation. *Proc. of the Romanian Academy, Series A*, 12(2): 109–116, 2011.
- A Crowther, N Zhang, D K Liu, and J K Jeyakumaran. Analysis and simulation of clutch engagement judder and stick-slip in automotive powertrain systems. *Proc IMechE., Part D: J. of Automobile Engineering*, 218(12):1427–1446, December 2004.
- P. Dolcini, C. Canudas de Wit, and H. Béchart. Improved optimal control of dry clutch engagement. *Proc. of the 16th IFAC World Congress*, 16(1), 2005.
- P. Dolcini, C. Canudas de Wit, and H. Béchart. Lurch avoidance strategy and its implementation in AMT vehicles. *Mechatronics*, 18(1):289–300, May 2008.
- P. J. Dolcini, C. Canudas de Wit, and H. Béchart. *Dry Clutch Control for Automotive Applications*. Advances in Industrial Control. Springer-Verlag London, 2010.
- G. Ercole, G. Mattiazzo, S. Mauro, M. Velardocchia, F. Amisano, and G. Serra. Experimental methodologies to determine diaphragm spring clutch characteristics. In *SAE Technical Paper: 2000-01-1151*, March 2000.
- J. Fredriksson and B. Egardt. Active engine control for gear shifting in automated manual transmissions. *Int. J. of Vehicle Design*, 32(3-4):216–230, 2003.
- F. Garofalo, L. Glielmo, L. Iannelli, and F. Vasca. Optimal tracking for automotive dry clutch engagement. In *2002 IFAC, 15th Triennial World Congress*, 2002.
- L. Glielmo and F. Vasca. Optimal control of dry clutch engagement. In *SAE Paper: 2000-01-0837*, March 2000.
- N. Heintz, M. Mews, G. Stier, A. J. Beaumont, and A. D. Noble. An approach to torque-based engine management systems. In *SAE Technical Paper: 2001-01-0269*, March 2001.
- S. Hong, S. Ahn, B. Kim, H. Lee, and H. Kim. Shift control of a 2-speed dual clutch transmission for electric vehicle. In *2012 IEEE Vehicle Power and Propulsion Conference*, October 2012.
- G. Lucente, M. Montanari, and C. Rossi. Modelling of an automated manual transmission system. *Mechatronics*, 17(1):73–91, November 2007.
- B. Mashadi and D. Crolla. *Vehicle Powertrain Systems*. John Wiley & Sons Ltd, first edition, 2012.

- G. Mattiazzo, S. Mauro, M. Velardocchia, F. Amisano, G. Serra, and G. Ercole. Measurement of torque transmissibility in diaphragm spring clutch. In *SAE Technical Paper: 2002-01-0934*, March 2002.
- S.E. Moon, M.S. Kim, H. Yeo, H.S Kim, and S.H Hwang. Design and implementation of clutch-by-wire system for automated manual transmissions. *Int. J. Vehicle Design*, 36(1):83–100, 2004.
- A. Myklebust and L. Eriksson. Road slope analysis and filtering for driveline shuffle simulation. In *2012 IFAC Workshop on Engine and Powertrain Control, Simulation and Modeling*, October 2012a.
- A. Myklebust and L. Eriksson. Torque model with fast and slow temperature dynamics of a slipping dry clutch. In *2012 IEEE VPPC*, October 2012b.
- M. Pettersson. *Driveline Modeling and Control*. PhD thesis, Linköpings Universitet, May 1997.
- F. Vasca, L. Iannelli, A. Senatore, and G. Reale. Torque transmissibility assessment for automotive dry-clutch engagement. *IEEE/ASME transactions on Mechatronics*, 16(3):564–573, June 2011.
- M. Velardocchia, G. Ercole, G. Mattiazzo, S. Mauro, and F. Amisano. Diaphragm spring clutch dynamic characteristic test bench. In *SAE Technical Paper: 1999-01-0737*, March 1999.
- M. Velardocchia, F. Amisano, and R. Flora. A linear thermal model for an automotive clutch. In *SAE Technical Paper: 2000-01-0834*, March 2000.
- A. Wikdahl and Å. Ågren. Temperature distribution in a clutch. Master’s thesis, Linköping University, 1999.
- H. Zeng, Y. Lei, Y. Fu, Y. Li, and W. Ye. Analysis of a shift quality metric for a dual clutch transmission. In *SAE Technical Paper: 2013-01-0825*, April 2013.

Modeling, Observability and Estimation of  
Thermal Effects and Aging on Transmitted  
Torque in a Heavy Duty Truck with a Dry  
Clutch\*

C

---

\*Submitted to *IEEE/ASME Transactions on Mechatronics*.



---

# Modeling, Observability and Estimation of Thermal Effects and Aging on Transmitted Torque in a Heavy Duty Truck with a Dry Clutch

Andreas Myklebust and Lars Eriksson

*Vehicular Systems, Department of Electrical Engineering,  
Linköping University, SE-581 83 Linköping, Sweden*

## ABSTRACT

---

A transmission with both high comfort and high efficiency is the Automated Manual Transmission (AMT). To be able to control and fully utilize this type of transmission it is of great importance to have knowledge about the torque transmissibility curve of the clutch. The transmitted torque in a slipping dry clutch is therefore studied in experiments with a heavy duty truck (HDT). It is shown that the torque characteristic has little or no dependence on slip speed, but that there are two dynamic effects that make the torque vary up to 900 Nm for the same clutch actuator position. Material expansion with temperature can explain both phenomena and a dynamic clutch temperature model that can describe the dynamic torque variations is developed. The dynamic model is validated in experiments, and it is shown to reduce the error in transmitted torque from 7 % to 3 % of the maximum engine torque compared to a static model. Clutch wear is also a dynamic phenomenon that is of interest to track and compensate for, and therefore the model is augmented with an extra state describing wear. An observability analysis is performed showing that the augmented model is fully or partially observable depending on the mode of operation. In particular, by measuring the actuator position the temperature states are observable, both during slipping of the clutch and when it is fully closed. An Extended Kalman Filter (EKF), which observes the temperature states, was developed since it is straight forward to incorporate different modes of operation. The EKF was evaluated on measurement data and the estimated states converged from poor initial values, enabling prediction of the translation of the torque transmissibility curve. The computational complexity of the EKF is low and thus it is suitable for real-time applications. Modeling, parameter estimation, observer design and validation are all carried out using production sensors only and therefore it is straight forward to implement the observer in a production HDT following the presented methodology.

---

# 1 INTRODUCTION

Increasing demands on comfort, performance, and fuel efficiency in vehicles lead to more complex transmission solutions. Historically high efficiency was best accomplished with a classical Manual Transmission and comfort with a classical Automatic Transmission. The Automated Manual Transmission (AMT) is one way to combine the best from two worlds. An important part in an AMT is clutch control that has a profound effect on vehicle performance. In clutch control it is of importance to know the torque transmitted in the clutch with high precision. Models have come to play an important role in estimation and control of the transmitted torque, since torque sensors are expensive.

## 1.1 OUTLINE AND CONTRIBUTIONS

After a short survey of related work the thermal clutch model from Myklebust and Eriksson (2012) is summarized while the effects of temperature on the transmitted torque are presented in detail. In Myklebust and Eriksson (2013) the thermal effects in the clutch is shown to have a significant effect on launch control and therefore a temperature state observer is built here. The first contribution is that a wear parameter is added to the clutch model and the observability of this new model is investigated. The observability varies with the mode of operation and subsequently an observer must be able to handle different modes of operation. Therefore an Extended Kalman Filter (EKF) is built using the clutch model to allow for compensation of the thermal dynamics and wear. The validation of the observer also provides a further validation of the clutch model. However clutch torque observers have been built before, e.g. Dolcini et al. (2005a, 2010); Kim and Choi (2010); Gao et al. (2012); the contribution here lies in that the thermal effects have been observed. This makes it possible to not only know the current torque, but also the translation of the torque transmissibility curve. As a result not only feedback control but also feedforward is supported. In particular, the model makes it possible to use measurements of the actuator position when the clutch is fully closed to estimate the temperatures. The observer utilizes production sensors only and in fact, the entire synthesis process, from model building to observer validation, is performed using the production sensors. All in all this gives an observer that is light weight and implementable in production trucks.

## 1.2 SURVEY OF CLUTCH MODELS

A sketch of a dry single-plate clutch is found in Fig. 1, while in-depth explanations are found in for example Mashadi and Crolla (2012) and Vasca et al. (2011). In clutch-modeling literature a wide range of models have been proposed. The most simple models have a clutch torque that is assumed to be a controllable input, see for example Dolcini et al. (2008) or Garofalo et al. (2002). These models rely on the assumption that there is perfect knowledge of how the clutch behaves.

More advanced models include submodels for slipping and sticking torques. For example a LuGre model is used in Dolcini et al. (2005b) and a Karnopp model in Bataus et al. (2011). The former is a one-state model that captures stick-slip behavior, varying break-away force, Stribeck effect, and viscous friction. The latter includes a dead-zone around zero speed to ease the simulation of stick-slip behavior.

Models for the clutch torque during slipping commonly use a function with the following structure,

$$M_{\text{trans,k}} = \text{sgn}(\Delta\omega) n \mu R_e F_N \quad (1)$$

where  $\Delta\omega$  is the clutch slip (speed),  $n$  the number of friction surfaces,  $\mu$  the friction coefficient,  $R_e$  the effective radius and  $F_N$  the clamping (normal) force. In these models  $F_N$  is often either given as input or a static nonlinear function of clutch position,  $x$ , i.e.  $F_N = F_N(x)$ , see for example Vasca et al. (2011) or Glielmo and Vasca (2000). In particular Dolcini et al. (2010) mentions that a third-order polynomial is suitable to describe the connection between throwout-bearing position and clutch transmitted torque, mainly governed by the flat (cushion) spring characteristics. These characteristics are reported to have a decreasing slope with temperature in Cappetti et al. (2012a). However in Cappetti et al. (2012b) thermal expansion in the axial direction of the spring is shown to be a more significant effect. From a graph in Hong et al. (2012) the normal force can be seen to be speed dependent. In Dolcini et al. (2010) that speed dependency is said to be due to centrifugal forces acting on the springs in the clutch. The papers Mashadi and Crolla (2012); Moon et al. (2004) and Szimandl and Németh (2012) report of hysteresis in the diaphragm spring, that could lead to hysteresis in the normal force. In Mattiazzo et al. (2002) a temperature and wear dependency of the normal force/bearing position characteristics is shown. There it decreases with temperature. In Myklebust and Eriksson (2012); Deur et al. (2012); Cappetti et al. (2012b) and Hoic et al. (2013) the change in normal force/bearing position characteristics is explained by thermal expansion of clutch parts and the normal force is increasing with temperature. Although with an exception for low forces in Hoic et al. (2013). There the normal force is decreasing with temperature due to the expansion of a return spring, which is not present in the more common setup studied here.

When studying the components of (1) besides the normal force, it is generally recognized that  $\mu$  can depend on temperature, slip speed, and wear while  $R_e$  can depend on temperature and wear as well, (Velardocchia et al., 1999). In Vasca et al. (2011) a slip speed dependency of  $\mu R_e$  is shown, this was especially pronounced for slip speeds below  $\sim 100$  RPM. In Deur et al. (2012)  $R_e$  is assumed constant and  $\mu$  is fitted to the following regression curve:

$$\begin{aligned} \mu = & a_0 + a_1 (e^{-a_2 \Delta\omega} - 1) T_b + (a_3 - a_4 \ln(\Delta\omega)) T_b^2 \\ & + (a_5 - a_6 \Delta\omega) F_N + a_7 T_b F_N \end{aligned} \quad (2)$$

where  $T_b$  is the temperature of the clutch body and  $a_0 - a_7$  are curve parameters.

It can be difficult to separate which parameter in (1) that is the reason for a change in  $M_{\text{trans},k}$ . Therefore the clutch torque is often studied as a lumped model. In Velardocchia et al. (1999)  $M_{\text{trans},k}$  is seen to decrease with temperature and  $\Delta\omega$ . However there are large variations with wear. In Ercole et al. (2000)  $M_{\text{trans},k}$  initially decreases with temperature for low temperatures and then increases for medium and high temperatures. Similarly there are variations with wear and in addition temperature-torque hysteresis are reported. In Velardocchia et al. (2000), Wikdahl and Ågren (1999) and Myklebust and Eriksson (2012) temperature models are established, but only Myklebust and Eriksson (2012) includes the effect of the temperature on  $M_{\text{trans},k}$ . The models in Velardocchia et al. (2000) and Wikdahl and Ågren (1999) could be complemented with (1) and (2) in order to give the clutch torque. Although that approach requires more parameters to be estimated compared to the model in Myklebust and Eriksson (2012). Furthermore the clamping load needs to be measured, which is not available in production vehicles. In Myklebust and Eriksson (2012) only sensors available in production vehicles are used. Furthermore the clutch is only modeled during slipping, there is no slip-speed dependency and torque is increasing with temperature, in accordance with the observations made there. It is also computationally simple enough to be used in control applications.

## 2 EXPERIMENTAL SETUP

Two rear-wheel drive Heavy Duty Trucks (HDT), called Ara and Ernfrid, have been used for experiments. Both are equipped with a 14-speed AMT and a 16.4 liter V8 capable of producing 3500 Nm. Ara weighs 105 tonnes and Ernfrid 21 tonnes. The clutch, that is in focus here, is a dry single-plate pull-type normally closed clutch. A schematic is seen in Fig. 1. The clutch is actuated by an electric motor that through a worm gear moves a hydraulic master cylinder that in turn moves a slave piston and via a lever pulls the throwout bearing. Both motor position,  $x_m$ , and slave piston position,  $x_p$ , are measured. In order to bring  $x_p$  to the same range as  $x_m$  and make data sets with different amount of wear comparable to each other the signal  $x = x_p - x_{0,\text{ref}}$  is used for the slave position, see Fig. 1.

The trucks used here are only equipped with production sensors, namely: engine speed, input shaft speed, coolant temperature, motor position and slave position. Hence no exact torque measurement, is available. In order to get a measurement of the clutch torque the reported engine torque is compensated for inertia effects of the engine and flywheel. The main benefit of this setup, with only production sensors, is that the resulting model and observer is directly applicable on a production truck. Furthermore the procedure for experiments, model building, model validation, and observer evaluation can easily be performed on other vehicles equipped with a dry clutch. On the other hand, the drawback, compared to a test stand, e.g. Velardocchia et al. (1999); Moon et al. (2004) or Deur et al. (2012), is fewer and less precise sensors. All these mentioned test

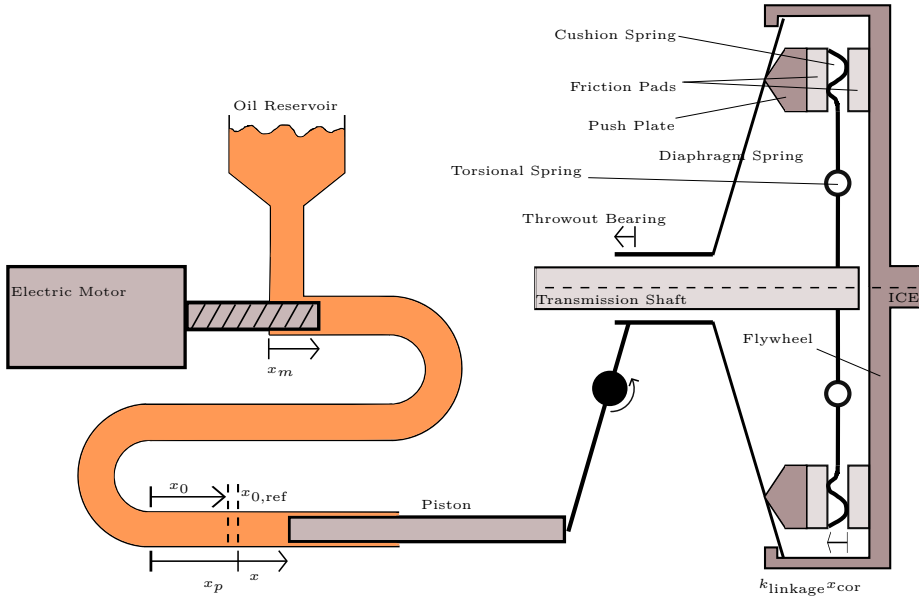


Figure 1: A schematic over the actuator and the dry single-plate pull-type clutch studied here.  $k_{\text{linkage}}$  is the combined ratio of all levers between the piston and the push plate.

stands consists of a stand-alone dry clutch that is cooled towards the stagnated room-temperature air. In a truck there might be an airflow, the clutch is installed below to the truck floor, bolted to the transmission, and especially the flywheel is bolted to a 1 tonne,  $\sim 90^\circ\text{C}$  warm engine. Naturally all this leads to different temperature dynamics.

### 3 CLUTCH MODEL

The modeled clutch is a single-plate dry clutch with two contact surfaces, see Fig. 1 for an overview. Torque is transferred between the flywheel and the clutch disc through friction. The friction is modeled as coulomb friction with stick-slip behavior. This is simply modeled with two friction coefficients, one static,  $\mu_s$ , and one dynamic,  $\mu_k$ . By defining the ratio of the friction coefficients,  $k_\mu = \frac{\mu_s}{\mu_k}$  the equation for the transmittable torque during sticking (the stiction torque) becomes:

$$M_{\text{trans},s} = k_\mu M_{\text{trans},k} \quad (3)$$

where  $M_{\text{trans},k}$  is given by (27). The modeling of the two modes, slipping and locked-up, is done by a state machine, described in Section 3.1. However here the focus is upon the clutch when it is slipping and it is the equations for the

clutch in slipping mode that is used by the observer in Section 4. Nevertheless it is useful to discuss some aspects of the mode switching to better understand the different modes introduced in Section 4.1.

### 3.1 LOCK-UP/BREAK-APART LOGIC

The clutch model has two modes, locked and slipping mode. While in locked mode, the clutch behaves as one rigid body, whereas during slipping the clutch consists of two bodies where each one has an angular velocity and position. Torque from the ICE,  $M_e$ , and transmission,  $M_t$ , are inputs and angular velocity on both sides,  $\omega_e$  and  $\omega_t$ , respectively, are states. The equations are:

Conditions for switching from slipping to locked mode:

$$\omega_e = \omega_t \quad (4)$$

$$|M_{\text{trans}}| \leq M_{\text{trans,s}} \quad (5)$$

Equations for the clutch in locked mode:

$$M_e - M_t = (J_e + J_{\text{fw}} + J_c) \dot{\omega}_e \quad (6)$$

$$\omega_c = \omega_e \quad (7)$$

$$M_{\text{trans}} = \frac{M_e J_c + M_t (J_e + J_{\text{fw}})}{J_e + J_{\text{fw}} + J_c} \quad (8)$$

Conditions for switching from locked to slipping mode:

$$|M_{\text{trans}}| \geq M_{\text{trans,s}} \quad (9)$$

Equations specific to the clutch in slipping mode:

$$M_{\text{trans}} = \text{sgn}(\underbrace{\omega_e - \omega_t}_{\Delta\omega}) M_{\text{trans,k}} \quad (10)$$

$$M_e - M_{\text{trans}} = (J_e + J_{\text{fw}}) \dot{\omega}_e \quad (11)$$

$$M_{\text{trans}} - M_t = J_c \dot{\omega}_t \quad (12)$$

The state machine is validated in Myklebust and Eriksson (2013).

### 3.2 SLIPPING TORQUE MODEL STRUCTURE

The rest of this section, Section 3, discusses how to model the clutch during slipping, or more precise, how to model  $M_{\text{trans,k}}$ . This discussion is an extension of the one in Myklebust and Eriksson (2012). As mentioned in Section 1.2,  $M_{\text{trans,k}}$  depends on several factors such as, actuator position, temperatures, rotational speeds and wear. In Fig. 2 it is seen how the transmitted torque varies with up to 900 Nm for a given position. Furthermore components are non-linear

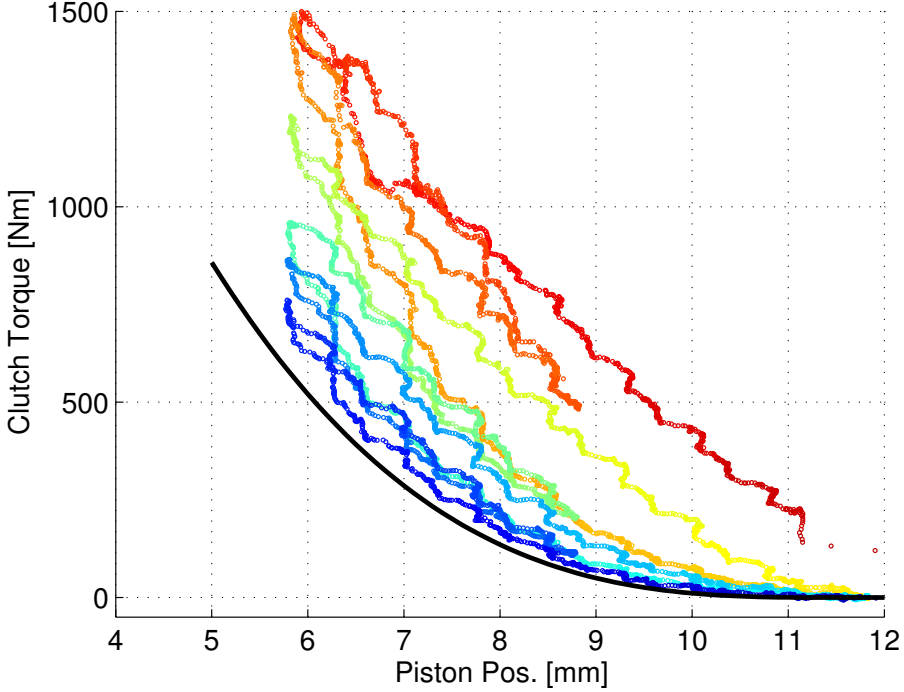


Figure 2: The clutch position,  $x$ , has been ramped back and forth while the clutch torque has been measured. The transmitted torque clearly depends on something more than the clutch position, in particular there is a drift with time (the color changes with time, blue=0 s and red=75 s). The torque difference between the first and last ramp is up to 900 Nm. The black line is a parameterization of (16).

e.g. spring characteristics, hysteresis, etc. However during experiments no clear hysteresis have been detected and therefore not modeled. Due to the difficulties involved in measuring wear, especially when access to test equipment is limited and non-exclusive, wear has been assumed slow enough to not have a significant effect in the experiments. The only exception is the parameter  $x_{0,\text{ref}}$  of Section 3.4, which is directly affected by the thickness of the friction pads.  $x_{0,\text{ref}}$  had to be parameterized to each measurement session (months apart). During the life time of an HDT more parameters would probably need to be adapted continuously. However more prolonged testing is required to reach any conclusion. With the above assumptions and the addition of  $n = 2$  leaves the clutch model structure at:

$$M_{\text{trans},k} = 2\mu(\Delta\omega, T) R_e(T) F_N(x, T, \omega_e) \quad (13)$$

In Section 3.4 the temperature effect will be explained by a changing  $F_N$ , at least for medium temperatures of the clutch. Nevertheless with the available sensors there is no way to truly separate the effects between the parameters. Therefore the model structure will be,

$$M_{\text{trans,k}} = M_{\text{trans,k}}(x, T, \Delta\omega) \quad (14)$$

In the next section the slip dependency will be investigated and in the subsequent section the position and temperature dependency will be handled.

### 3.3 SLIP DEPENDENCY

Slip speed,  $\Delta\omega$ , dependency is recognized in the literature, (Vasca et al., 2011), (Velardocchia et al., 1999), this is therefore further investigated here. Experiments have been carried out as follows. A truck has been driven to an uphill and has been kept stationary by slipping the clutch at a constant position. This way the vehicle will accelerate forwards if more torque is transmitted and backwards if less torque is transmitted. Furthermore it is easy to initially keep the input shaft speed stationary this way, and by doing so the engine speed can be used to control the slip speed. Slip-speed steps are made and an abrupt change in torque/input shaft acceleration should be seen if there is a slip-speed dependency, Fig. 3. Note that the engine torque will see a transient during the edges of a step due to the acceleration of the engine. A smaller transient is present in the clutch torque signal due to imperfections in the compensation for the acceleration. No significant change is seen in the input shaft acceleration and no correlation between steady-state clutch torque and slip speed is seen neither, Fig 4. Therefore (14) can be reduced to

$$M_{\text{trans,k}} = M_{\text{trans,k}}(x, T) \quad (15)$$

This is somewhat in contrast to the data in Velardocchia et al. (1999) where a slip dependency is shown. The slip has only been investigated at relatively large speeds and does therefore not contrast the data in Vasca et al. (2011).

### 3.4 TEMPERATURE EFFECTS AND MODELS

The shape of the torque transmissibility curve is mainly due to the cushion spring characteristics. In Dolcini et al. (2010) it is mentioned that this curve can be described by a third order polynomial,

$$M_{\text{ref}}(x_{\text{ref}}) = \begin{cases} a(x_{\text{ref}} - x_{\text{ref,ISP}})^3 + \\ + b(x_{\text{ref}} - x_{\text{ref,ISP}})^2 & \text{if } x_{\text{ref}} < x_{\text{ref,ISP}} \\ 0 & \text{if } x_{\text{ref}} \geq x_{\text{ref,ISP}} \end{cases} \quad (16)$$

where  $x_{\text{ISP}}$  (Incipient Sliding Point) is the kiss point, where the push plate and clutch disc first meet and torque can start to transfer. There is no first or

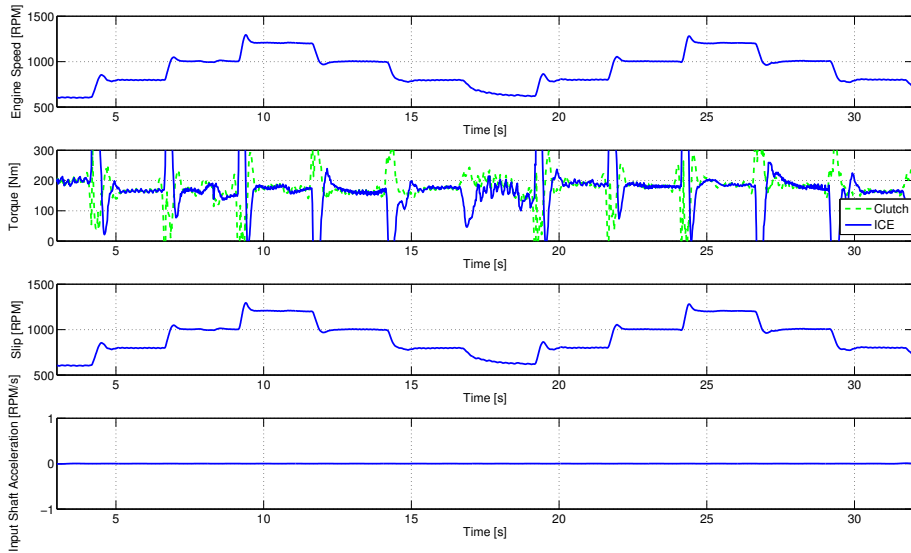


Figure 3: Slip steps are made through engine-speed control when the truck is held stationary in a slight uphill using a constant clutch position. No reaction is seen in neither clutch torque or input shaft acceleration.

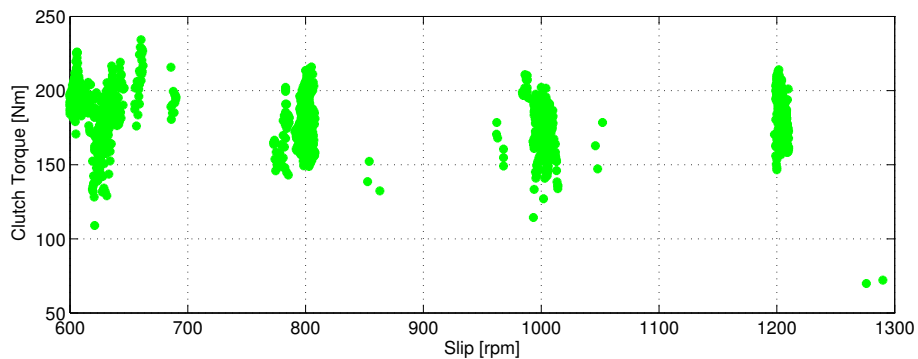


Figure 4: The data points from Fig. 3 when the engine speed is constant. No correlation is seen between clutch torque and slip speed.

zeroth order term in the equation since it is desired to have zero torque and derivative at  $x_{\text{ref,ISP}}$ . The exact value of  $x_{\text{ISP}}$  can be difficult to find since the transmissibility curve is very flat around  $x_{\text{ISP}}$ . However it is only important to find a  $x_{\text{ISP}}$  that gives a good curve fit, as errors will be small near  $x_{\text{ISP}}$ . A suggestion in Mattiazzo et al. (2002) is to define  $x_{\text{ISP}}$  as the point that transmits a certain small torque. That method should give sufficient estimates of  $x_{\text{ISP}}$  for

the application described here.

Experimental data confirms that (16) is a good approximation for a given temperature,  $T_{\text{ref}}$ , see Fig. 2. However during slipping of the clutch, heat is dissipated from the friction surface into the cast iron parts of the clutch that naturally will expand. When the actuator motor is fully retracted (position=0) the expansion can be measured through the position sensor on the slave. This slave position is called the zero position,  $x_0$ , see Fig. 1.

A set of experiments has been performed to investigate the dynamics of the clutch expansion. In order to be able to measure the zero position during heating, the clutch has been alternating between closed and slipping with short time intervals. After some time of heating the clutch has been held closed for a prolonged time while the zero position has been constantly monitored as the clutch cools down. The measurement results are found in Figure 5. The zero position increases in a repeatable way with dissipated energy in the clutch and decays in an exponential manner with time. This supports the hypothesis that temperature is causing the change in zero position.

#### MATERIAL EXPANSION ANALYSIS

In order to see that the change in zero position is due to material expansion, the temperature increase is calculated in two ways. During the first heating period of Fig. 5, 1.5 MJ of energy is dissipated. The pressure plate and flywheel have a combined mass of 81 kg and are made of cast iron that has a specific heat of 0.5 kJ/(kg K), (Nording and Österman, 1999). If cooling of the clutch is neglected a slightly high estimation of the temperature increase is obtained.

$$\frac{1.5 \cdot 10^6}{500 \cdot 81} = 37 \text{ K}$$

The measured expansion of the clutch during the same period is 0.3 mm at the piston. With a linkage ratio of 8.8, a 100 mm thick clutch and an expansion coefficient for cast iron of  $11 \cdot 10^{-6} \text{ K}^{-1}$ , (Nording and Österman, 1999), this corresponds to a temperature increase of,

$$\frac{0.3}{8.8 \cdot 100 \cdot 11 \cdot 10^{-6}} = 30 \text{ K}$$

The two temperature estimates are practically the same, which indicates that the measured expansion depends on temperature.

#### EXPANSION MODEL

In order to model the expansion a temperature model is required. In Velardocchia et al. (2000) a linear model with one thermal mass in the pressure plate and one in the flywheel is proposed. All parts of the clutch are cooled towards the air in the clutch housing. Here the model is extended to capture the changes in the housing temperature,  $T_h$ . In contrast to Velardocchia et al. (2000) the

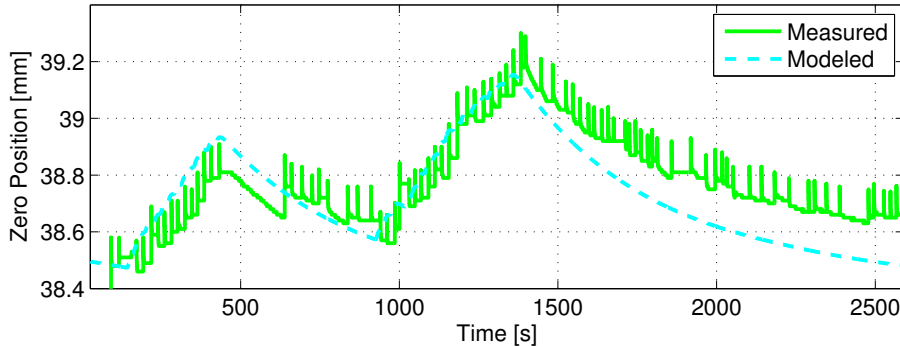


Figure 5: The clutch has been heated through slipping and then left to cool down. The zero position has been recorded as a measure of the expansion. The temperature model (17)-(20) shows good agreement with the measurement. Parameters have been fitted to a separate set of data.

clutch studied here is mounted in a vehicle, therefore the clutch is, in addition, thermally connected to both the ICE and transmission. However only a few percent of the dissipated power,  $P$ , goes into the transmission, Wikdahl and Ågren (1999). Therefore the heat flow to the transmission has been neglected. Moreover it has been found that the thermal masses of the flywheel and pressure plate can be taken as one mass,  $(mc_p)_b$ , for the clutch body, without losing accuracy with respect to the expansion. For an electrical analogy of the model see Fig. 6. The corresponding equations are:

$$(mc_p)_b \dot{T}_b = k_{\text{ICE}2b}(T_{\text{coolant}} - T_b) + k_{b2h}(T_h - T_b) + P \quad (17)$$

$$(mc_p)_h \dot{T}_h = k_{b2h}(T_b - T_h) + k_{h2\text{amb}}(T_{\text{amb}} - T_h) \quad (18)$$

where,

$$P = M_{\text{trans},k} \Delta\omega \quad (19)$$

In order to connect the temperature model with the change in zero position, the levers and the expansion of the clutch body as function of temperature are assumed linear.

$$x_0 = k_{\text{exp},1} (T_b - T_{\text{ref}}) + x_{0,\text{ref}} \quad (20)$$

The eight parameters in the equations have been fitted against measured data and the validation results, on a different set of data, can be seen in Fig. 5. Using these results the piston position can be corrected for the expansion effect to correspond to the actual compression of the flat spring, see Fig. 1.

$$\Delta x_0 = x_0 - x_{0,\text{ref}} \quad (21)$$

$$x_{\text{cor}} = x - \Delta x_0 \quad (22)$$

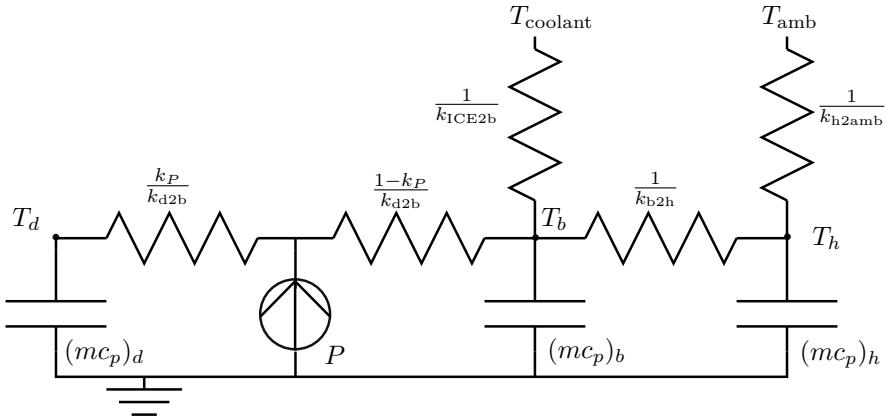


Figure 6: An electrical analogy of the temperature model (23)-(25). If  $(mc_p)_d = 0$  the model can also be described by (17)-(18).

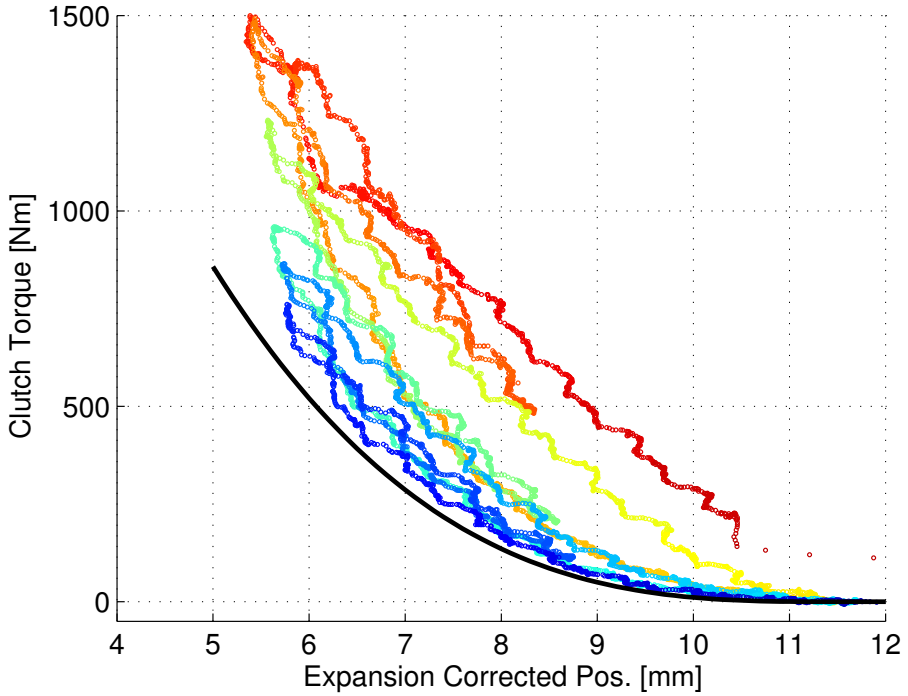


Figure 7: The data from Figure 2 has been corrected for expansion of the clutch body using (20)-(22). The correction is not sufficient to explain the torque drift.

Nevertheless the expansion model does not fully explain the torque drift, see Fig. 7. The time scale in Fig. 2 is significantly smaller than that of Fig. 5. The torque drift is also much larger than what is explained by the modeled expansion. In fact the remaining relative torque drift is of the same magnitude as that reported in Cappetti et al. (2012b) due to flat spring axial expansion. This has led to the hypothesis that the clutch disc, or at least the flat spring, is also expanding with heat. In particular the clutch disc/flat spring has a much smaller (thermal) mass, which could correspond to the faster time constant phenomenon seen in the data.

#### INCLUDING FAST DYNAMICS

The clutch disc temperature,  $T_d$ , has been modeled in a similar fashion, see Fig. 6 for an electrical analogy and below for equations.

$$(mc_p)_b \dot{T}_b = k_{\text{ICE2b}}(T_{\text{coolant}} - T_b) + k_{\text{b2h}}(T_h - T_b) + k_{\text{d2b}}(T_d - T_b) + k_P P \quad (23)$$

$$(mc_p)_h \dot{T}_h = k_{\text{b2h}}(T_b - T_h) + k_{\text{h2amb}}(T_{\text{amb}} - T_h) \quad (24)$$

$$(mc_p)_d \dot{T}_d = k_{\text{d2b}}(T_b - T_d) + (1 - k_P)P \quad (25)$$

A new situation with this extended model is that the dissipated energy has to be split between the clutch disc and the body. In the model it is split by the parameter  $k_P$ , which is 1 if all energy goes to the body and 0 if all goes to the disc. However the model is not sensitive to  $k_P$  due to two facts. Firstly the vast difference in time constants, a factor of  $\sim 50$ , between the disc and the body decouples (23) from (25), i.e.  $k_{\text{d2b}}(T_d - T_b) + k_P P \approx (1 - k_P)P + k_P P = P$ , leaving the dynamics of  $T_b$  almost unchanged. Secondly the parameters are fitted to data, i.e. if  $k_P$  is 0 instead of 0.5 the value of  $(mc_p)_d$  and  $k_{\text{d2b}}$  will double, leaving the dynamics of  $T_d$  almost unchanged. In the data the expansion has been seen to lag the dissipated power. The lag is maximized by  $k_P = 0$  this is thus the choice of  $k_P$ .

The expansion of the clutch disc is modeled by extending (20) with an extra term

$$\begin{aligned} \Delta x_0 &= k_{\text{exp}}(T_b - T_{\text{ref}}) + k_{\text{exp},2}(T_d - T_{\text{ref}}) = \\ &= k_{\text{exp}}(T_b - T_{\text{ref}}) + k_{\text{exp},2}((T_d - T_b) + (T_b - T_{\text{ref}})) = \\ &= \underbrace{(k_{\text{exp}} + k_{\text{exp},2})}_{k_{\text{exp},1}}(T_b - T_{\text{ref}}) + k_{\text{exp},2}(T_d - T_b) \end{aligned} \quad (26)$$

where the second term was practically zero during the zero-position measurements due to the fast dynamics of  $T_d$ . Therefore the new parameters can be estimated separately from the old parameters. After estimation of the new parameters the position can be corrected with (23)-(26) and Fig. 8 is obtained.

The model works well until the temperatures become too high (state  $T_d$  reaches more than 200 °C). It has been found empirically that saturating the

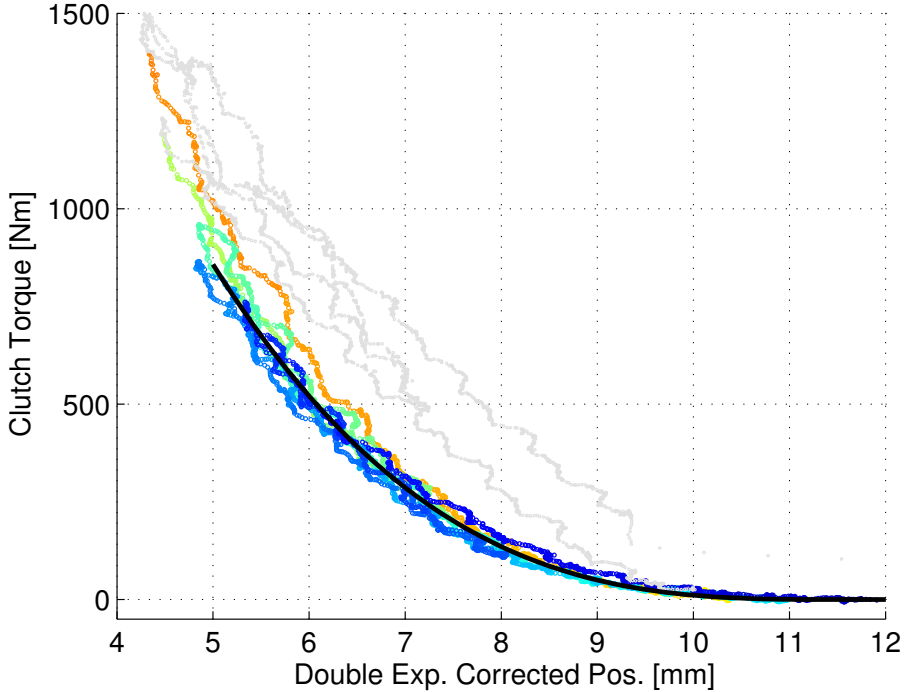


Figure 8: The data from Figure 2 has been corrected for expansion of the clutch body using (22) and (26). The correction explains the torque drift until the temperatures get too high (somewhere when state  $T_d$  becomes greater than  $200\text{ }^\circ\text{C}$ , marked with gray thin lines).

term  $(T_d - T_b)$  at  $110\text{ }^\circ\text{C}$  improves the model at higher temperatures. One should note that values of the temperature states have not been validated against any measurement but they have reasonable magnitudes.

The transmitted torque can now be calculated as,

$$M_{\text{trans},k} = M_{\text{ref}}(x_{\text{cor}}) \quad (27)$$

Note that  $x_{\text{cor}}$  increases with temperature which in turn makes  $M_{\text{trans},k}$  increase with temperature. This is in contrast with the data in Velardocchia et al. (1999) where the torque is decreasing with temperature. Although in the experiments performed here the clutch mostly has a medium to high temperature and could comply with the data in Ercole et al. (2000).

#### POWER AS INPUT?

It can be discussed whether the dissipated power,  $P$ , should be considered an input signal since it is calculated using (19). On one hand, calculating the

power from the measured torque gives a better power signal that in turn gives a better estimate of the current transmissibility curve, which could be used for feedforward in control applications. On the other hand the measured torque is not always available, e.g. some special driving scenarios, when evaluating new controllers through simulation, or in the prediction made by a model-based controller. Then  $P$  has to be calculated using the modeled torque. In Section 3.5 the model will be evaluated using both a measured  $P$  and a modeled  $P$ .

In summary, the model is a three state model with one static non-linearity. All calculations are simple and therefore the model is suitable for running in real time, for example in a clutch-control application.

### 3.5 CLUTCH MODEL VALIDATION

The model has been validated on several data sets, separate from those used for parameter identification, and one of these is shown in Fig. 9. At the end of the torque pulses, the modeled torque drops faster than the measured torque, when the clutch is fully opened in 0.3 s. This is however believed to be due to delays in the computation of the engine torque, sensors and other data processing. Therefore the residuals,  $M_{\text{sim}} - M_{\text{meas}}$ , have been filtered using a moving median of five samples (10 Hz). The result is presented in Fig. 10. The residuals are less than 200 Nm and most of the time less than 100 Nm. Considering that 100 Nm is less than 3 % of maximum engine torque, the model works well. In fact the estimated engine torque can have errors of similar magnitude.

Note that when the dissipated power is measured the simulation shows a slightly low clutch torque. If instead the dissipated power is calculated from

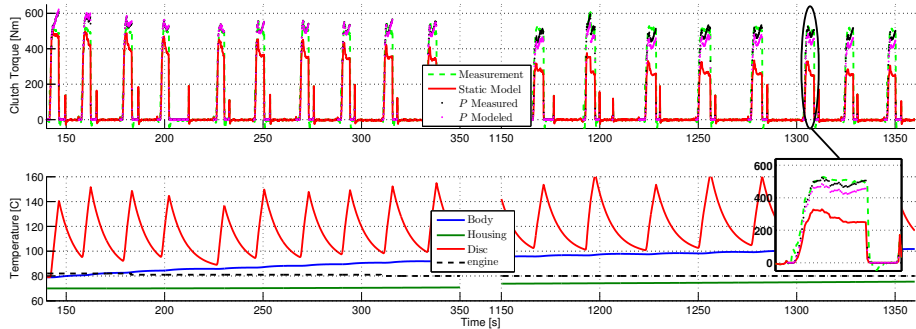


Figure 9: The dynamic torque model shows good agreement with measurements in a validation data set. There is a slight decay in torque when  $P$  is modeled instead of measured. However both implementations are significant improvements compared the static model,  $M_{\text{trans}} = M_{\text{ref}}(x)$ , with parameters fitted to the rising edge of the first torque pulse. The open-loop simulation started at 0 seconds. In the lower plot  $P$  is measured.

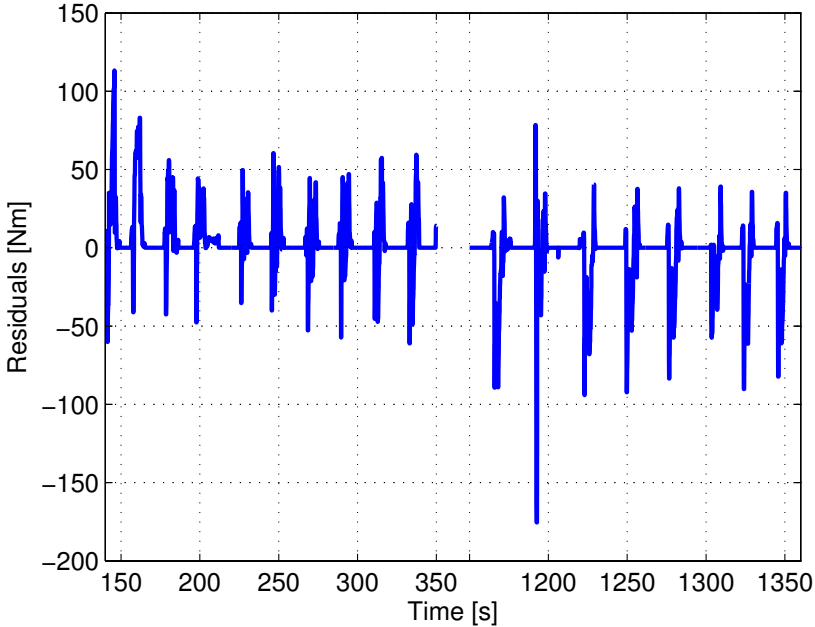


Figure 10: The residuals between the model and data presented in Figure 9. The residuals are less than 200 Nm and most of the time less than 100 Nm. Or in other words, most of the time less than 3 % of maximum ICE torque. The mean absolute relative error is a mere 0.3 %

the simulated torque the torque error makes the simulated power dissipation too low and therefore the temperature states get lower. In turn this will lead to even lower simulated torque in the next torque pulse. This is the explanation for the decay in the simulated torque when also the power is simulated. In spite of this it still models the torque better than the more common static model.

A validation of a launch is shown in Fig. 11. The static and dynamic models are compared to measurement data. The dynamic model has a small error that is always less than 104 Nm, and has better performance than the static model.

In other data sets it has been seen that when  $T_d$  is greater than 200 °C the model deteriorates. This however is of small concern since these temperatures are only reached during extreme driving, where other measures can be taken. The accuracy of the model has also been seen to be less good when the truck is cold.

The clutch temperatures can not be quantitatively validated as no temperature measurements are available. Therefore only a qualitative validation is performed, showing that the magnitudes of the temperature states are reasonable for an HDT clutch, see Fig. 9 and 11.

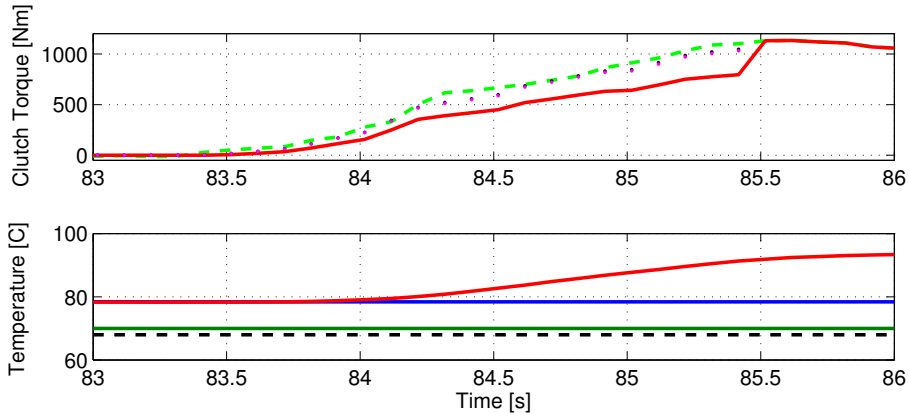


Figure 11: The dynamic torque model shows good agreement with measurement data of a start. The open-loop simulation started at 0 seconds. Line colors and styles are the same as in Fig. 9. The clutch is locked up when there are no black or magenta dots. In the lower plot  $P$  is measured.

## 4 OBSERVER

As shown in Myklebust and Eriksson (2013) the thermal effects in a dry clutch can have a significant effect on launch control of a vehicle. Controllers that assume the clutch torque to be an controllable input signal, e.g. Dolcini et al. (2008) and Garofalo et al. (2002), would need an underlying compensation of the thermal effect. This could be done like in Deur et al. (2012), however there measurements of the temperature is used. Due to the difficulties involved in measuring the temperatures of rotating bodies, this is not a feasible solution for production vehicles. Instead the here proposed model can be used to estimate the temperatures. With the help of an observer the model can be made insensitive to poor initial values and wear (here only considered as a change in  $x_{0,\text{ref}}$ ). The latter is taken care of by adding a fourth equation to the state space (23)-(25).

$$\dot{x}_{0,\text{ref}} = 0 \quad (28)$$

The following definitions are made: state vector  $X = [T_b, T_h, T_d, x_{0,\text{ref}}]^T$ , input vector  $U = [x, P, T_{\text{coolant}}, T_{\text{amb}}]^T$  and intermediate output variable  $\tilde{y} = [x_0, x_{\text{cor}}]^T$ . Now, with (26), (21), (22), (27) and (16) the model can be expressed as:

$$\dot{X} = AX + BU \quad (29)$$

$$\tilde{y} = CX + DU + \begin{bmatrix} -1 \\ 1 \end{bmatrix} k_{\text{exp},1} T_{\text{ref}} \quad (30)$$

where,

$$A = \begin{pmatrix} -\frac{k_{b2h} + k_{ICE2b} + k_{d2b}}{(mc_p)_b} & \frac{k_{b2h}}{(mc_p)_b} & \frac{k_{d2b}}{(mc_p)_b} & 0 \\ \frac{k_{b2h}}{(mc_p)_h} & -\frac{k_{b2h} + k_{h2amb}}{(mc_p)_h} & 0 & 0 \\ \frac{k_{s2b}}{(mc_p)_d} & 0 & -\frac{k_{s2b}}{(mc_p)_d} & 0 \\ 0 & 0 & 0 & 0 \end{pmatrix} \quad (31)$$

$$B = \begin{pmatrix} 0 & 0 & \frac{k_{ICE2b}}{(mc_p)_b} & 0 \\ 0 & 0 & 0 & \frac{k_{h2amb}}{(mc_p)_h} \\ 0 & \frac{1}{(mc_p)_d} & 0 & 0 \\ 0 & 0 & 0 & 0 \end{pmatrix} \quad (32)$$

$$C = \begin{pmatrix} C_1 \\ C_2 \end{pmatrix} = \begin{pmatrix} k_{exp,1} - k_{exp,2} & 0 & k_{exp,2} & 1 \\ -k_{exp,1} + k_{exp,2} & 0 & -k_{exp,2} & 0 \end{pmatrix} \quad (33)$$

$$D = \begin{pmatrix} D_1 \\ D_2 \end{pmatrix} = \begin{pmatrix} 0 & 0 & 0 & 0 \\ 1 & 0 & 0 & 0 \end{pmatrix} \quad (34)$$

and the measurable model outputs are,

$$y = \begin{bmatrix} x_0 \\ M_{trans,k} \end{bmatrix} = \begin{bmatrix} \tilde{y}_1 \\ M_{ref}(\tilde{y}_2) \end{bmatrix} \quad (35)$$

However all measurements are not always available. The zero position is only available when the clutch is fully closed and slipping torque only when the clutch is slipping. This naturally affects observability and observer design, and is therefore analyzed below.

#### 4.1 OBSERVABILITY

When studying the observability of a system the structure of the output function (35) is important. Due to the varying nature of that structure in this application it is natural to break down the problem into different cases: fully closed, engaged and locked-up, engaged and slipping, and open clutch.

##### FULLY CLOSED CLUTCH

When the clutch is fully closed it is not restrictive to assume that the clutch is locked up. Then the clutch torque is a direct response of the engine torque and not temperature or clamp load dependent. Therefore the transmitted torque does not contribute with information regarding the states, but the zero position does and can be measured so in this mode the output is:

$$y = C_1 X - k_{exp,1} T_{ref} \quad (36)$$

This subsystem, (29) together with (36), is locally observable according to linear theory, (Rugh, 1996).

#### ENGAGED AND LOCKED-UP CLUTCH

The clutch does not need to be fully closed in order to be locked-up. If the clutch is not fully closed the piston position does not contain any information about the thermal expansion since an expansion does not alter the piston position, instead it compresses the cushion spring. Furthermore the transmitted torque only gives a lower bound of the stiction torque and therefore the states can be bounded, but not observed.

#### ENGAGED AND SLIPPING CLUTCH

When the clutch is slipping the output is given by:

$$y = M_{\text{ref}}(C_2X + D_2U + k_{\text{exp},1}T_{\text{ref}}) \quad (37)$$

This subsystem is structured as a linear state space and a non-linearity on the output. The non-linearity, i.e. the torque transmissibility curve, is invertible in the range where the clutch is engaged. Therefore the nonlinearity does not affect the observability of this mode.

When looking at the structure of the rest of the subsystem, (29) together with the second row of (30), it can be seen that  $x_{0,\text{ref}}$  does not enter  $y$  nor any of its time derivatives. Therefore  $x_{0,\text{ref}}$  is not observable in this mode. If this state is removed the observability matrix receives full rank. In conclusion the temperature states are locally observable whereas  $x_{0,\text{ref}}$  is not observable

#### OPEN CLUTCH

When the clutch is open the transmitted torque is simply zero. This gives a bound on the kiss point and thereby a bound on the states but no observability.

Since the system is unobservable in certain modes a trajectory that takes the system into the observable modes is required to acquire observability for the system. The only mode in which all states are observable is fully closed clutch. Conveniently enough this mode is frequently visited.

## 4.2 OBSERVER SELECTION AND PRECAUTIONS

Since the system is observable an EKF can be used to observe the states. Two main reasons exist for choosing the EKF. First the implementation is straight forward and the EKF has been successful in many applications, especially if the non-linearity is mild. Second it is easy to adjust the number of measurements according to system mode with the EKF. In addition to the different modes discussed in Section 4.1 there are driving scenarios when  $M_e$ , and thereby  $y_2$ , is not available or reliable.

When the system is in a mode that makes one or more states unobservable the respective covariances will naturally grow, this helps the estimate to converge quickly when the state(s) become observable again, see e.g. Höckerdal et al.

(2011). If the system stays in an unobservable mode for a prolonged time the covariance can grow too large and cause numerical issues in the observer. Nevertheless there exists a simple remedy to this problem; limit the covariance with its initial value, only the diagonal elements need to be limited, (Höckerdal et al., 2011). This needs to be considered in an online application.

Another practical issue is that the torque estimate from the engine control unit is slightly biased. Even if just by a few Newton meters the bias has a profound effect on the estimate during longer periods of open clutch. When the clutch is fully open the temperature would have to increase immensely in order to explain a non zero torque output. This can be remedied in many ways and a simple method is to set the torque to zero, when it is under a threshold governed by the accuracy. Here the threshold on measured torque was set to 20 Nm.

### 4.3 SELECTION OF EKF COVARIANCE MATRICES

In order to make the covariance matrix for the measurement noise roughly match data the following procedure has been carried out: Both measurements have been manually examined at arbitrary time points and the amplitude of the noise was taken as the standard deviation for an assumed white noise. Then the variances are put on the diagonal elements of the covariance matrix:

$$R = \begin{bmatrix} 10^{-2} & 0 \\ 0 & 10^2 \end{bmatrix} \quad (38)$$

The covariance matrix for the process noise is also given a diagonal structure as this gives one parameter to tune for each equation. Manual tuning of the observer resulted in the following matrix:

$$Q = \begin{bmatrix} 10^{-1} & 0 & 0 & 0 \\ 0 & 10^{-3} & 0 & 0 \\ 0 & 0 & 10^{-1} & 0 \\ 0 & 0 & 0 & 10^{-8} \end{bmatrix} \quad (39)$$

where  $Q(4,4)$  has a very low value since  $x_{0,\text{ref}}$  varies very slowly.

### 4.4 OBSERVER EVALUATION

The observer has been validated using measurement data. Since no temperature measurements are available the model has been simulated using manually tuned initial values,  $[T_b, T_h, T_d, x_{0,\text{ref}}] = [80, 70, 80, 38]$ . Given these initial values the model predicts the torque and zero position well, see Fig. 12, and therefore these trajectories of the temperature states are those sought by the observer. To test the convergence of the observer the states are given poor initial values,  $[T_b, T_h, T_d, x_{0,\text{ref}}] = [20, 20, 20, 41]$ , see Fig. 12. The

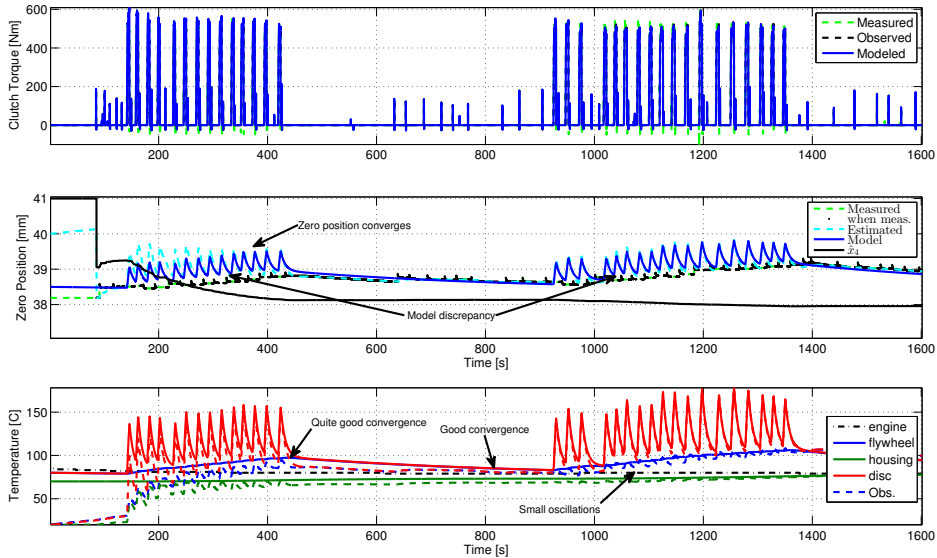


Figure 12: The model simulates the torque and zero position well given good initial values. The observer states are able to approach the model states although the initial states for the observer are far off. There is some oscillation in  $T_b$  due to a model discrepancy that is present in the  $x_0$  signal but not the torque signal.

estimate-error covariance matrix is initially set to,

$$P_0 = \begin{bmatrix} 15 & 0 & 0 & 0 \\ 0 & 15 & 0 & 0 \\ 0 & 0 & 15 & 0 \\ 0 & 0 & 0 & 15 \end{bmatrix} \quad (40)$$

Note that the value of 15 is relatively seen largest for the initial estimation error of  $x_{0,\text{ref}}$ . During the first 85 s almost nothing happens since the clutch is open which makes the system unobservable. Only a slight increase in temperature is present since the observed states are below their equilibrium points. At 85 s when the clutch is closed (neutral gear) the sum of  $\hat{x}_{0,\text{ref}}$  and the expansion should equal the measured  $x_0$ . As a consequence  $\hat{x}_{0,\text{ref}}$  is drastically improved due to the large value in  $P_0(4, 4)$ , while the temperature estimates are not. As the temperature estimates continue to slowly rise towards equilibrium  $\hat{x}_{0,\text{ref}}$  follows. At 142 s when the clutch is slipping for the first time the temperature states start to converge quicker. Between slipping phases in the data the clutch is fully closed and the zero position is given time to converge. Around 400 s  $\hat{x}_{0,\text{ref}}$  approaches the models value and subsequently the temperature states do so as well. After 430 s the clutch is closed over a longer period of time.

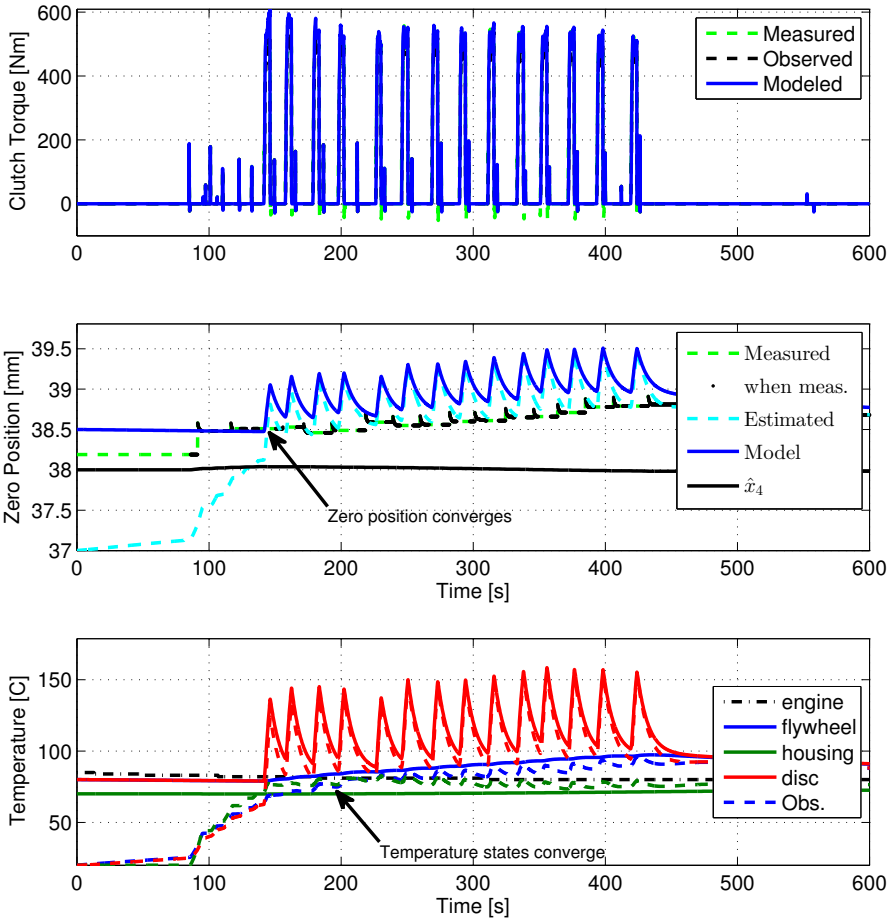


Figure 13: When  $\hat{x}_{0,\text{ref}}$  has a good initial value and low covariance the temperature states converge quickly, compared to the case in Fig. 12.

During this time the convergence rate is low since the zero position is estimated well. The small oscillations seen in  $\hat{T}_b$  are a consequence of that the observer is compensating for the discrepancy between modeled and measured zero position without losing accuracy in the torque estimate.

The observer is working, although it takes time to converge. However this is an extreme case, the temperature states could be given better initial guesses using the engine temperature and in particular,  $x_{0,\text{ref}}$  does not change while the truck is powered off. Therefore  $\hat{x}_{0,\text{ref}}$  can be given its final value from the last run as an initial guess, and  $P_0(4,4)$  can be given the end value of  $P(4,4)$  from the last run. For the case in Fig. 12 the end values are  $\hat{x}_{0,\text{ref}} = 38$  mm (as in

the model) and  $P_0(4, 4) = 2 \cdot 10^{-6} \text{ mm}^2$ . Rerunning the observer on the same data, with  $\hat{x}_{0,\text{ref}}$  initialized from data in the last run, yields the result in Fig. 13. Now the temperature states can be seen to converge quickly, almost even before the clutch starts slipping. Herein lies the power of the proposed observer, it can estimate the clutch temperature, and hence the torque transmissibility curve, without slipping the clutch, since it uses the measurement of the zero position. This is very useful since the clutch is closed for extended time periods during long haulage and during that time, the clutch temperature can change due to the engine and ambient temperature. This gives the possibility to track and know the torque transmissibility curve before the clutch starts to slip which is of great value for clutch and torque control.

## 5 CONCLUSION

The transmitted torque in an HDT dry clutch at slipping conditions has been studied. Experiments show no direct slip-speed dependency at the levels of slip investigated here, instead dynamic effects are clearly visible. In particular the measurements show that the transmitted torque can vary with up to 900 Nm for a given position. The dynamic behavior has two vastly different time constants, approximately a factor 50 apart, where both parts affect the transmitted torque through thermal expansion of clutch parts. A third-order state-space model with an output nonlinearity captures the behavior of the clutch.

In validations, on driving sequences with intense use of the clutch, the open-loop simulation error was kept under 200 Nm and most of the time under 100 Nm, which is less than 3 % of maximum engine torque and comparable to the accuracy of the engine torque estimate. The dynamic model that includes temperature states is a significant improvement compared to a static model. The model was developed, fitted and validated on a production HDT using production sensors only.

The model was then augmented with a wear parameter corresponding to thinning of the clutch disc. In this augmented model the temperature states are observable both during slipping of the clutch and when the clutch is fully closed, the latter is due to the utilization of the zero-position measurement. The clutch disc wear on the other hand is only observable when the clutch is fully closed.

The implemented EKF can, using real data, converge from poor initial values, enabling prediction of the translation of the torque transmissibility curve. If, as often is the case, given good initial knowledge about the disc wear but poor initial temperatures the observer can converge within a minute without slipping the clutch. The EKF is simple and suitable for real-time applications.

All modeling, design and validation steps have been performed using production sensors only, efficiently demonstrating that the EKF can be implemented in a production truck.

## REFERENCES

- Marius Bataus, Andrei Maciac, Mircea Oprean, and Nicolae Vasiliu. Automotive clutch models for real time simulation. *Proceedings of the Romanian Academy, Series A*, 12(2):109–116, 2011.
- Nicola Cappetti, Mario Pisaturo, and Adolfo Senatore. Modelling the cushion spring characteristic to enhance the automated dry-clutch performance: The temperature effect. *Proc IMechE, Part D: Journal of Automobile Engineering*, 226(11):1472–1482, 2012a.
- Nicola Cappetti, Mario Pisaturo, and Adolfo Senatore. Cushion spring sensitivity to the temperature rise in automotive dry clutch and effects on the frictional torque characteristic. *Mechanical Testing and Diagnosis*, 3(2):28–38, 2012b.
- Josko Deur, Vladimir Ivanovic, Zvonko Herold, and Milan Kostelac. Dry clutch control based on electromechanical actuator position feedback loop. *International Journal of Vehicle Design*, 60(3-4):305–326, 2012.
- Pietro Dolcini, Hubert Béchart, and Carlos Canudas de Wit. Observer-based optimal control of dry clutch engagement. In *44th IEEE Conference on Decision and Control, and the European Control Conference*, December 2005a.
- Pietro Dolcini, Carlos Canudas de Wit, and Hubert Béchart. Improved optimal control of dry clutch engagement. *Proceedings of the 16th IFAC World Congress*, 16(1), 2005b.
- Pietro Dolcini, Carlos Canudas de Wit, and Hubert Béchart. Lurch avoidance strategy and its implementation in AMT vehicles. *Mechatronics*, 18(1):289–300, May 2008.
- Pietro J. Dolcini, Carlos Canudas de Wit, and Hubert Béchart. *Dry Clutch Control for Automotive Applications*. Advances in Industrial Control. Springer-Verlag London, 2010.
- G. Ercole, G. Mattiazzo, S. Mauro, M. Velardocchia, F. Amisano, and G. Serra. Experimental methodologies to determine diaphragm spring clutch characteristics. In *SAE Technical Paper: 2000-01-1151*, March 2000.
- Bingzhao Gao, Hong Chenc, Jun Li, and Lu Tian. Observer-based feedback control during torque phase of clutch-to-clutch shift process. *International Journal of Vehicle Design*, 58(1):93–108, 2012.
- Franco Garofalo, Luigi Glielmo, Luigi Iannelli, and Francesco Vasca. Optimal tracking for automotive dry clutch engagement. In *2002 IFAC, 15th Triennial World Congress*, 2002.

- Luigi Glielmo and Francesco Vasca. Optimal control of dry clutch engagement. In *SAE Technical Paper: 2000-01-0837*, March 2000.
- Erik Höckerdal, Erik Frisk, and Lars Eriksson. EKF-based adaptation of look-up tables with an air mass-flow sensor application. *Control Engineering Practice*, 19(5):442–453, 2011.
- Matija Hoic, Zvonko Herold, Nenad Kranjcevic, Josko Deur, and Vladimir Ivanovic. Experimental characterization and modeling of dry dual clutch thermal expansion effects. In *SAE Technical Paper: 2013-01-0818*, April 2013.
- Sungwha Hong, Sunghyun Ahn, Beakyou Kim, Heera Lee, and Hyunsoo Kim. Shift control of a 2-speed dual clutch transmission for electric vehicle. In *2012 IEEE Vehicle Power and Propulsion Conference*, October 2012.
- Jinsung Kim and Seibum B. Choi. Control of dry clutch engagement for vehicle launches via a shaft torque observer. In *2010 American Control Conference*, June 2010.
- Behrooz Mashadi and David Crolla. *Vehicle Powertrain Systems*. John Wiley & Sons Ltd, first edition, 2012.
- G. Mattiazzo, S. Mauro, M. Velardocchia, F. Amisano, G. Serra, and G. Ercole. Measurement of torque transmissibility in diaphragm spring clutch. In *SAE Technical Paper: 2002-01-0934*, March 2002.
- S.E. Moon, M.S. Kim, H. Yeo, H.S Kim, and S.H Hwang. Design and implementation of clutch-by-wire system for automated manual transmissions. *International Journal Vehicle Design*, 36(1):83–100, 2004.
- Andreas Myklebust and Lars Eriksson. Torque model with fast and slow temperature dynamics of a slipping dry clutch. In *2012 IEEE Vehicle Power and Propulsion Conference*, October 2012.
- Andreas Myklebust and Lars Eriksson. The effect of thermal expansion in a dry clutch on launch control. In *7th IFAC Symposium on Advances in Automotive Control*, September 2013.
- Carl Nording and Jonny Österman. *Physics Handbook*. Studentlitteratur, 1999.
- Wilson J. Rugh. *Linear System Theory*. Prentice-Hall, Inc., second edition, 1996.
- Barna Szimandl and Huba Németh. Dynamic hybrid model of an electro-pneumatic clutch system. *Mechatronics*, 23(1):21–36, 2012.
- Francesco Vasca, Luigi Iannelli, Adolfo Senatore, and Gabriella Reale. Torque transmissibility assessment for automotive dry-clutch engagement. *IEEE/ASME transactions on Mechatronics*, 16(3):564–573, June 2011.

M. Velardocchia, G. Ercole, G. Mattiazzo, S. Mauro, and F. Amisano. Diaphragm spring clutch dynamic characteristic test bench. In *SAE Technical Paper: 1999-01-0737*, March 1999.

M. Velardocchia, F. Amisano, and R. Flora. A linear thermal model for an automotive clutch. In *SAE Technical Paper: 2000-01-0834*, March 2000.

Anna Wikdahl and Åsa Ågren. Temperature distribution in a clutch. Master's thesis, Linköping University, 1999.

Road Slope Analysis and Filtering for Driveline  
Shuffle Simulation\*

D

---

\*Published in *2012 IFAC Workshop on Engine and Powertrain Control, Simulation and Modeling*.



---

# Road Slope Analysis and Filtering for Driveline Shuffle Simulation

Andreas Myklebust and Lars Eriksson

*Vehicular Systems, Department of Electrical Engineering,  
Linköping University, SE-581 83 Linköping, Sweden*

## ABSTRACT

---

In powertrain analysis, simulation of driveline models are standard tools, where efficient and accurate simulations are important features of the models. One input signal with high impact on the accuracy is the road slope. Here it is found that the amplitude discretization in production road-slope sensors can excite vehicle shuffle dynamics in the model, which is not present in the real vehicle. To overcome this problem road-slope information is analyzed with the aid of both measured and synthetic road profiles, where the latter are generated from regulatory road specifications. The analysis shows that it is possible to separate vehicle shuffle resonances and road-slope information, and designs are proposed for on- and off-line filtering of the road-slope-sensor signal in spatial coordinates. Applying the filter to measured data shows that vehicle shuffle is significantly attenuated, while the shape of the road slope profile is maintained. As a byproduct the use of smoothing the rolling resistance is shown.

---

## 1 INTRODUCTION

When analyzing powertrains and their controls, the results will of course depend on the model but also on the input signals. The quality of the input signals have a big impact on simulation results, e.g. noise components in the inputs can have a profound effect on the outputs. A motivating example is given in Figure 3 where powertrain oscillations are induced due to sensor discretization levels, of integer percentage points, in road slope.

This example of discretization noise in the road-slope signal and how it influences simulated dynamics of a driveline is in focus here. Attention is also given to how a measured road-slope-sensor signal can be filtered so that the high frequency content, that can excite driveline dynamics and might result in vehicle shuffle, is removed while the relevant information is maintained. This is of importance when powertrains are simulated for control applications where vehicle shuffle has to be avoided. Examples of such control applications are vehicle-speed control, (Petterson and Nielsen, 2002), driver-filter design, (Gerhardt et al., 1998), gear-shift control, (Fredriksson and Egardt, 2003), (Petterson and Nielsen, 2000), and launch control, (Garofalo et al., 2002), (Dolcini et al., 2008).

Little work exists in the area of analyzing and filtering road slope data, even though road-grade information is used in different applications. For example Gao et al. (2011) studies road slope estimation and also how an incorrect estimation of the constant road slope effects the control of clutch disengagement. Estimation of the road slope for various applications is also treated in e.g. Lingman and Schmidbauer (2002), Sebsadji et al. (2008) and Bae et al. (2001). In Sahlholm (2011), where a road slope estimator is developed, low frequency errors are introduced to study the effect on look-ahead control and motivate the need of a good road grade estimator. Sahlholm (2011) filtered the road data using a third-order Butterworth low-pass filter with spatial cut-off frequency of  $9 \cdot 10^{-3} \text{ m}^{-1}$  before being used. In the related literature there is no quantitative analysis of the frequency content in the road-slope data.

A driveline model is developed for analysis of the interaction between road-slope data and vehicle shuffle. Measurement data is collected from a heavy duty truck, in order to both validate the model and to get realistic signals for the study. In addition the frequency content of different roads is analyzed, both theoretically and through measured road-slope data.

## 2 POWERTRAIN MODEL

In order to investigate how the quality of the road-slope signal affects simulation, a simulation model is required. A longitudinal model of a heavy-duty truck has therefore been developed. The model has to capture important dynamics in the driveline and how they make the truck shuffle. The model is an extension of the model in Petterson (1997) that was used for evaluation of oscillation damping by engine control during tip-in maneuvers. Petterson (1997) identified

the important flexibilities in the driveline that cause vehicle shuffle and therefore the same model structure is used here. The model is built in a modular way and then condensed into a state space model.

An overview of the different modules and their information exchange is given in Figure 1, which also defines the nomenclature used in this paper. Each module corresponds to a part in the powertrain, Internal Combustion Engine (ICE), clutch, gearbox, propeller shaft, final drive, drive shafts and vehicle dynamics.

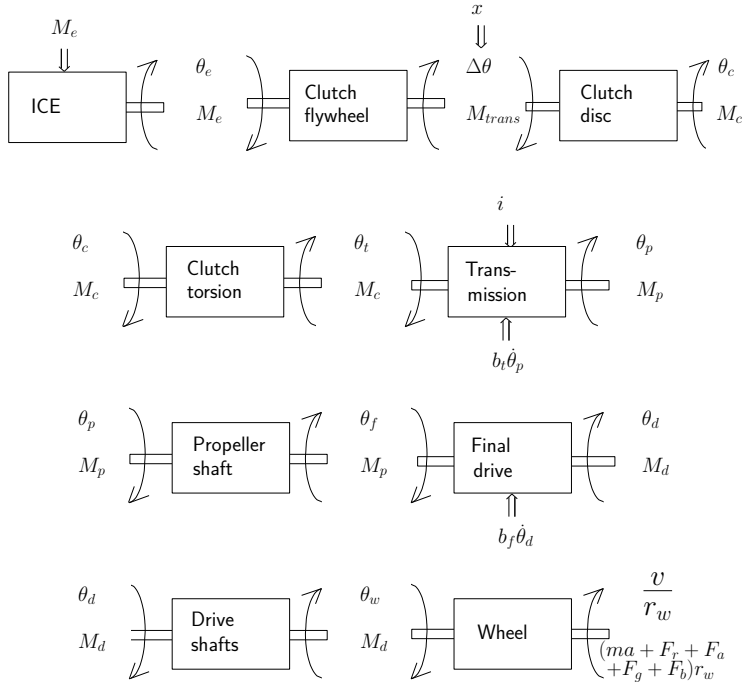


Figure 1: Sketch of the subsystems and their information exchange in the truck model.

## 2.1 INTERNAL COMBUSTION ENGINE

The ICE produces the engine torque,  $M_e$ , that is given as model input. Note that this is the net (brake) torque of the ICE, e.g.  $M_e = 0$  with open clutch will keep the engine speed constant.

## 2.2 CLUTCH

The clutch is modeled in three separate parts. The actuator, the clutch disc where slip might occur, and a torsional part that is flexible.

## CLUTCH ACTUATOR

The clutch position,  $x$ , is normalized by its maximum stroke,  $x_{\max}$  to get a relative position. The relative position is assumed to have an effective range,  $x_{\text{eff}}$  where the resulting normal force between the clutch plates are unsaturated. This effective range is transformed so that 0 corresponds to zero normal force and 1 corresponds to maximum normal force. This transformed signal is assumed to be proportional to the applied normal force.

The natural output from the actuator is the clamping force,  $F_N$ . Nevertheless the clamping force is directly recalculated into a transmittable torque,  $M_{\text{trans}} = k\mu F_N$ , that is used as actuator output. There are two friction coefficients, one static,  $\mu_s$ , and one dynamic,  $\mu_k$ . Let  $\mu_k$  be part of  $k_{\text{clutch}}$  and define the ratio of the friction coefficients,  $k_\mu = \frac{\mu_s}{\mu_k}$ . Then the equations for the clutch actuator become:

$$x_{\text{eff}} = \begin{cases} L_l, & \frac{x}{x_{\max}} < L_l \\ \frac{x}{x_{\max}}, & L_l \leq \frac{x}{x_{\max}} \leq L_u \\ L_u, & L_u < \frac{x}{x_{\max}} \end{cases} \quad (1)$$

$$M_{\text{trans},k} = k_{\text{clutch}} \frac{L_u - x_{\text{eff}}}{L_u - L_l} \quad (2)$$

$$M_{\text{trans},s} = k_\mu M_{\text{trans},k} \quad (3)$$

Note that (2) is a simple model of the slipping clutch compared to Myklebust and Eriksson (2012).

## CLUTCH DISC

The modeled clutch is a single-plate dry clutch with two contact surfaces. Torque is transferred between the clutch disc and flywheel through friction. The friction is modeled as coulomb friction with stick-slip behavior. Torque from the ICE,  $M_e$ , and driveline,  $M_c$ , are inputs and angular velocity & angle on both sides,  $\dot{\theta}_e$  &  $\theta_e$  and  $\dot{\theta}_c$  &  $\theta_c$ , respectively, are outputs.

The clutch model has two modes, locked and slipping mode. While in locked mode, the clutch behaves as one rigid body, whereas during slipping the clutch consists of two bodies where each one has an angular velocity and position. The condition for the transition from slipping to locked mode is that the speed difference is zero and the transmitted torque,  $M_{\text{trans}}$  is less than the static transmittable torque,  $M_{\text{trans},s}$ . The condition for transition from locked to slipping mode is when  $M_{\text{trans}}$  rises above  $M_{\text{trans},s}$ .

Using  $\theta_e$ ,  $\dot{\theta}_e$ ,  $\theta_c$ , and  $\dot{\theta}_c$  as states gives the following equations for the clutch disc:

Conditions for switching from slipping to locked mode:

$$\dot{\theta}_e = \dot{\theta}_c \quad (4)$$

$$M_{\text{trans}} \leq M_{\text{trans,s}} \quad (5)$$

Equations for the clutch in locked mode:

$$M_e - M_c = (J_{\text{ICE}} + J_{\text{fw}} + J_c) \ddot{\theta}_e \quad (6)$$

$$\dot{\theta}_c = \dot{\theta}_e \quad (7)$$

$$M_{\text{trans}} = \frac{M_e J_c + M_c (J_e + J_{\text{fw}})}{J_e + J_{\text{fw}} + J_c} \quad (8)$$

Conditions for switching from locked to slipping mode:

$$M_{\text{trans}} \geq M_{\text{trans,s}} \quad (9)$$

Equations specific to the clutch in slipping mode:

$$M_{\text{trans}} = \text{sgn}(\dot{\theta}_e - \dot{\theta}_c) M_{\text{trans,k}} \quad (10)$$

$$M_e - M_{\text{trans}} = (J_e + J_{\text{fw}}) \ddot{\theta}_e \quad (11)$$

$$M_{\text{trans}} - M_c = J_c \ddot{\theta}_c \quad (12)$$

## TORSIONAL PART

The main flexibility of the clutch is in the torsion springs in the clutch disc. They are located on the vehicle side of the friction surfaces. Therefore the flexibility of the clutch is modeled as a separate part of the clutch, located on the transmission side of the clutch disc, like in Moon et al. (2004).

The clutch torsional part is modeled as a torsional spring and damper. It takes speed & angle from the clutch disc,  $\dot{\theta}_c$  &  $\theta_c$ , and the input shaft of the transmission,  $\dot{\theta}_t$  &  $\theta_t$ , as input and returns a torque,  $M_c$ . The equation for the torsional part is:

$$M_c = c_c(\dot{\theta}_c - \dot{\theta}_t) + k_c(\theta_c - \theta_t) \quad (13)$$

## 2.3 TRANSMISSION

The gear number (input) is converted to a gear ratio,  $i_{t,i}$ , and gearbox inertia,  $J_{t,i}$ . The gear ratio scales the input-side torque,  $M_c$ , & inertia into output-side torque,  $M_t$ , & inertia,  $J_t$ . The speed is calculated from the output side to the input side and then integrated to an angle,  $\theta_t$ . There is also a speed proportional (viscous) friction in the transmission. On the output side the outputs torque & inertia are summed with the propeller shaft torque,  $M_p$ , & inertia,  $J_p$ , to produce the outputs speed,  $\dot{\theta}_p$ , & angle,  $\theta_p$  using Newton's second law.

Note that no synchronizers are modeled and the model can not engage neutral gear. Therefore gear shifting will be instantaneous. This is an acceptable

approximation when the clutch is disengaged, since the transmission input side has low inertia compared to the rest of the vehicle.

With the states  $\dot{\theta}_p$ ,  $\theta_p$ , and  $\theta_t$  the equations become:

$$M_t = M_c i_{t,i} \quad (14)$$

$$(J_{t,i} + J_p) \ddot{\theta}_p = M_t - b_t \dot{\theta}_p - M_p \quad (15)$$

$$\dot{\theta}_t = \dot{\theta}_p i_{t,i} \quad (16)$$

## 2.4 PROPELLER SHAFT

The flexible propeller shaft is modeled in the same way as the clutch flexibility, (13). The equation for the propeller shaft is:

$$M_p = c_p(\dot{\theta}_p - \dot{\theta}_f) + k_p(\theta_p - \theta_f) \quad (17)$$

## 2.5 FINAL DRIVE

The final drive with differential is assumed to act symmetrically on the drive shafts. Therefore it can be modeled as the transmission but with fixed gear ratio,  $i_f$ , and inertia,  $J_f$ . With the states  $\dot{\theta}_d$ ,  $\theta_d$  the equations become:

$$(J_p i_f^2 + J_f + J_d) \ddot{\theta}_d = M_p i_f - b_f \dot{\theta}_d - M_d \quad (18)$$

$$\dot{\theta}_f = \dot{\theta}_d i_f \quad (19)$$

## 2.6 DRIVE SHAFTS

The flexible drive shafts can, with the symmetrical differential, be lumped into one and modeled in the same way as the clutch flexibility, (13). The equation is:

$$M_d = c_d(\dot{\theta}_f - \dot{\theta}_w) + k_d(\theta_f - \theta_w) \quad (20)$$

This is the main flexibility in the driveline.

## 2.7 VEHICLE DYNAMICS

The non-driveline parts that affect the longitudinal dynamics are modeled in this block. That is, the wheels and vehicle. Tire dynamics are neglected and rolling condition is assumed. The wheels simply consists of a radius,  $r_w$ , an inertia,  $J_w$  and a rolling resistance force,  $F_r$ .

Model inputs that directly affect the vehicle dynamics are braking force and road-slope angle,  $\alpha$  (in radians). The road-slope angle is used to calculate the gradient force that is added with the braking force, rolling resistance and aerodynamic drag. The sign of the vehicle velocity is used so that rolling resistance, braking force and air resistance will oppose the vehicle movement.

The drag forces are subtracted from the drive shaft torque and divided by the vehicle mass,  $m$ , in order to calculate the vehicle acceleration,  $a$ , which is integrated to velocity and fed back to the drive shafts as angular velocity.

## DISCONTINUITY OF ROLLING RESISTANCE

The rolling resistance has a static component that changes sign with the velocity of the vehicle. Around zero velocity this leads to a large discontinuity in the rolling resistance. If this is not properly handled there can be significant

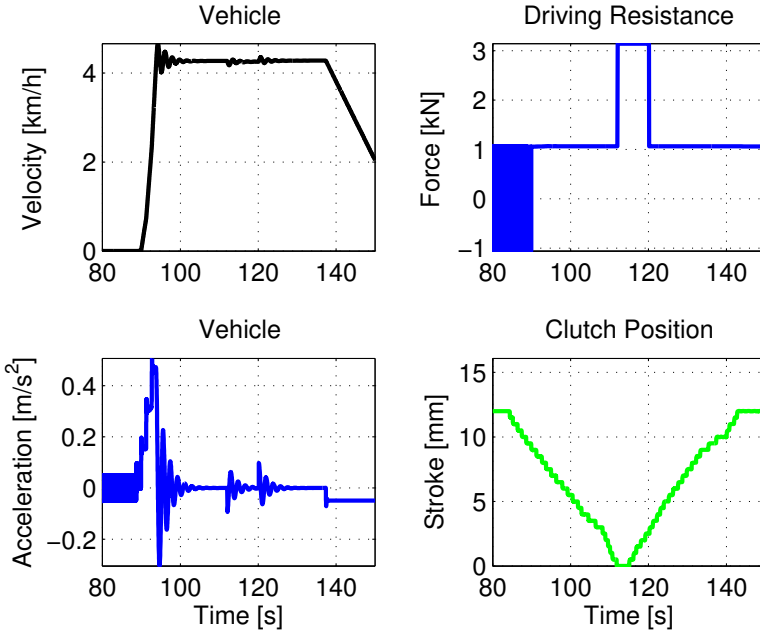


Figure 2: In the upper right plot it is seen how the rolling resistance is constantly switching sign during the first ten seconds of the simulation. In the lower left plot it is seen in addition how the acceleration is switching, while the speed is practically zero, upper left plot.

oscillations in the vehicle velocity and loading torque. See Figure 2 for a simulation example of this. One possibility is to use a state machine to control the states and transition between rolling and stand still. Another simpler cure to this problem is to smooth the rolling resistance using e.g. the following smoothing function

$$f(v) = 1 - e^{-c_{sr}v^2} \quad (21)$$

where  $v$  is the vehicle speed (in m/s) and  $c_{sr}$  is a tuning parameter. A smaller  $c_{sr}$  gives more smoothing, which speeds up the simulation more but affects the rolling resistance higher up in the speed range. Here  $c_{sr} = 16$  is selected as an empirical value that gives large reductions in simulation time without a significant effect on the rolling resistance at speeds above 0.5 km/h, see Figure 3. The simulation time was reduced with up to 85% when the smoothing function

was used in cases similar to that in Figure 3. With the states  $v$  ( $\dot{v} = a$ ) and  $\theta_w$  the equations become:

$$F_a = \frac{1}{2}\rho_a c_w A_f v^2, \quad F_g = mg \sin(\alpha) \quad (22)$$

$$F_r = f(v)(c_{r1} + c_{r2}|v|)mg, \quad \dot{\theta}_w = v/r_w \quad (23)$$

$$\begin{aligned} \frac{M_d}{r_w} - \text{sgn}(v)(F_r + F_a + F_b) - F_g = \\ = \left( m + \frac{J_w + J_d}{r_w^2} \right) a \end{aligned} \quad (24)$$

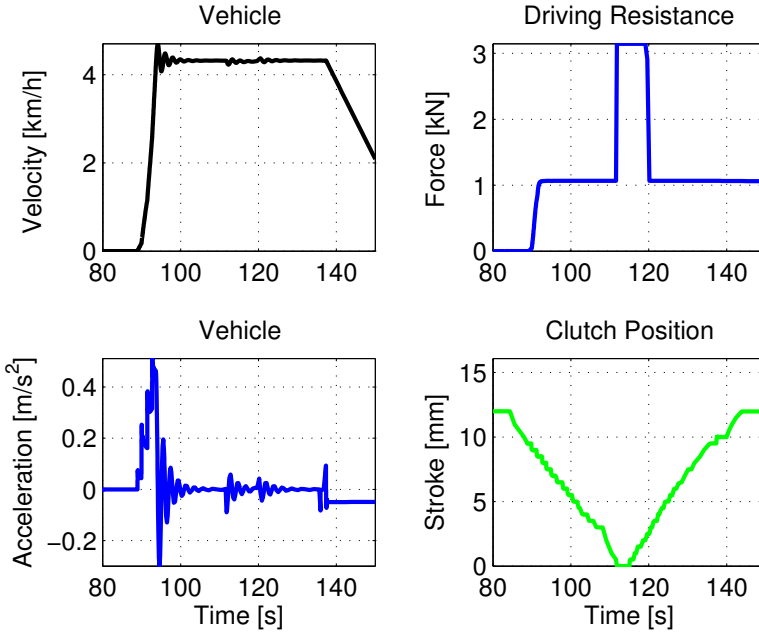


Figure 3: Simulation with the smoothed rolling resistance model. In the upper right plot it is seen that the rolling resistance does not increase until the velocity starts to increase (upper left plot). Moreover the acceleration can be seen to be zero until movement starts. Moreover it can clearly be seen that when the driving resistance, due to discretization levels of road slope signal, makes steps, at 110 s and 120 s, there are longitudinal oscillations.

## 2.8 STATE-SPACE MODEL

The vehicle speed,  $y = v$ , is the output and the velocities and torsions are chosen as state variables

$$\begin{aligned} x &= (x_1, x_2, x_3, x_4, x_5, x_6, x_7)^T = \\ &= (\omega_e, \theta_e - \theta_t, \omega_p, \theta_p - \theta_f, \omega_d, \theta_d - \theta_w, \omega_w)^T \end{aligned} \quad (25)$$

In order to get a compact representation of the model, the engine torque,  $g_1 = u_1 = M_e$ , and driving resistance,  $g_2 = F_{\text{dr}} = F_r + F_a + F_g + F_b = F_r + F_a + u_2$ , are collected into two separate signals. In the analysis in Section 3 the clutch is closed, gear is fixed, and velocity is positive. Then the system can be conveniently written as:

$$\begin{aligned} \dot{x} &= Ax + Bg(x, u) \\ y &= Cx \end{aligned} \quad (26)$$

with,

$$\begin{aligned} g(x, u) &= \left[ u_1, \frac{\rho_a c_w A_f r_w^2 x_7^2}{2} + (c_{r1} + c_{r2} r_w x_7) mg + u_2 \right]^T, \\ A &= \begin{pmatrix} \frac{-c_c}{J_1} & \frac{-k_c}{J_1} & \frac{c_c i_t}{J_1} & 0 & 0 & 0 & 0 \\ 1 & 0 & -i_t & 0 & 0 & 0 & 0 \\ \frac{c_c i_t}{J_2} & \frac{k_c i_t}{J_2} & \frac{-c_1}{J_2} & \frac{-k_p}{J_2} & \frac{c_p i_f}{J_2} & 0 & 0 \\ 0 & 0 & 1 & 0 & -i_f & 0 & 0 \\ 0 & 0 & \frac{c_p i_f}{J_3} & \frac{k_p i_f}{J_3} & \frac{-c_2}{J_3} & \frac{-k_d}{J_3} & \frac{c_d}{J_3} \\ 0 & 0 & 0 & 0 & 1 & 0 & -1 \\ 0 & 0 & 0 & 0 & \frac{c_d}{J_4} & \frac{k_d}{J_4} & \frac{-c_d}{J_4} \end{pmatrix}, \end{aligned} \quad (27)$$

$$J_1 = J_e + J_c, \quad J_2 = J_t + J_p,$$

$$J_3 = J_p i_f^2 + J_f + J_d, \quad J_4 = m_v r_w^2 + J_w + J_d,$$

$$c_1 = c_c i_t^2 + b_t + c_p, \quad c_2 = c_p i_f^2 + b_f + c_d,$$

$$B^T = \begin{pmatrix} \frac{1}{J_1} & 0 & 0 & 0 & 0 & 0 & 0 \\ 0 & 0 & 0 & 0 & 0 & 0 & \frac{-r_w}{J_4} \end{pmatrix}$$

$$C = (0 \quad 0 \quad 0 \quad 0 \quad 0 \quad 0 \quad r_w)$$

Note that (26) is a non-linear system as  $g_2$  depends on  $x_7^2$ .

## 2.9 LINEARIZATION

The Bode diagram is used to analyze the gain and resonances in the system, and to facilitate this the system is linearized. Noting that the only non-linearity in the state-space model is in  $g_2$  we can easily do the linearization by augmenting the  $A$ -matrix. This is done by doing the first-order Taylor expansion around  $v_0$  of the aerodynamic drag

$$F_a = \frac{1}{2} \rho_a c_w A_f (2v_0 v - v_0^2) + \mathcal{O}((v - v_0)^2) \quad (28)$$

giving the addition

$$\Delta a_{7,7} = \frac{-r_w^2 (c_{r2}mg - \rho_a c_w A_f v_0)v}{J_4} \quad (29)$$

to element  $a_{7,7}$  in  $A$ . The constant terms in the linearization are taken care of by the torque and torsions that correspond to steady state at  $v_0$ .

$$\begin{aligned} \dot{x}_\Delta &= A_{\text{aug}} x_\Delta + B u_\Delta \\ y_\Delta &= C x_\Delta \end{aligned} \quad (30)$$

where  $A_{\text{aug}}$  is the  $A$ -matrix augmented with  $\Delta a_{7,7}$ .

## 2.10 MODEL VALIDATION

The modular truck model has been validated using measurements from tip-in and tip-out maneuvers. Measurements of engine torque and road grade have been used as input for open-loop simulation of the model. Note that it is of great importance to have accurate road-grade information, when simulating the system. Otherwise the vehicle speed would have a large drift compared to the measurement. The model agrees well with measurement data for low gears, see Figure 4, and quite well for high gears, see Figure 5. In the latter case there were some small high frequency oscillations that were not captured in the model. Nonetheless the main vehicle shuffle frequency and amplitude have been captured in both cases. Therefore the model is suitable for simulations of cases where vehicle shuffle is a concern.

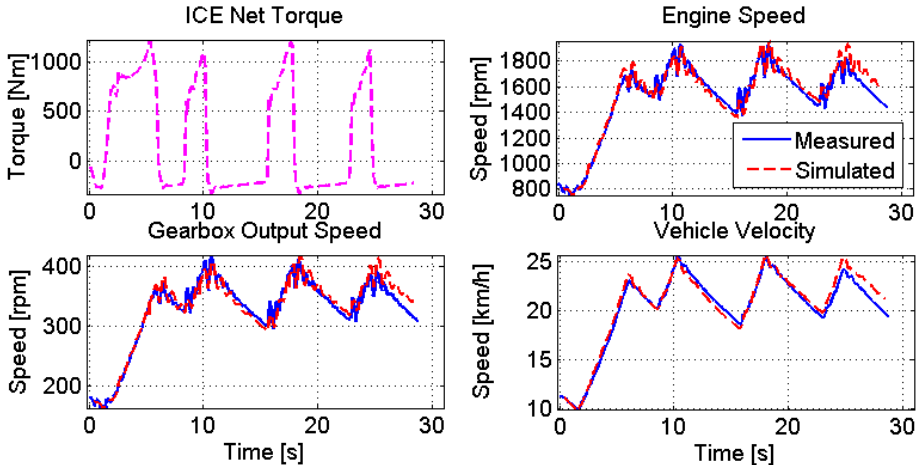


Figure 4: Model validation using tip-in/tip-out maneuvers for fifth gear. The model is run in open loop and it agrees well with data.

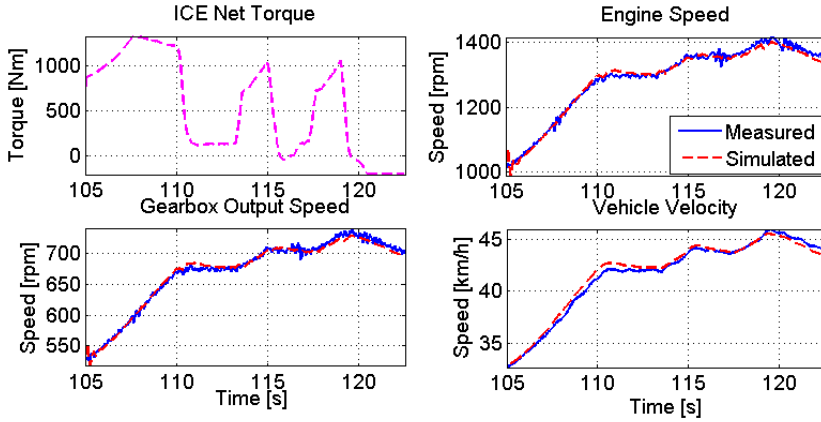


Figure 5: Model validation using tip-in/tip-out maneuvers for ninth gear. The model is run in open loop and it captures the trends in speed variations as well as the shuffle oscillations well. There are some quick oscillations that are missed.

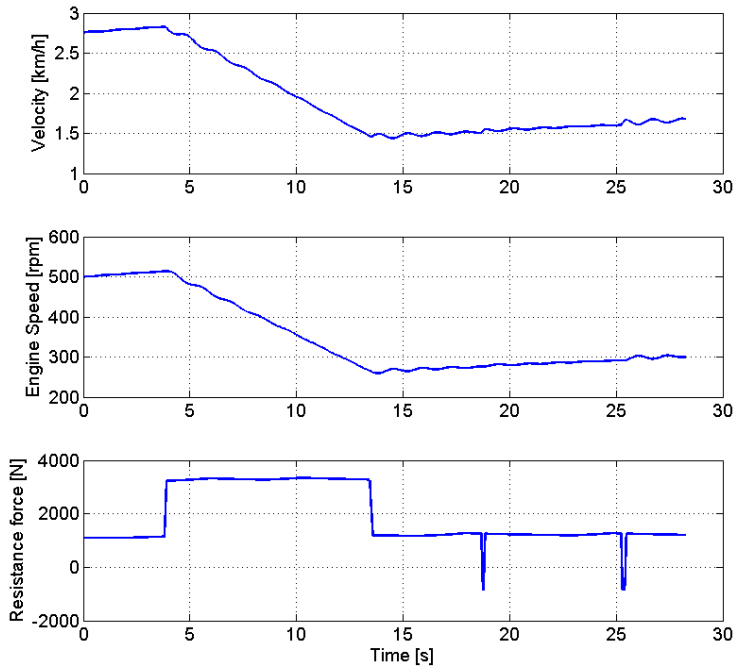


Figure 6: Showing how a one percentage point step in road slope affects truck behavior in 1<sup>st</sup> gear when engine torque is constant. A change in vehicle velocity with an oscillation superimposed can be seen.

### 3 SLOPE SIGNAL EFFECT ON SIMULATION

The linearized state-space model (30) is used to investigate the effect of a discretized slope signal on vehicle shuffle. First, no braking is assumed. Second, for slopes less than 20%,  $\sin(\alpha)$  can, with great accuracy, be considered equal to the road slope in percent ( $= \tan \alpha$ ). Since roads made for heavy duty trucks in Sweden have a maximum slope of 12% (highways have a maximum of 8% slope), (Swedish Road Administration, 2004), this is a very sound simplification. These two assumptions make  $u_{\Delta,2}$  proportional to the road slope, and therefore suitable as input signal for this study.

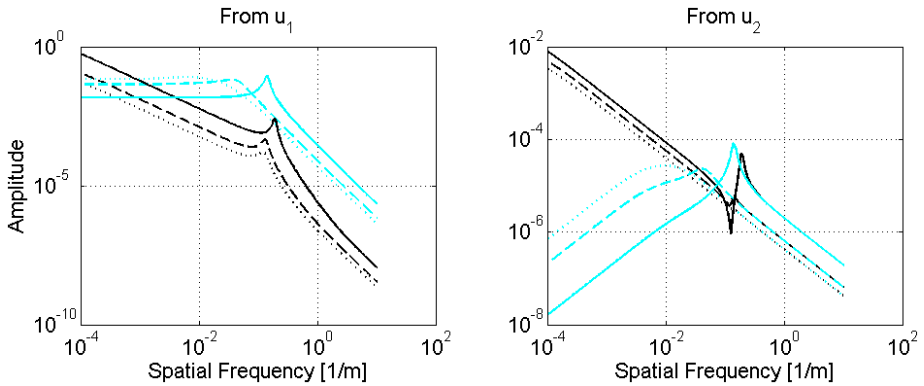


Figure 7: Bode plot of the open-loop system (black) and the closed-loop system (cyan), both systems in first (solid), sixth (dashed), and eighth (dotted) gear. Spatial frequency is used in order to enable comparisons with the road spectra in Section 4. The spatial frequency has been calculated using the maximum speed of each gear. For the open loop system  $u = [M_e \ F_{dr}]^T$  and for the closed loop system  $u = [w_{e,ref} \ F_{dr}]^T$ . For both cases  $y = v$ . It can be seen that the resonance peaks vanishes at eighth gear. For the closed loop case, in the right plot, the peak moves towards lower frequencies as the gear number is increased.

The truck has been simulated, in first gear with constant engine torque, using a measured driving resistance as input. The measured driving resistance contains three pulses, one long and two short, see Figure 6. The changes in driving resistance are due to that the road-slope signal is discretized in amplitude. This kind of signal contains a very wide frequency range. Therefore it induces oscillations in the driveline that are visible alongside the ramp changes in velocity. This can be explained by viewing the Bode plot of the system found in Figure 7. In the bode plot, there is a resonance peak in the transfer function from  $F_{dr}$  to  $v$ . This peak is the reason for the oscillations, however the peak has a low amplitude compared to the low frequency gain. Therefore the ramp changes in velocity are much greater than the oscillations. Note that also the transfer function from  $M_e$  to  $v$  has a resonance peak that can result in driveline oscillations. Consequently

if the system is under feedback, e.g. speed control, then both resonance peaks can be excited by a slope step, leading to even more driveline oscillations.

To highlight this a PI-controller for engine speed control is introduced

$$e = \dot{\theta}_{e,\text{ref}} - \dot{\theta}_e \quad (31)$$

$$\dot{x}_8 = e \quad (32)$$

$$M_e = K_P e + K_I x_8 \quad (33)$$

where  $K_P$  and  $K_I$  are the controller parameters. With the speed controller the

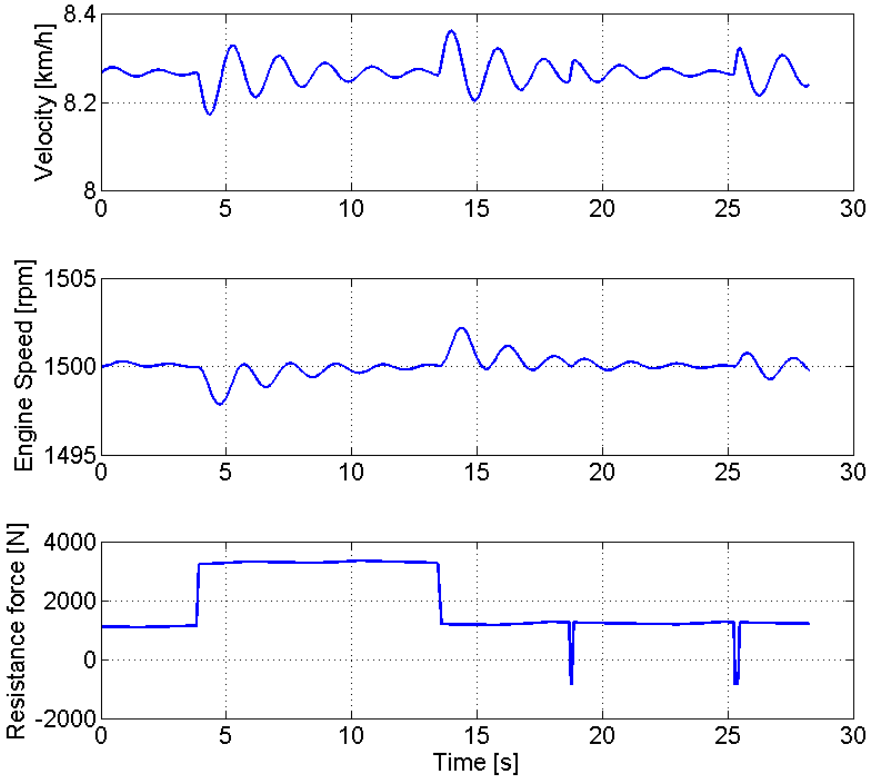


Figure 8: Oscillations in vehicle speed (longitudinal shuffle) can be seen when one-percentage-point pulses in road slope are present. Engine speed is kept constant by a PI-controller.

results in Figure 7 and Figure 8 are obtained. The driveline oscillations are now more clearly seen as well as the resonance peak in the transfer function from  $F_{\text{dr}}$  to  $v$ , which now also attains its maximum at the resonance. A better tuning or a more advanced controller could perhaps avoid the oscillations in the closed loop case, but this would only cure the symptoms and not the cause, which is

the high frequency content in the input. It can thus be concluded that some kind of filtering should be applied to the road slope signal.

It should however be noted that the occurrence of the sharp resonance peak, and therefore the need for filtering, is dependent on the selected gear. In the closed loop case, higher gear means that the peak in the transfer function moves towards lower frequencies, while in the open loop case it moves slightly towards higher frequencies. The peak also becomes less pronounced with higher gear numbers and vanishes at gear eight. So no filtering is needed for gears higher than seven.

## 4 ROAD FREQUENCY

When filtering the road-slope signal, it is of great interest to keep the important information in the signal. In order to achieve this it must be understood how a road-slope profile typically looks like.

According to official road-design policies (see Swedish Road Administration (2004) for Swedish and AASHTO (2004) for US), the road segments between constant slopes have a parabolic shape,

$$z = \frac{x^2}{2R} \quad (34)$$

where  $z$  is the elevation,  $x$  the longitudinal position and  $R$  the curve parameter. The parabola works as an approximation of a circle with radius  $R$ . For Swedish highways (89 km/h for heavy duty trucks)  $R$  can be as low as 1250 m and in cities (50 km/h)  $R$  can be as low as 300 m. The slope can be calculated as,

$$\begin{aligned} \tan \alpha &= \lim_{x_2 \rightarrow x_1} \left( \frac{z_2 - z_1}{x_2 - x_1} \right) = \lim_{x_2 \rightarrow x_1} \left( \frac{x_2^2 - x_1^2}{2R(x_2 - x_1)} \right) = \\ &= \lim_{x_2 \rightarrow x_1} \left( \frac{x_2 + x_1}{2R} \right) = \frac{x}{R} \quad (35) \end{aligned}$$

As stated earlier, slopes can be considered small and together with  $x \approx vt$  it yields,

$$\alpha = \frac{v}{R}t \quad (36)$$

This means that the slope varies as a piece-wise linear and continuous function. A piece-wise linear function contains sharp knees and has an infinite frequency content but the amplitude decreases with frequency. To get an idea of the spectrum a synthetic road is constructed by picking a number of random inclinations with random lengths, then connecting these slopes with vertical curves of random radii. For simplicity reasons uniform distributions are assumed for all variables. The inclinations have been selected from the range dictated by Swedish Road Administration (2004). The radii have been selected from a narrow range above the minimum value. The range of the slope-length distributions are

set exponentially with respect to the inclination, with flat ground giving the widest range. This is to mimic that in reality flat segments usually are longer than steep slopes. These assumptions are used to construct an approximation of a worst-case road. The resulting frequency spectrum is seen in Figure 9. Most of the power is in spatial frequencies below  $3 \cdot 10^{-4}$  1/m.

This theoretical "worst-case road" has been complemented with frequency spectra of different measured road segments<sup>1</sup> that indicate similar cut-off frequencies and roll-off rates, Figure 9. This indicates that the synthetisation method is sound and therefore it has been used for making a city road (50 km/h speed limit). The different limitations on maximum slope and  $R$  results in a road with higher frequency content. The main power is below  $1 \cdot 10^{-3}$  1/m.

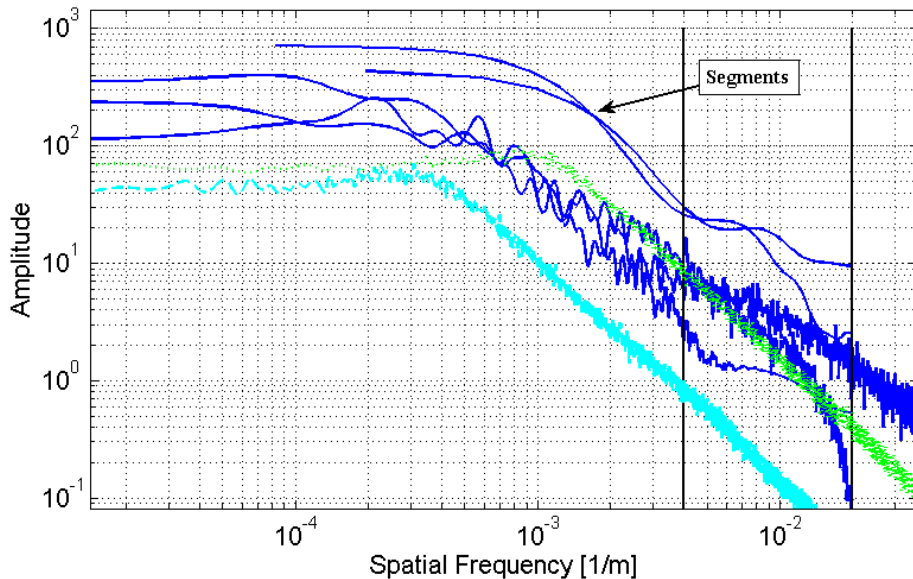


Figure 9: Frequency spectra for five measured highways (blue solid), one synthetic highway (cyan dashed), and one synthetic city road (green dotted). They all have similar shapes and most of their energy in frequencies below  $1 \cdot 10^{-3}$  1/m. The two shorter curves correspond to segments of the longer roads. The two black vertical lines mark the cut-off frequency and the -30 dB frequency of the filter.

Looking at the data for the road slope frequency content, Figure 9, and the Bode diagram for the model, Figure 7, one sees that the road data starts to fall off for frequencies below the resonance frequency of the driveline. This provides an opportunity to reduce the problem of oscillations by filtering the road slope signal. Especially since the Bode diagram represents the case with lowest spatial

<sup>1</sup>The road segments are the Järna segment, Jönköping-Linköping, Koblenz-Trier, Norrköping-Södertälje and the Olstorp segment

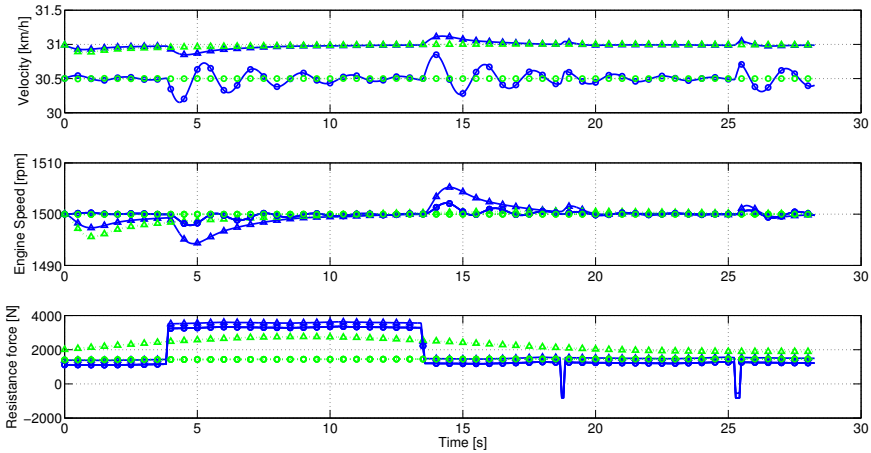


Figure 10: Original slope signal with its simulation response in solid blue. The acausally filtered signal and its response are shown in dashed green. Triangles are seventh gear and circles are first gear. The velocity response in first gear has been scaled. The oscillations are successfully filtered. Note that in first gear the slope signal is filtered more since the pulses are shorter in spatial coordinates.

frequency (highest speed for each gear), which represents the worst case with minimum separation between frequencies.

## 5 FILTER DESIGN

The design rules for the filter are that it should have little impact on the naturally occurring road frequencies and damp those that could excite driveline oscillations.

According to the investigation in the previous section the important road frequencies lie below  $1 \cdot 10^{-3}$  1/m, the location of the knee of the synthetic city road. However note that the two shorter segments in Figure 9 have a later roll off than the long roads because these particular segments are rich on high frequency content. Likewise choosing the filter cut-off frequency at the knee of the city road profile might lead to filtering of naturally occurring frequencies on a segment of this profile. Therefore the cut-off frequency is taken with one decade of margin compared to the knee, i.e.  $f_{co} = 4 \cdot 10^{-3}$  1/m. However there is never any guarantee that no real frequencies will be filtered as the theory have shown an infinite frequency content.

Frequencies that need to be damped are those around the resonance peak, see Figure 7, that exists for gear seven or lower. Maximum speed in seventh gear is about 50 km/h so it makes sense to choose  $f_{co}$  from the city road. The lowest frequency for any resonance peak is  $f_{lo} = 2 \cdot 10^{-2}$  1/m, which is that of

gear seven in closed loop. As the resonance peak is quite low in seventh gear, -30 dB of attenuation is chosen at  $f_{lo}$ . The filter will naturally attenuate more at the peaks for lower gears.

These requirements can be fulfilled by, for example a third or higher order low pass Butterworth filter with a cut-off frequency of  $4 \cdot 10^{-3}$  1/m (-40 dB at  $f_{lo}$ ). Note that while on one hand higher order gives a steeper gain curve and more margin to the requirements, on the other it gives more phase lag, i.e. time delay. In addition a higher filter order is more complex so computation time will increase. Therefore the lowest possible order is desirable in an on-line application. It might also be desirable to filter in the time domain, in that case the filter will be speed dependent. In an off-line application computational time is of less importance and the signal can be filtered both in the forward and reverse direction in order to get a zero phase filter.

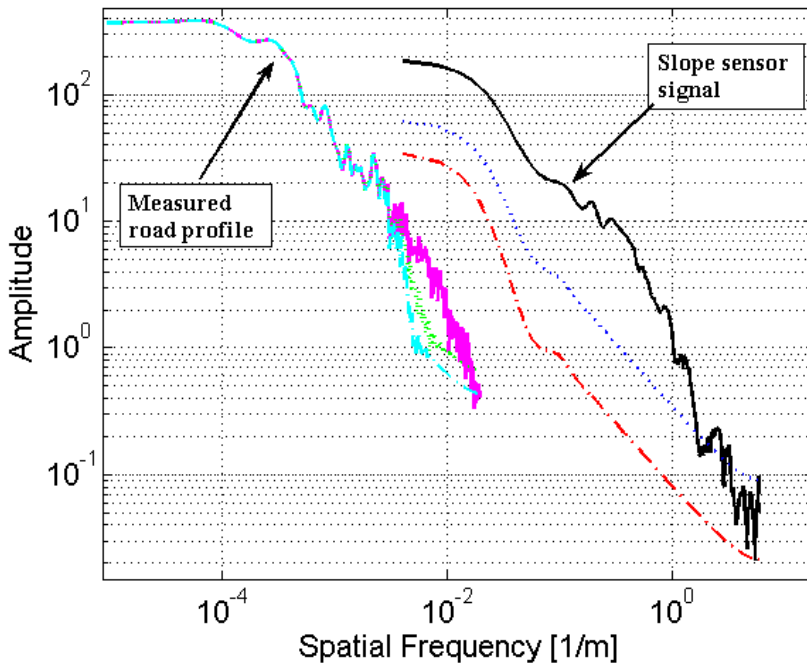


Figure 11: A real road profile in solid. With its filtered ditos in dashed-dotted (non-causal) and dotted (causal) slightly below (hard to tell apart). The short measured slope signal is also found in solid. It too has its filtered ditto in dashed-dotted (non-causal) and dotted (causal) below. The measured signal has lost a lot of its high frequency content whereas the road profile has kept its low frequency content. Just as intended.

## 6 RESULTS

Figure 10 shows that third order filtering of driving resistance effectively eliminates the oscillations in both first and seventh gear. In Figure 11 it can be seen that the high frequency content in the road slope sensor is significantly reduced whereas the real road profile is essentially the same. A road profile together with causally and non-causally filtered versions are displayed in Figure 12, showing that the general behavior of the road profile is preserved. It can thus be concluded that the filter design works as intended. Furthermore a third order filter is sufficient even in the off-line application, where it would be trouble free to increase the order.

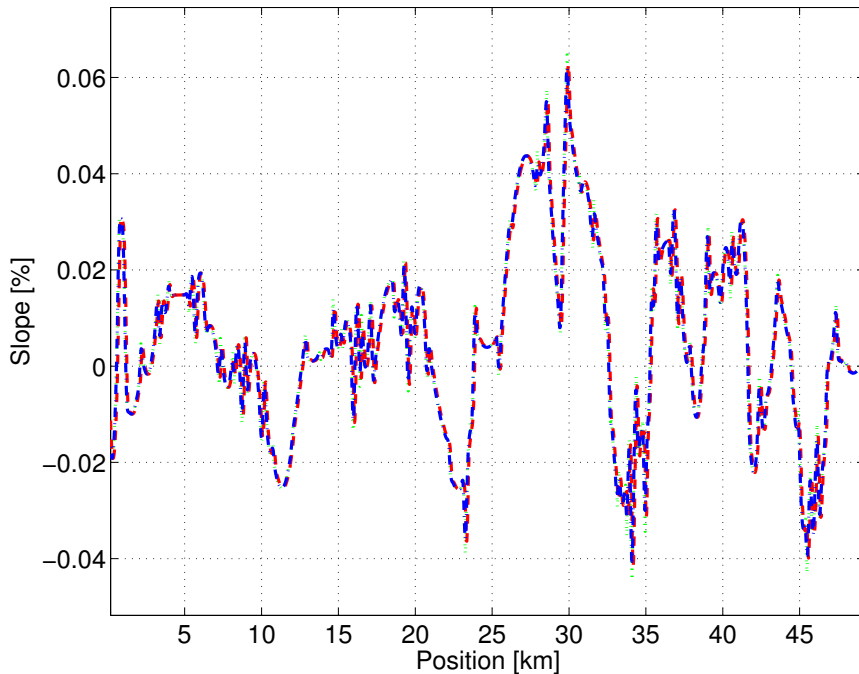


Figure 12: The road profile as function of position. Unfiltered in dotted green, causally filtered in dashed red and non-causally filtered in dash-dotted blue. The three signals are practically the same.

## 7 CONCLUSIONS

In this paper a model that describes vehicle shuffle of a heavy duty truck has been summarized and validated. Special emphasis was given to the interaction between driveline and road. In particular it was shown that smoothing the

rolling resistance around zero speed gives a significant reduction in simulation time for driving with start and stop scenarios.

Furthermore, experimental data from a production road slope sensor was shown to have a big impact on the simulation of the vehicle. In particular the high frequency content, introduced by amplitude discretization in the sensor, was shown to excite driveline oscillations. The oscillations also become more pronounced when the driveline had a feedback speed controller.

The frequency content in a theoretical worst-case road and measured roads, have been investigated and found to be below the resonance frequency of the model in every gear. It was also shown that the frequency separation was large enough to make a low-pass-filter design possible for the road-slope sensor.

Finally a design is proposed for a filtering method consisting of a low pass Butterworth filter in the spatial domain that eliminates erroneous behavior caused by high frequency disturbances in the slope signal, e.g. discretization. Applying the filter to measured data shows that the driveline oscillations are significantly attenuated, while the shape of the road-slope profile is maintained.

## REFERENCES

- AASHTO (2004). *A policy on geometric design of highways and streets: 2004*. American Association of State Highway and Transportation Officials.
- Bae, H.S., Ryu, J., and Gerdes, J.C. (2001). Road grade and vehicle parameter estimation for longitudinal control using gps. In *2001 IEEE Intelligent Transportation Systems*.
- Dolcini, P., de Wit, C.C., and B echart, H. (2008). Lurch avoidance strategy and its implementation in AMT vehicles. *Mechatronics*, 18(1), 289–300.
- Fredriksson, J. and Egardt, B. (2003). Active engine control for gear shifting in automated manual transmissions. *International Journal of Vehicle Design*, 32(3-4), 216–230.
- Gao, B., Lei, Y., Ge, A., Chen, H., and Sanada, K. (2011). Observer-based clutch disengagement control during gear shift process of automated manual transmission. *Vehicle System Dynamics*, 49(5), 685–701.
- Garofalo, F., Glielmo, L., Iannelli, L., and Vasca, F. (2002). Optimal tracking for automotive dry clutch engagement. In *2002 IFAC, 15th Triennial World Congress*.
- Gerhardt, J., H onninger, H., and Bischof, H. (1998). A new approach to functional and software structure for engine management systems - bosch me7. In *SAE Technical Paper: 980801*.
- Lingman, P. and Schmidtbauer, B. (2002). Road slope and vehicle mass estimation using kalman filtering. *Supplement to Vehicle System Dynamics*, 37(1), 12–23.
- Moon, S., Kim, M., Yeo, H., Kim, H., and Hwang, S. (2004). Design and implementation of clutch-by-wire system for automated manual transmissions. *International Journal Vehicle Design*, 36(1), 83–100.
- Myklebust, A. and Eriksson, L. (2012). Torque model with fast and slow temperature dynamics of a slipping dry clutch. In *2012 IEEE Vehicle Power and Propulsion Conference*.
- Pettersson, M. (1997). *Driveline Modeling and Control*. Ph.D. thesis, Link opings Universitet.
- Pettersson, M. and Nielsen, L. (2000). Gear shifting by engine control. *IEEE Transactions Control Systems Technology*, 8(3), 495–507.
- Pettersson, M. and Nielsen, L. (2002). Diesel engine speed control with handling of driveline resonances. *Control Engineering Practice, Advances in Automotive Control*, 11(3), 319–328.

Sahlholm, P. (2011). *Distributed road grade estimation for heavy duty vehicles*. Ph.D. thesis, KTH School of Electrical Engineering.

Sebsadji, Y., Glaser, S., Mammar, S., and Dakhllallah, J. (2008). Road slope and vehicle dynamics estimation. In *2008 American Control Conference*.

Swedish Road Administration (2004). Văgar och gators utformning - linjeföring. Technical report, Văgverket Publikation 2004:80.